Integrated Seismic Interpretation, Modeling, Rock Physics Study along with Complex Velocity Model Building and AVO Analysis to predict Hydrocarbon Potential of Bitrisim, Pakistan.

By

Khurram Shahzad

M.Sc. Geophysics

(2012-2014)

DEPARTMENT OF EARTH SCIENCES

QUAID-I-AZAM UNIVERSITY

ISLAMABAD

IN THE NAME OF ALLAH,

THE MERCIFUL, THE COMPASSIONATE

AND FROM HIM DO WE SEEK HELP.

ALL PRAISE BE TO ALLAH, THE SUSTAINER OF ALL THE WORLDS,

AND BLESSINGS AND PEACE BE UPON OUR MASTER MUHAMMAD (S.A.W.W),

AND ON ALL HIS FAMILY AND COMPANIONS.

Certificate

It is certified that **Khurram Shahzad** S/O **Muhammad Ilyas** compiled the work contained in this dissertation under my supervision and accepted in its present form by department of earth sciences as satisfying the requirements for M.Sc. degree in Geophysics.

RECOMMENDED BY

Dr. Muhammad Gulraiz Akhter _____

Supervisor /Chairman

Department of Earth Sciences.

Quaid-i-Azam University, Islamabad.

Pakistan.

External Examiner _____

Dedicated to my Grand father

With love to my father and mother.

My brothers and my angel.

ABSTRACT

The current study involves integrated seismic interpretation, rock physics and seismic attributes analysis of Bitrisim area, with special emphasis on velocity processing and modeling techniques. The study area lies in the Southern Indus basin which is known for its huge hydrocarbon reserves. Interpretation and analysis have been done on four seismic lines among the 25 seismic lines assigned to our group along with petrophysical logs of four wells. The complete workflow has been carried out using licensed software.

The integrated study involves; structural interpretation of seismic data, time to depth conversion and generation of depth sections, synthetic seismograms, crustal shortening analysis, well correlations, 1D and 2D Rock physics and Engineering properties along with seismic attributes analysis.

Horst and graben structures have been identified on the time sections which are more prominent on the depth sections created by using the velocity model. Well correlation section of four wells has been created along with a 2D seismic model, to study the seismic amplitude response in terms of contrast between alluvium or clay and limestone successions.

Seismic velocities have been calibrated through borehole velocities from sonic logs and velocity model has been generated using spatio-temporal and horizon based interpolation algorithms. The results indicate that horizon based interpolation generates the best velocity model and therefore it is used in time to depth conversion and other analysis. More over for the confirmation of the marked horizons and their behaviour, seismic attribute analysis have been carried out which helps in understanding the lateral continuity, bedding sequences and thickness of desired beds.

Amplitude Versus Offset/Angle Modeling was done for Upper Goru and Lower Goru Formations. P-wave reflection coefficient for Water and Gas saturated cases were computed for angles ranging from 40 to 70 degrees. The curve shows good separation between water and gas saturated cases, indicating the presence of Oil or Gas reservoir.

ACKNOWLEDGEMENT

In the name of *Allah Almighty*, the most Gracious, the most Compassionate. Almighty, on whom ultimately we depend for sustenance and guidance. I bear witness that *Hazrat Muhammad (SAWW)* is the last messenger, whose life is role model for the whole mankind till the Day of Judgment. I thank *Allah Almighty* for giving me strength and skill to finalize this study.

I acknowledge the cooperation extended by the Department of Earth Sciences at Quaid-i-Azam University Islamabad .Principally I would like to manifest my appreciation to my Supervisor; The Chairperson of the Department, Dr. Muhammad Gulraiz Akhter who not only guided me but also having faith in me by giving me a chance to do my dissertation under the guidance of Dr. Khalid Amin Khan, The Chief Geophysicist, OGTI (Oil and Gas Training Institute), Islamabad. I would like to pay special thanks to Dr. Khalid Amin Khan cordially who helped me thoroughly from his golden time.

I would like to thank the faculty and the staff of the department for their attention and co-operation with me throughout my Masters. I must acknowledge the prayers and efforts of my family for their encouragement, support and devotion throughout the study without whom I am nothing. I must acknowledge the help, reassurance, eternal love, support and prayers of all of my class fellows and friends especially The *KUNDANS* [Shahroz Azeem, Waleed Ahmed Raza, Umair Ahmed, Muhammad Waqas and Imran Rasheed].

I would also like to mention Mr Tahir Javed with respect and Wajahat Nawaz, Usman Zaib and Muhammad Junaid Abassi for the coordination throughout my dissertation.

Khurram Shahzad

January, 2014

Contents

List of Figures

List of Tables

Chapter 1

1. Introduction

1.1 Introduction to the Study Area

An essential element in the growth of the national economy is hydrocarbon reserves. Hydrocarbons have wide use in everyday life. Geophysical imaging techniques are becoming more and more complex due to continued research and development. Geophysical methods are the most widely used techniques for the delineation of hydrocarbons; in this regard seismic method is of supreme importance in this respect.

Pakistan has a high potential of hydrocarbons and consists of three major sedimentary basins (covering more than 2/3rd of its area) namely, Indus Basin in the east, Baluchistan Basin in the west and Pishin basin in the northwest. Indus and Baluchistan basin are separated by Ornach Bela transform fault zone and the Pishin basin lies between Indus and Chamman transform fault. A variety of sub-basins, fold belts and monoclines with variable structural styles resulting from diverse geodynamic conditions have been identified in Baluchistan Basin and Indus Basin (Kadri, 1995)

A deep seated north-south trending fossil failed rift has been indicated by the aeromagnetic data in the southern Indus basin. Horst and Graben structures have been recognized in the subsurface that are connected with the Indus fossil rift. The seismic epicentres distribution in the Indus plain has close association with regional east-west trending system of transcurrent faults that are related to the fossil rift of the Indus basin seems to be presently active, which is causing deformation of the overlaying mountain ranges. (Zaigham & Mallick., 2000)

1.2 Geographical Location

The study area is located in Khairpur district ,Sindh. Sanghar is the main town which is about 40 km south of the location.

It is located in central Sindh Province and is bounded on the North by Jacobabad High (Sukkar ridge), on the East by Jaisalmir High (Indian Border), on the south by Thar Slope and Nagarparkar Ridge and on the west by Thatha and Hyderabad High. Geographically

- Latitude: **26° 18′ 41.92′′** to **26° 29′ 32.06′′ North.**
- Longitude: **68° 55′ 0.63′′** to **69° 4′ 2.03′′ East.**

Figure 1.1 Satellite image of Pakistan showing Bitrisim area (Khan et al., 2008).

The imagery has been obtained from the Image Base databank developed using the Projection Independent Multi-Resolution Imagery Tiles Architecture (PIMRITA) (Khan et al., 2008) (Fig 1.1).

1.3 Base Map

A base map shows spatial location of seismic lines and wells and is considered as an important component of interpretation, as time, velocity and depth contours are finally posted

on this map. The base map of the area is generated by plotting data in Universal Transverse Mercator (UTM, Zone 42) geodetic reference system. The base map given in Fig 1.2 shows the orientation of the 25 seismic lines assigned to the group. Four lines; 20017-BTM-02, 20017-BTM-09, 20027-BTM-01 and 986-BTM-09; that have been used in this study are highlighted with yellow color. The wells used for marking the horizons are Fateh-01, Ichhri-01, Hakeem Daho -01 and Chak 05 Dim South -01 which are given in Table 1.1. Hakeem Daho-01 and Chak 05 Dim South-01 lie at southern part of the study area and having good distance to the seismic lines. These are only used for well correlation in this research work to understand the surrounding lithology.

Table 1 Orientation, nature and names of seismic lines along with wells used.

Sr. No.	Line name	Nature of line	Orientation	Wells
1	**20027-BTM-01**	**Dip**	**SW-NE**	
2	**20017-BTM-09**	**Dip**	**SW-NE**	**FATEH_01**
3	**20017-BTM-02**	**Strike**	**NW-SE**	
4	**986-BTM-09**	**Dip**	**SW-NE**	
5	20017-BTM-03	Dip	SW-NE	
6	20017-BTM-04	Dip	SW-NE	
7	20017-BTM-05	Dip	SW-NE	ICHHRI_01
8	20027-BTM-06	Dip	SW-NE	
9	20017-BTM-07	Dip	SW-NE	
10	20017-BTM-08	Dip	SW-NE	
11	20027-BTM-02	Dip	SW-NE	
12	20027-BTM-03	Dip	SW-NE	

13	20027-BTM-04	Dip	SW-NE	
14	20027-BTM-05	Dip	SW-NE	
15	20027-BTM-06	Dip	SW-NE	
16	20027-BTM-07	Dip	SW-NE	HAKEEM DAHO_01
17	20027-BTM-08	Strike	NW-SE	
18	20027-BTM-09	Strike	NW-SE	
19	20027-BTM-16	Strike	NW-SE	
20	986-BTM-08	Dip	SW-NE	CHAK-5 DIM SOUTH _01
21	986-BTM-10	Strike	NW-SE	
22	986-BTM-11	Dip	SW-NE	
23	986-BTM-12	Dip	SW-NE	
24	986-BTM-13	Dip	SW-NE	
25	986-BTM-14	Dip	SW-NE	

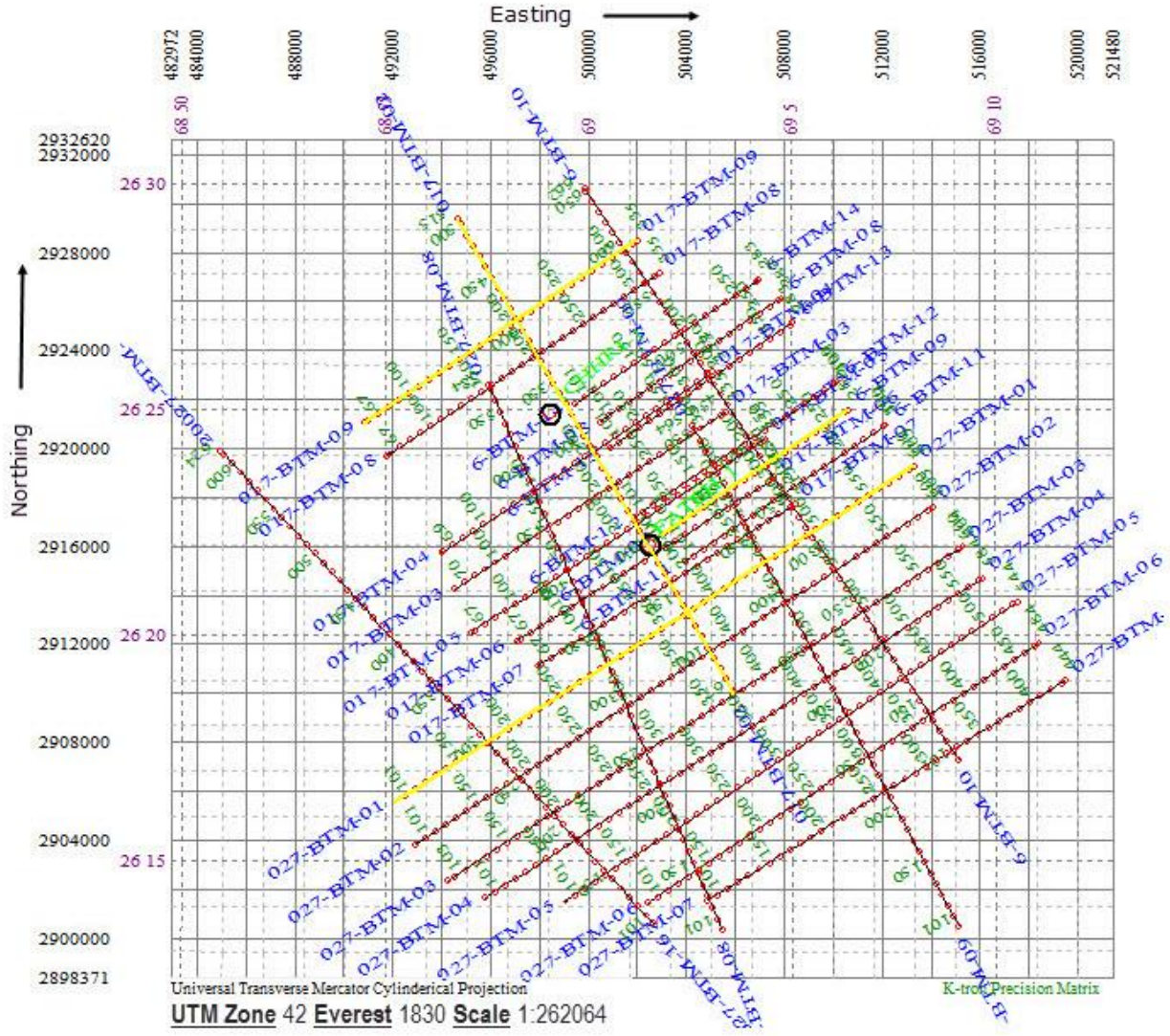

Figure 1.2 Base map showing seismic lines and wells. Study lines labelled yellow while wells with black colour.

These maps have been prepared using Precision Matrix an Integrated Geo Systems (Khan, 2000) application.

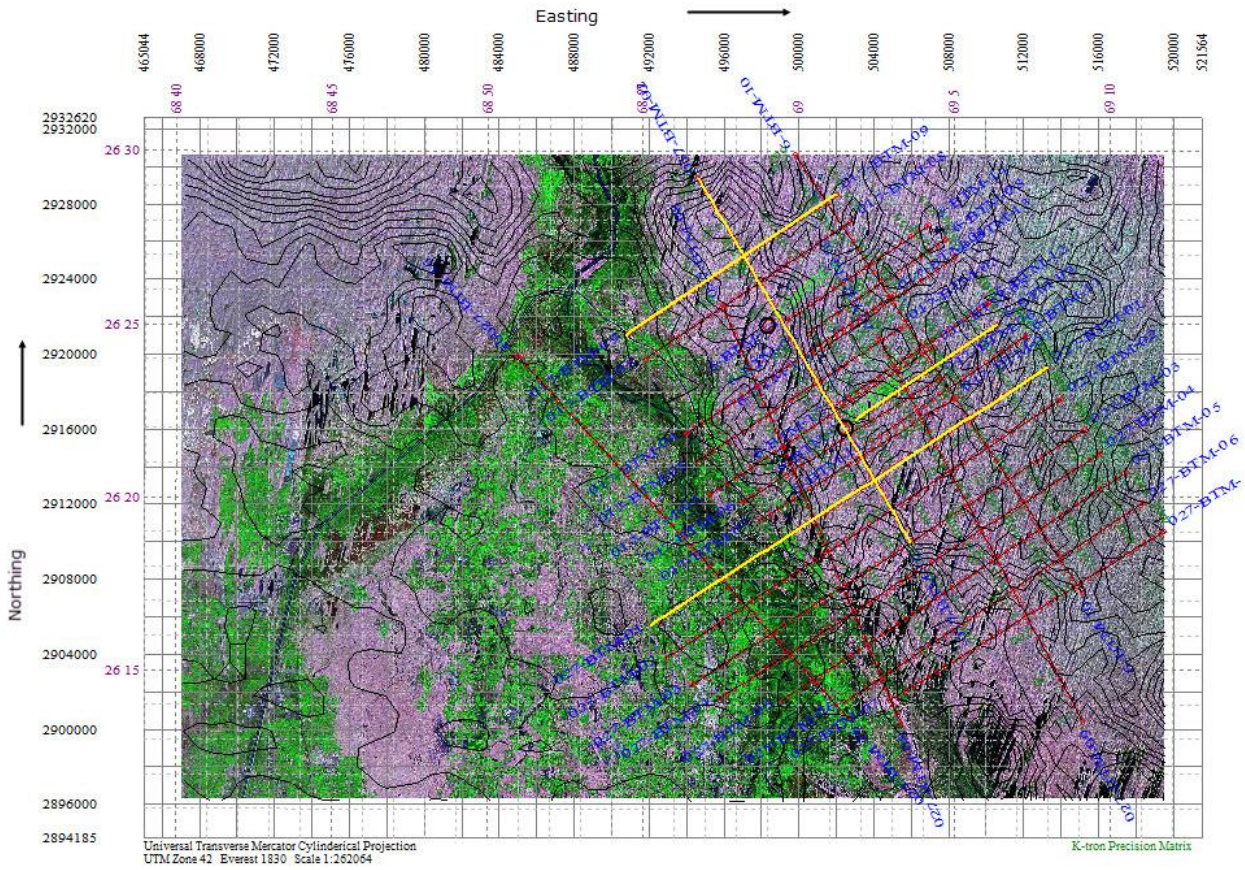

Figure 1.3 Base map having Satellite Imagery and SRTM30 digital elevation model contours (black). Yellow coloured under study seismic lines along with wells used (black).

1.4 Data Formats

The migrated seismic time section along with supporting data and the petro physical data obtained in following formats.

- Seismic — SEG-Y format
- Navigation — DBO format
- Petro physics — LAS format
- DEM — GRD Grid format
- Seismic Velocities — VEL format
- Well — KGD Vector format
- Georeference satellite image — GRF,JPG format

SEG-Y, LAS, navigation and velocity data was provided by the Directorate General Petroleum Concession (DGPC), Government of Pakistan while imagery, SRTM30 Digital Elevation Model (DEM) and other cultural mapping data was obtained from Pakistan Digital databank.

1.5 Introduction to Seismic Lines

Migrated time seismic sections of the lines "20017-BTM-02, 20017-BTM-09, 20027-BTM-01 and 986-BTM-09 "are provided for analysis and interpretation. These lines have been processed to get the final migrated stacks which have been used for interpretation. A generalized seismic data processing flow (Khan, 2009) is shown in Fig 1.3. The breakage in the reflectors helps in identifying the faults. Basement and other prominent reflectors show high amplitudes, indicating strong reflection coefficients.

1.6 Seismic Acquisition Parameters

Generation of (artificial) seismic signals on land (on surface, or, buried) or in water, reception of the signals after they travel through the interior of the earth, and their (digital) recording for later analysis.

Below mentioned seismic data had been recorded by O.G.D.C (Oil and Gas Development Corporation) in the study area.

- Datum M.S.L
- Datum Velocity 1800 m/sec

1.6.1 Instruments

The essential instrumental requirements are to generate a seismic pulse with suitable source, detect the seismic waves in the ground with a suitable transducer and record and display the seismic waveforms on suitable seismograph. Following parameters are attained in the study area.

- System SN388
- Format DMUX SEGD
- Aliasing filter 120 Hz
- Notch filter OUT
- Sampling interval 2 msec
- Record length 6 seconds
- No. of data traces 120

1.6.2 Source Information

Seismic source is a localized region within which the sudden release of energy leads to a rapid stressing of the surrounding medium. Requirements for a seismic source are; sufficient energy, waveform must be repeatable, must be safe, environmentally acceptable and efficient. Detail of the source parameters used in the study area is given below.

- Energy Source — Dynamite
- Charge Pattern — 1 Hole
- Average Charge — 5 kilogram
- Average Shot Depth — 18 meters
- Shot Interval — 50 meters

1.6.3 Receiver Information

Seismic signals are carried from geophones to recorders as varying electric currents, in cables which must contain twice as many individual wires as there are geophones. Cables and plugs are the most risky part of seismic system where they join.

A geophone consists of a coil wound on a high permeable magnetic core and suspended by leaf spring in the field of a permanent magnet as shown in Fig 1.4. Detail of the cable used in study area is given below.

- Spread — 3075-125- * - 125-3075
- Group interval — 50 meters
- Type of Geophones — SM.4 SERCEL
- Geophone Code — 0312 LINEAR
- Group Length — 97.30 meters
- Geophone Interval — 2.78 meters

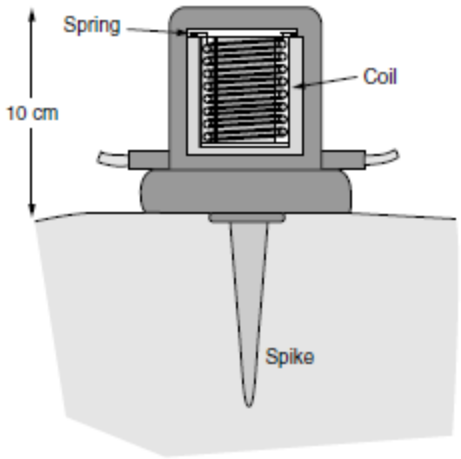

Figure 1.4 Moving coil Geophone

1.7 Data Processing

When the data has been acquired, it passes through the whole processing sequence that includes data processing techniques that are used to enhance the quality of the data. The raw seismic data is processed to enhance the signal to noise ratio and get the final seismic sections. The processing sequence flow chart is given below in Fig 1.5.

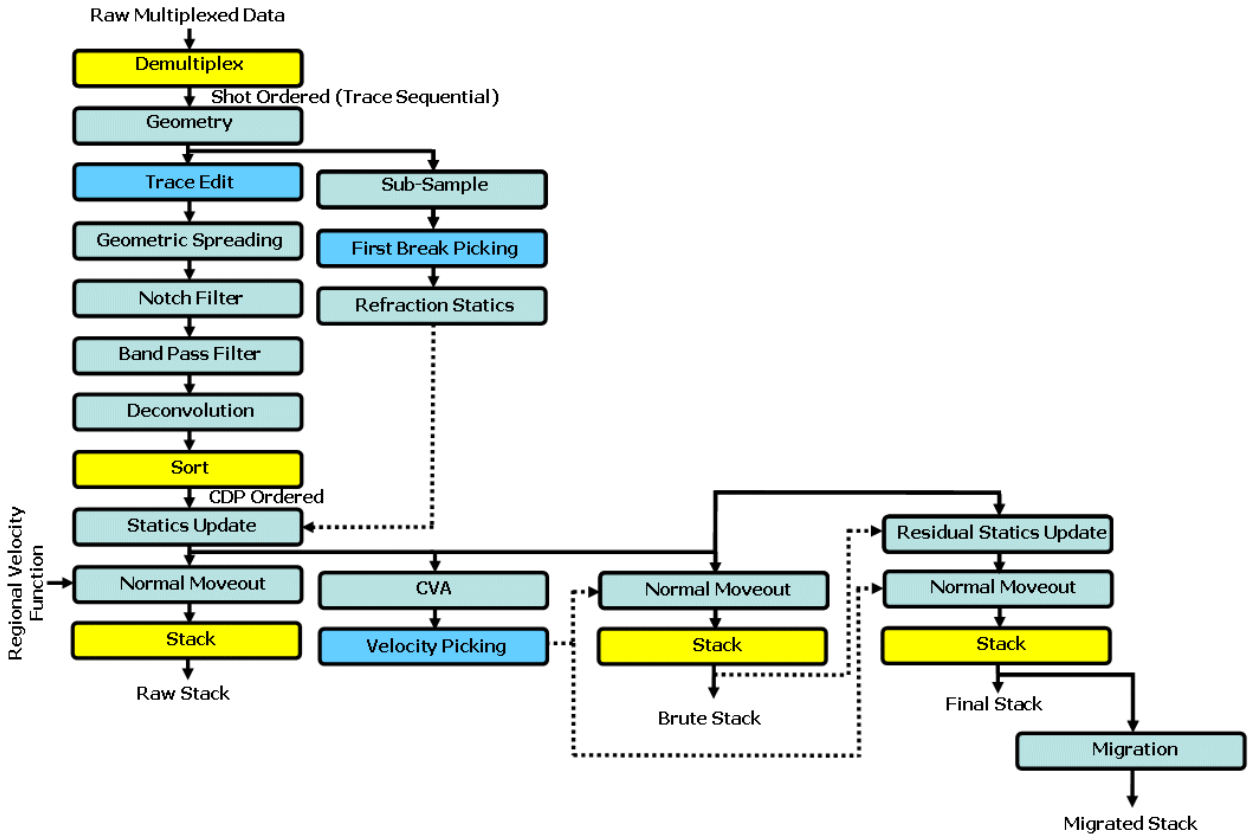

Figure 1.5 Seismic data processing flow chart. (Khan, 2009).

1.8 Spatial Data Infrastructure

Spatial Data Infrastructure in simple words is "a collection of geo-referenced databases and their associated processing & visualization tools". [Geo-reference means data w.r.t. some location reference to Earth or data for a given position on Earth]. The imagery (Khan et al., 2008) and SRTM-30 Digital Elevation Model (DEM) (Farr et al., 2007) are obtained from Digital Pakistan (Khan et al., 2012), a Spatial Data Infrastructure consisting of an array of database servers for imagery, binary grids, digitized vector layers and geological and geophysical databanks, linked with integrated visualization and processing applications as in Fig 1.6.

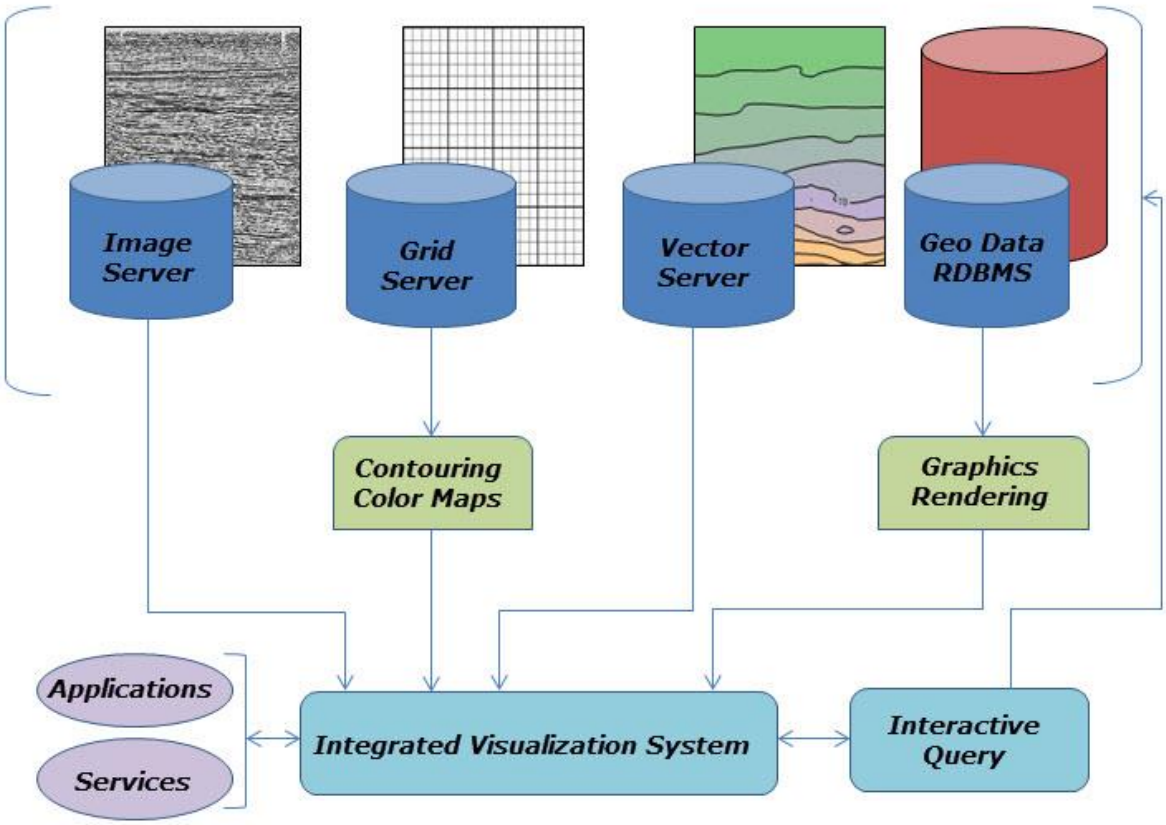

Figure 1.6 Block diagram of spatial data infrastructure for Digital Pakistan (Khan et al, 2012).

1.9 Software Purposes

Various software tools used in the thesis workflow have been summarized below along with their functionality.

1. **Precision matrix**
   - ❖ Base map generation with imagery
   - ❖ Well correlation profile
   - ❖ DEM contours
2. **X-Works**
   - ❖ Interactive interpretation.
   - ❖ Velocity overlay.
   - ❖ Time to depth conversion.
   - ❖ Integrated depth surfaces.
   - ❖ Crustal Shortening.
   - ❖ 2D seismic Modeling.
   - ❖ Velocity Model Building.

- ❖ Well correlation.
- ❖ Geological columns.

3. **Visual OIL**
   - ❖ Velocity inversion/ Rock physics.
   - ❖ AVO Analysis.
4. **Wavelets**
   - ❖ Petro physics.
   - ❖ Rock physics and Engineering properties.
5. **Kingdom SMT**
   - ❖ Seismic Attributes Analysis.
6. **K-tron Quick Contours**
   - ❖ Horizon time contour maps.
   - ❖ Horizon depth contour maps.
   - ❖ Horizon velocity contour maps.
7. **Surfer**
   - ❖ Rock physics parameters cross-section.

1.10 Analysis of Workflow

Interpretation and analysis were carried forward using different software tools and techniques with each involve different processes which were performed as mentioned above. The simplified workflow used in the dissertation is given in Fig 1.7 which provides the complete scenario depicting how the dissertation has been carried forward from the initial phase till its completion.

1.11 Objectives of Study

- ❖ The delineation of the potential reservoir of the area under study.
- ❖ Structural interpretation using 2D seismic reflection data to understand subsurface geologic framework and its relation with surface geology.
- ❖ The preparation of average velocity, mean velocity and Iso-velocity graph to investigate the lateral and vertical variation in velocity.
- ❖ The preparation of the time sections and generation of the depth sections using processed velocities to understand the real subsurface structures.

- Generate time, velocity and depth contour maps on different levels of strata to analyse structural and stratigraphic trend of the area and get acknowledge with the variation in the velocities vertically as well as laterally.

- Well correlation along with crustal shortening to see the seismic behaviour at lithological boundaries.
- Seismic Attribute Analysis for the confirmation of the horizon marking.
- Velocity interpolation using time slice and horizon slice interpolation for the building of velocity model.
- Rock physics analysis to understand the variation in the rocks with respect to elastic moduli.
- Gassmann Fluid Substitution based AVO/AVA modeling of the reservoir.

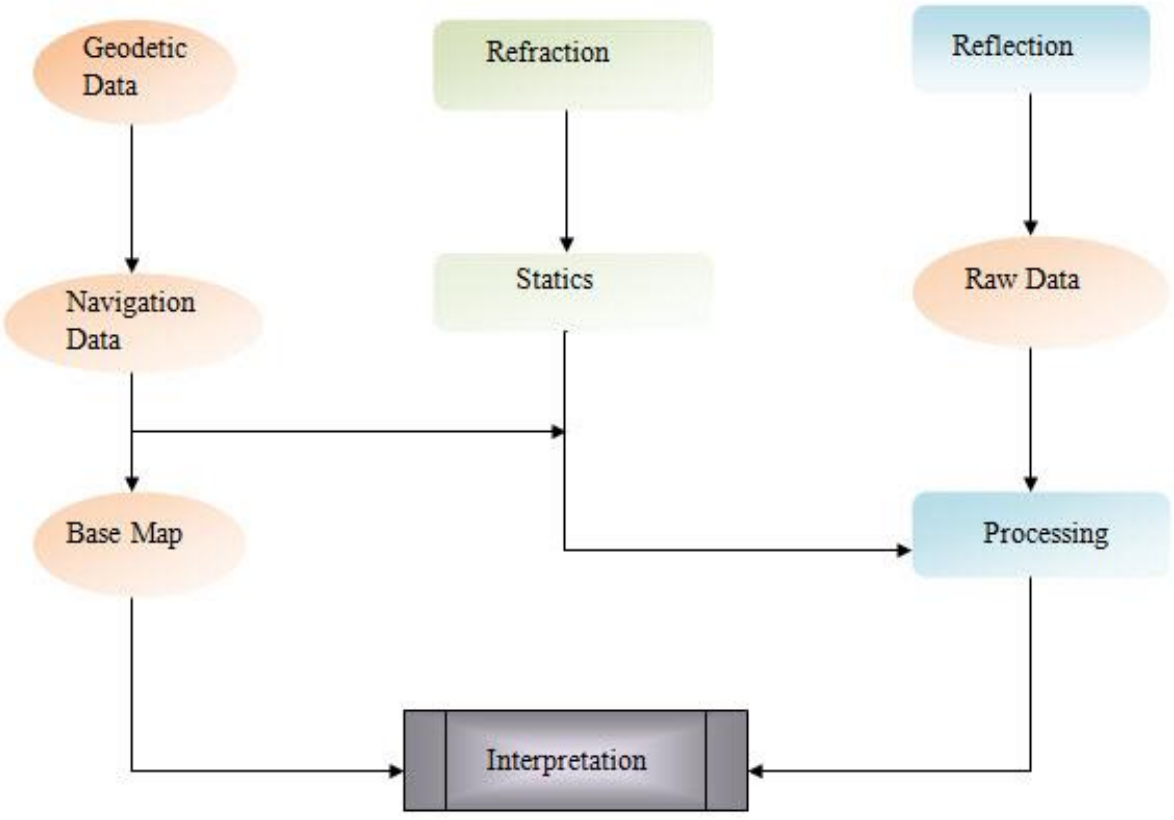

Figure 1.7 Seismic data interpretation workflow.

Chapter 2

2. General Geology and Stratigraphy

2.1 Introduction

Geology is the science comprising the study of solid Earth, the rocks of which it is composed, and the processes by which it evolves. Geology gives insight into the history of the Earth, as it provides the primary evidence for plate tectonics, the evolutionary history of life, and past climates. In modern times, geology is commercially important for mineral and hydrocarbon exploration and for evaluating water resources. It is also publicly important for the prediction and understanding of natural hazards.

Geology of an area plays very important role for a precise interpretation of seismic data, because same velocity effects can be generated from formations of different lithology. Also different velocity effects can be generated from same lithological horizons depending on their position and depth in the subsurface. Therefore as long as we don't know about geological formations and the history of its evolution in the area we cannot recognize different reflectors appearing in the seismic section. The information about location of faults, their penetration in subsurface and the presence of unconformities between rocks of different ages is also very important from interpretation point of view.

2.2 Structural Setting of the Study Area

The basinal history of the study area is related mainly to rifting and break up of Gondwana in Jurassic period. The Indian plate separated from East Gondwana in Aptian Time (120 ma). At the end of Cretaceous/early Paleocene, the Seychelles and Madagascar separated from India with associated faulting accompanied by Basaltic flows(Deccan Volcanics) in the southern part of Lower Indus Basin. The regional base Tertiary unconformity is due to thermal doming associated with the separation of the Seychelles and Madagascar from India. After the Paleocene there was a continuing oblique convergence of India and Asia throughout Tertiary time and the collision of India with Asia caused a westward tilting of the entire region. Domal lifting in during the Early Cretaceous is responsible for the Jacobabad-khairpur high on which the study area is located. Later on along deep seated faults in the Late Cretaceous and Paleocene have been generated. On the Jacobabad- Khairpur high, Eocene carbonates

(Sui Main Limestone) are widely distributed and form good hydrocarbon reservoirs. But in study area it is not acting as an economical reservoir.

2.2.1 Structural Zones

The Indus platform and foredeep comprise the following main structural zones.

Zones of upwarp	Mari-Kandhkot High
	Jacobabad-Khairpur High

Jacobabad Khairpur upwarp divides the Indus platform into two segments. The lower segment is comprised of lower Indus trough. It is bounded by Nawabshah and Nabisar slopes which are in turn flanked by Thatta-Hyderabad and Tharparkar highs. The upper segment is traversed by Sargodha Shahpur Ridge splitting into northern Punjab monocline and southern Punjab monocline. Some basement faults straddle major structures such as the Sargodha Shahpur ridge and Kandhkot-Mari and Jacobabad-Khairpur horsts. In Jacobabad Kandhkot zone, some of faults are likely to be post Eocene and post Miocene. South of Sargodha-Shahpur ridge and extending upto Kandhkot-Mari High is a roughly triangular area; the quaternary deposits are underlain by post Eocene, largely fluviatile deposits.

Structurally as a platform of the Indus basin, the Jacobabad-Khairpur horst started becoming a positive area in Late Jurassic. It consists of Mesozoic, Tertiary and Quaternary sediments with the Cretaceous and Jurassic reduced in thickness over horst. Mesozoic and Tertiary plays are significant targets for exploration.

2.2.2 Structural Setting

Normal faults are generated as a result of entire southern basin exhibiting the extensional tectonics, showing the Horst and Graben structures with former being of great exploratory importance. The extensional tectonics during the Cretaceous time created the tilted fault blocks over a wide area of the Eastern Lower Indus sub-basin (Kemal et al, 1992).

The southern Indus basin is identified as an extension basin resulting from an inferred fossil-rift crustal feature overlain by a thick sedimentary sequence. Extension was a consequence of temporal divergence of the Indo-Pakistan subcontinent from Gondwanaland during the early Paleozoic. Based on magnetic anomaly trends, the Indus basin fossil-rift feature is characterized by horst and graben structures, together with a system of transcurrent faults. The association of seismicity events and basement crustal features suggests that Tertiary reactivation of individual segments of the inferred rift structure has deformed overlying

sequences of the Indus basin and also the surrounding areas, particularly the fold and thrust belt of Pakistan on the western side of the basin. (Zaigham and Mallick, 2000)

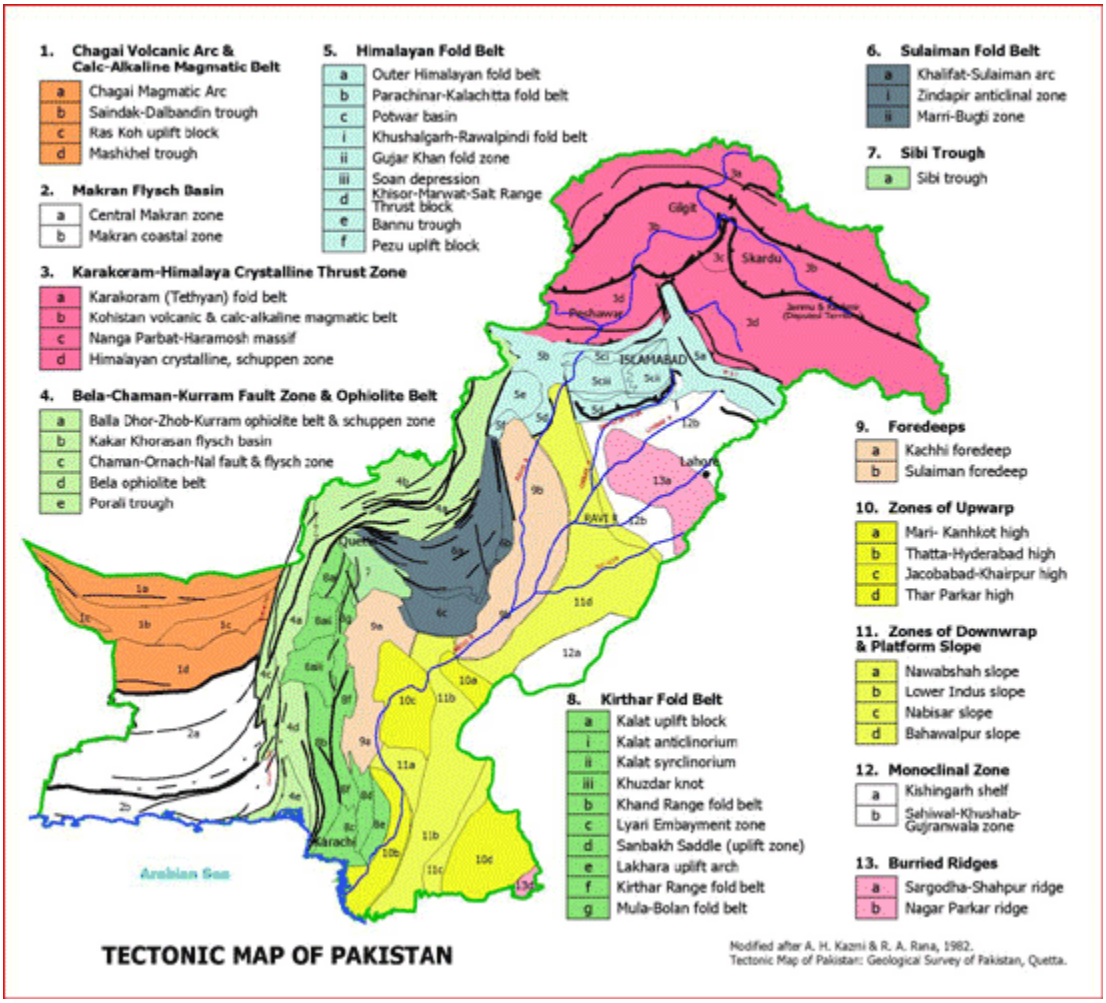

Figure 2.1 Tectonic map of Pakistan Tectonic map of Pakistan showing 13 tectonic sub division of Pakistan including study area (after Kazmi 1982).

2.3 Basins of Pakistan

The structure in Pakistan or we can write it as Indus basin is divided into number of regime i.e. compression regime at foreland margins, basement uplift in the Central Indus Basin and extensional regime in the Lower Indus Basin (Kadri, 1995).

The Basin and their subdivision includes the following

1. Indus Basin
    i. Upper Indus Basin
    ii. Lower Indus Basin
    iii. Central Indus Basin
    iv. Southern Indus Basin

2. Baluchistan Basin
3. Kakar Khorasaan Basin

2.3.1 Lower Indus Basin

The Lower Indus Platform Basin is bounded to the north by the Central Indus Basin, Sulaiman Fold belt to the northwest and Kirthar Fold Belt in the south-west. The main tectonic events which have controlled the structures and sedimentology of the Lower Indus Basin are rifting of the Indian Plate from Gondwanaland (Jurassic or Early Cretaceous) which probably created NE-SW to N-S rift systems, isostatic uplift or ridge-push at the margins of the newly developed ocean probably caused uplift and eastwards tilting at the start of the Cretaceous. Separation of the Madagascan and Indian plates in the Mid to Late Cretaceous which may have caused some sinistral strike-slip faulting in the region, hotspot activity and thermal doming at the Cretaceous-Tertiary boundary. It comprises the following main units:

a) Thar Platform
b) Karachi Trough
c) Kirthar Foredeep
d) Kirthar Fold Belt
e) Offshore Indus

Fig 2.2 shows different zones on the basis of the damage record which has been done by the earthquake events of past. Study area lies in the range where minor to moderate damage has been done. It can help us in interpreting the sub surface structure in the regard of not having complex faulting.

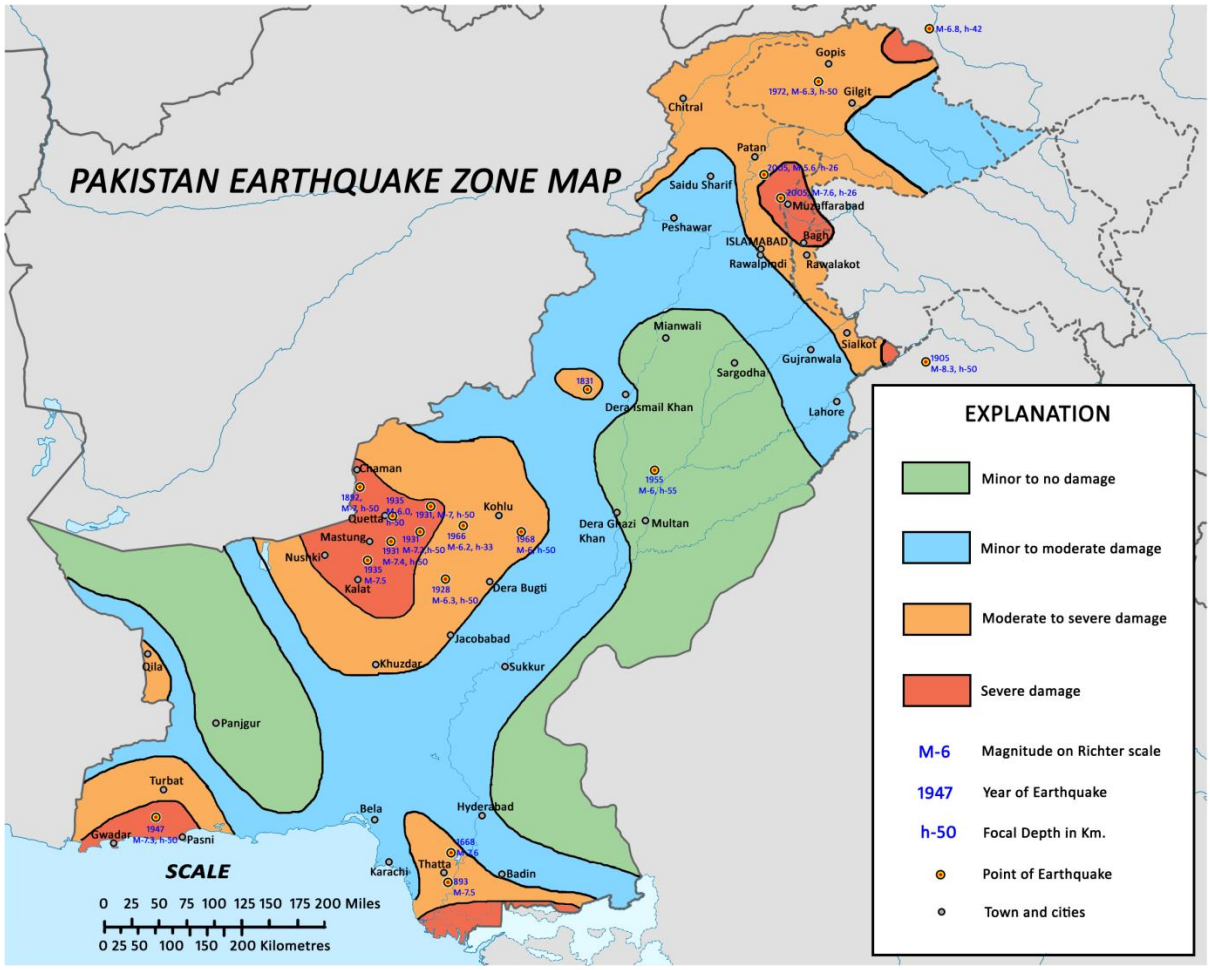

Figure 2.2 Earthquake hazard map of Pakistan showing the different zones on the basis of damage record (www.gsp.gov.pk).

2.4 Stratigraphy of Lower Indus Basin

Stratigraphy of the South Indus Basin ranges from Infracambrian to Recent with non-deposition and erosion at various stratigraphic levels.

Stratigraphic succession of the Punjab and Lower Indus Platform area, changes from east to west with regional unconformities at base Permian and base Tertiary levels.

Middle Jurassic to Eocene strata truncate below base Miocene-Pliocene unconformity eastward in the Punjab Platform while Tertiary sequence has direct contact with the Jurassic sequence in eastern part of the Lower Indus Platform. The thickness of the sediments increases westward. Stratigraphy known in Sulaiman and Kirthar foldbelt ranges from Permian to Recent age. Intra-formational sedimentation breaks are pronounced in Permian and Jurassic, while Cretaceous Tertiary unconformity is regional. Erosion in some parts of

the Foldbelt is so deep that it has exposed the Jurassic rocks at or near the surface (Ahmed et al, 2011).

The stratigraphic succession changes from east to west. Precambrian basement is exposed in the south-eastern corner the basin. The thickness of the sediments increases westward. In the eastern part of the basin Tertiary sequence has direct contact with Jurassic sequence. The stratigraphic chart of the study area is given in Figure 2.3.

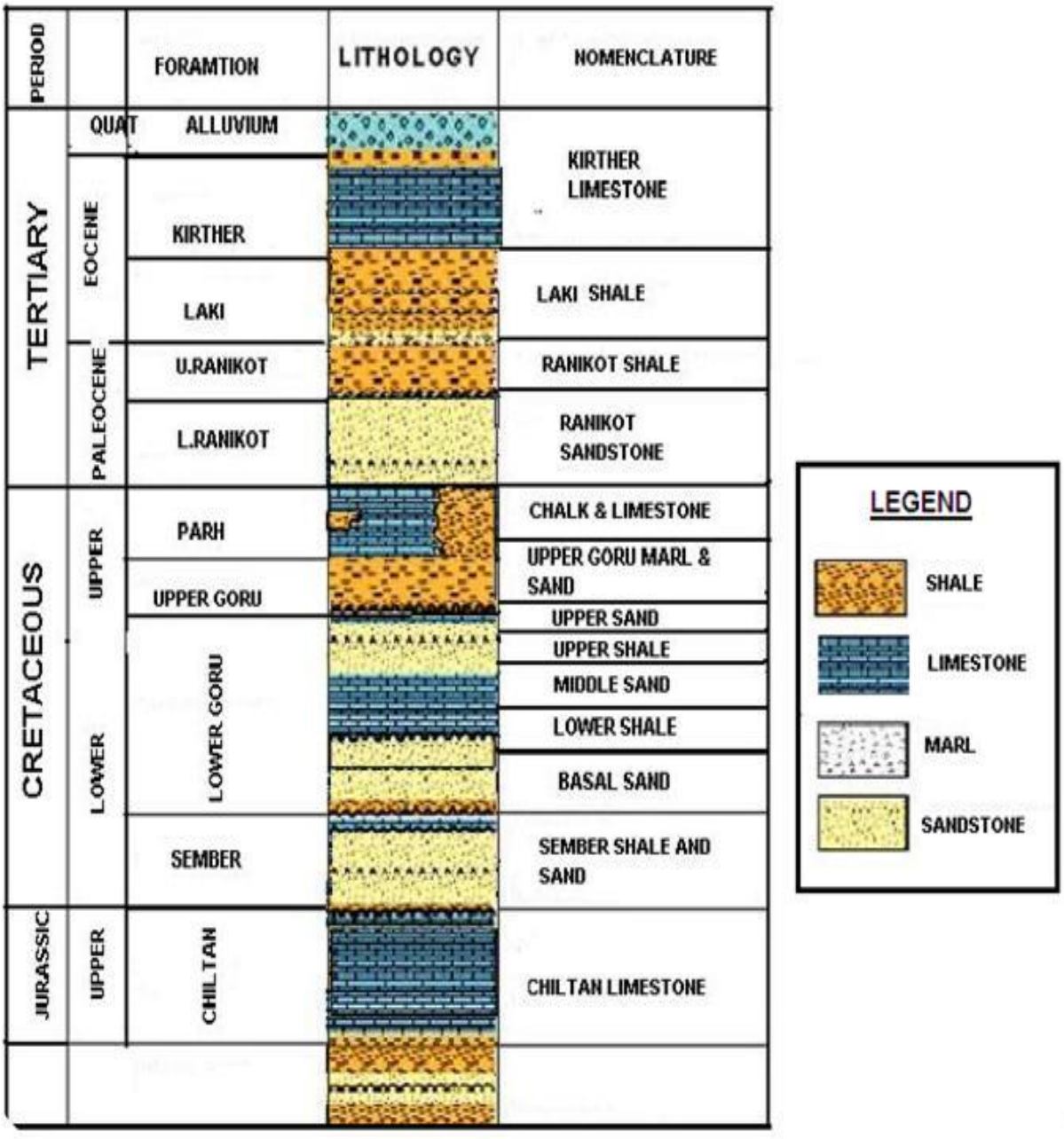

Figure 2.3 Stratigraphic successions in Lower Indus basin.

2.4.1 Chiltan Limestone

The Jurassic System is represented by limestone, shale and sandstone with subordinate dolomitic and ferruginous beds. It consists of massive thick bedded limestone. The limestone, where developed, overlies the Shirinab formation conformably. Its upper contact with Mazar Drik formation is transitional. The Chiltan limestone correlates with the Samana Suk Formation of the Upper Indus Basin (Shah et.al, 1977).

2.4.2 Sembar Formation

This is the lowermost unit of the Cretaceous sequence in the Kirthar-Sulaiman region, consisting of black shale interbedded with siltstone and nodular, argillaceous limestone. The shale and siltstone are commonly glauconitic. The Formation is 133 m thick in type area (Sembar Pass) and 262 m in the Mughal Kot section. It has a gradational contact with the overlying Gom Formation though at places an unconformity.

The fossils most commonly found in the Sembar Formation are belemnites *Hibolithes pistilliformis, H. subfusiformis*, and *Duvalia sp*. It is mainly Neocomian in age. According to Fatmi (1977) it may extend to the Late Jurassic.

2.4.3 Goru Formation

The Goru formation consists of interbedded sandstone, shale and siltstone. The limestone is grained, thin bedded, light to medium grey in color (Shah ,2009).

On the basis of lithology Goru Formation is divided in two parts:

a) **Lower Goru**

   The lower Goru is main reservoir rock within the area. The lower Goru horizon as a general 5 divisions based on predominant lithologies. The Basal sand unit, lower shale, middle sand unit (good reservoir potential), upper shale and upper sand.

b) **Upper Goru**

   The upper Goru sequence of middle to late cretaceous overlies the lower Goru formation which consists of mainly marl and calcareous claystone occasionally with interbeds of silt and limestone. The Goru Formation is widely distributed in the Kirthar and Sulaiman Province. It grades into overlying Pab formation which has not been reported in Fateh_01 and Icchri_01 wells of the study area.

The lower contact with the Sembar formation is conformable and is very locally reported unconformable by Williams (1959).The upper contact is transitional with the Goru

formation may be correlated with the Lumshiwal Formation of the Kohat-Potwar Province. The formation contains foraminifers and bivalves and age given is Early Cretaceous (Shah, 2009).

2.4.4 Ranikot

Blanford (1876) was the first to give the name Ranikot group. Vredenberg (1909a) subdivided the Ranikot group into Lower Ranikot (sandstone) an Upper Ranikot (shale).
One division of Ranikot group suggests that it comprise of three formations which are Khadro formation, consists of olive, yellowish brown sandstone and shale with interbeds of limestone. Keeping ascending stratigraphy order, Above Khadro formation is Bara formation (Lower Ranikot sandstone) consists of variegated sandstone and shale and the upper one is the Lakhra formation (Upper Ranikot limestone) consists of grey limestone, grey to brown sandstone and shale. Various authors have given it different divisions. Below are explained the three formations as part of the Ranikot group with details (Shah ,2009).

2.4.5 Laki

It lies over the Ranikot Group unconformably and is exposed mainly in the southern Kirthar Range and in the southern Sulaiman Range. The type locality is near Meting and near Mari Nai in the northern Lakhi Range. The formation comprises cream coloured to grey limestone, with subordinate marl calcareous shale, sandstone and lateritic clay. It contains a rich fossil assemblage of foraminifera, gastropods, bivalves, echinoid and algae. The lower part of the formation has been divided into the Sonari member and Meting limestone and shale member.

2.4.6 Kirthar

Top most lithology lying below the alluvium is the Kirthar which is primarily composed of limestone of Eocene. Kirthar formation as predominantly limestone, shale and marl.

2.5 Petroleum Plays

A play is "a group of geologically related prospects having similar conditions of source, reservoir and trap. (Kadri, 1995)

2.5.1 Play Elements

Within a basin the presence of play elements plays important role in hydrocarbon accumulation. The seven play elements are:

- Source
- Maturation
- Migration
- Seal or Cap
- Reservoir
- Trap
- Timing

2.5.2 Petroleum Prospects of the Area

i. Source Rocks

Shale sequences in the Sember formation and Lower Goru formation are known to be well developed source rocks of the area. Of all the possible source rocks in the Indus Basin, however, the Sembar is the most likely source for the largest portion of the produced oil and gas in the Indus foreland.

The Sembar was deposited over most of the Greater Indus Basin in marine environments and ranges in thickness from 0 to more than 260 m (Shah et al., 1977).

ii. Reservoir Rocks

The basal sands of lower guru formations are the main objective in the area these sands are hydrocarbon producer. Massive sands are another interesting producing reservoir from its various sand sheet of multiple thickness possibility of reservoir in lower guru sand overlain on basal sands could not be ruled out; however they have not yet proved to be such up till now.

These principle reservoirs are deltaic and shallow-marine sandstones in lower part of the Goru in this area. Reservoir qualities generally diminishes west ward while reservoir thickness increases.

iii. Seal or Cap Rocks

Fine-grained rocks such as shale or evaporites have the tendency as effective cap rocks. Additional seals that may be effective include: faults, and up-dip facies changes. The known seals in the study area are composed of inter bedded shale which is over lained the reservoirs. The thick sequence of shale and marl member of Upper Goru formation acts as a seal for underlying Lower Goru formation.

iv. Traps

All production in the study area is from structural traps. The tilted fault traps in the Lower Indus Basin are a product of extension related to rifting and the formation of horst and graben structures. The temporal relationships among trap formation and hydrocarbon generation, expulsion, migration, and entrapment are variable- throughout the Indus Basin. These provide the significant trapping system along tilted fault blocks and negative flower structures.

Chapter 3

3. Seismic Data Interpretation

3.1 Introduction

Conventional seismic interpretation implies picking and tracking laterally consistent seismic reflectors for the purpose of mapping geologic structures, stratigraphy and reservoir architecture. The ultimate goal is to delineate hydrocarbon accumulation and their extent and also calculate their volumes. Conventional seismic interpretation is an art that requires skill and experience in geophysics and geology.

Seismic interpretation can also be defined as "Transformation of seismic data into structural picture". Similarly, Coffeen (1986) writes "Seismic interpretation is the process of determining information about subsurface by using different types of seismic data". It can also act as a development of already established field.

Seismic interpretation is the process of determining the subsurface information of the earth from seismic data. It may determine general information about an area, locate prospects for drilling exploratory wells, or guide development of an already-discovered field (Coffeen, 1986).

To meet the challenges of exploring ever increasingly complex targets, there have been tremendous advancements in data acquisition equipment, computer hardware and seismic processing algorithms in the last three decades (Khan, 1995). The seismic method has thus evolved into a computationally complex science. The computer based working (Processing & Interpretation) is more accurate, precise, efficient and satisfactory which provides more time for further analysis of data. This whole work is carried out using a combination of computer software products, which include all K-tron Software, SMT Kingdom suit and Golden software Surfer. To make my interpretation praiseworthy SnagIt editor has been used.

3.2 Types of Seismic Interpretation

Seismic interpretation is the transformation of seismic reflection data into a structural picture by the application of correlation of seismic reflectors with geological boundaries and their time-depth conversion.

Main approaches for the interpretation of the seismic section are:

- Structural Analysis

To identify structural features

- Stratigraphic Analysis

To identify stratigraphic boundaries

3.2.1 Structural Analysis

This type of analysis is very satisfactory in case of Pakistan, as most of the hydrocarbon is being extracted from the structural traps. It is study of reflector geometry on the basis of reflection time. The main application of the structural analysis of seismic section is in the search for structural traps containing hydrocarbon. Most structural interpretation use two way reflection time rather depth and time structural maps are constructed to display the geometry of selected reflection events. Discontinue reflections clearly indicate fault sand undulating reflection several folded beds (Telford et al., 1990).

3.2.2 Stratigraphic Analysis

Stratigraphic analysis greatly enhances the chances of successfully locating hydrocarbon traps in sedimentary basin environment. Seismic stratigraphy is used to find out the depositional processes and environmental settings, because genetically related sedimentary sequence normally consists of concordant strata that show discordance with sequence above and below it. We want to distinguish the features that are not marked by the sharp boundaries. Geologists ordinarily group the sequence of sedimentary rocks into units called "Formations". These formations can be described in term of age, thickness, and lithology of the constituent layer. To distinguish different formations on the basis of seismic reflections is an important question in interpreting seismic data that may be structural, stratigraphic or lithological (Robinson & Coruh, 1988).

3.3 Work Procedure

The provided Navigation Data was in DAT file, which was transformed to DBO format in UTM Zone 42 by using K-tron Visual OIL (Output Input Language). All digital maps along with geo-referenced imagery were produced by using K-tron Precision Matrix. The interpretation was done on K-tron X-Works which provides an interactive interface for marking horizons and faults, exporting horizon's time, velocity and depth data for contouring

and for further analysis such as crustal shortening, 2D seismic modeling and well columns correlation as shown in Fig 3.1.

The seismic velocities are processed (Converted, Interpolated and Smoothed) by using X-works software, which is then used in different applications like time to depth conversion, Modeling and Rock Physics is shown in Fig 3.1.

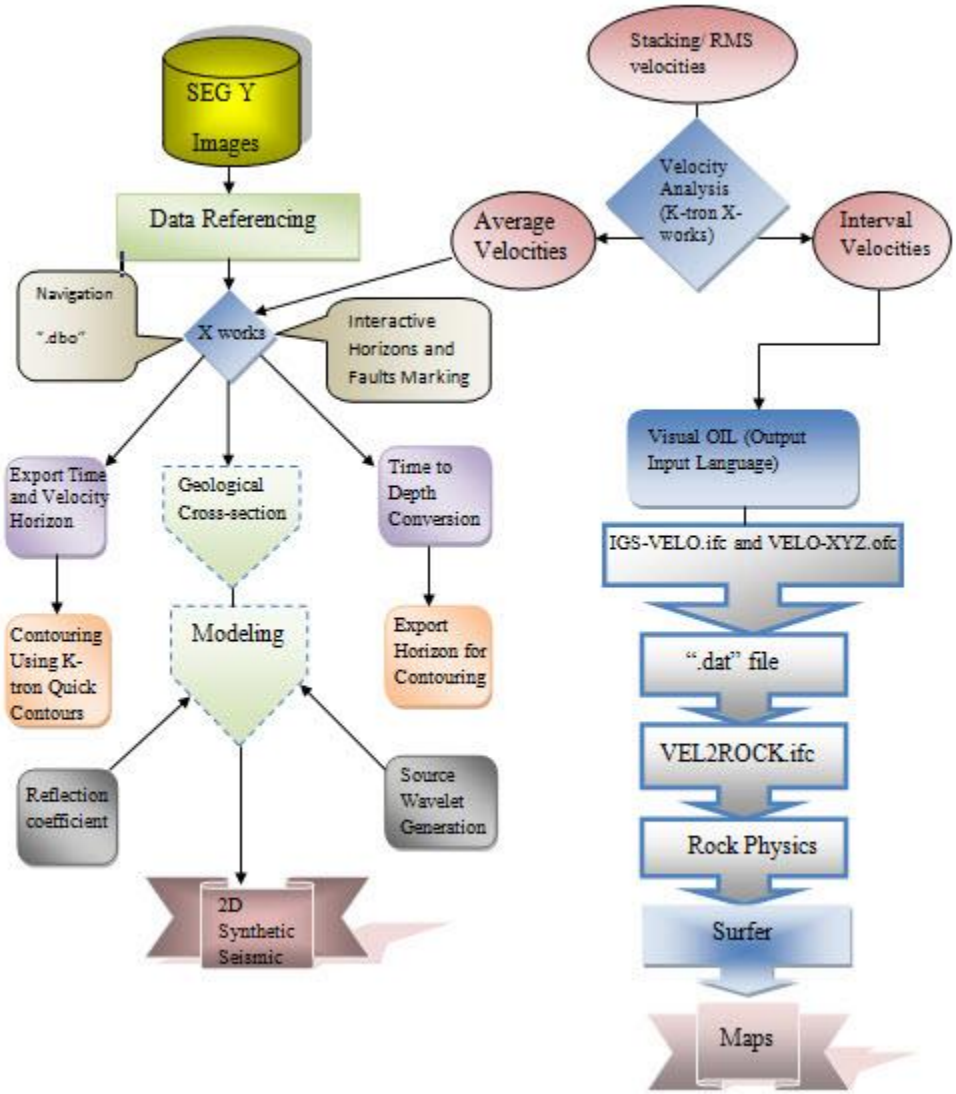

Figure 3.1 Work flow of Seismic Interpretation.

3.4 Seismic Horizons Identification

The main task of interpretation is to identify various reflectors or horizons as interface between geological formations. This requires good structural and stratigraphic knowledge of the area (Mcquillin et al., 1984). Thus during interpretation the horizons and faults are marked on the seismic section.

As seismic data in SEG-Y digital format for the four seismic lines is loaded into X-Works as The software provides interactive interpretation and the interpreted information is stored in a digital format. Another advantage of the application is that the times for the prospective horizon can be sent to gridding and contouring software for generating time, horizon velocity and depth contour maps. The software can also load the velocity functions and convert the time section into depth section. Since velocity varies vertically as well as laterally it does not apply a regional velocity function, instead it generates a processed velocity model which is used in time to depth conversion. Each reflector is marked with different colors so that they can be easily distinguished and faults are marked with black color.

The basic way to interpret multiple seismic lines is, first interpret that seismic line on which there is well, so according to well tops that seismic line is interpreted and further considered it as a reference line for the interpretation of other lines. If it is a dip line then a strike line will tie it at a certain source point, note that source point from the base map and multiplying with 2 to convert source point into CDP numbers and the time along y-axis at which the reflectors are marked on that reference line, so marked all the reflectors at the tie points and extend them on the bases of character and continuity. Now this interpreted strike line will tie all the dip lines so interpret them at the tie points and same were the procedure for the interpretation of other lines.

Fateh-01 well lies on the seismic line 20017-BTM-02 and the well tops were matched with the five seismic reflectors (Kirthar, Laki, Lower Ranikot, Upper Goru and Lower Goru) in depth domain to identify the geologic formations. Total depth of Fateh-01 is 3000.5 but well tops provided only to the depth of 2083m.

3.4.1 Well Information

The well is the basic component on which seismic interpretation is based. It is used to confirm the depth of the subsurface formation. Details of well used for the interpretation are given in the Table 2.

Table 2 Detailed information of the well used for interpretation.

Well Name	FATEH_01
Longitude	69.024497°
Latitude	26.366536°
K.B. Elevation	35.23 meters
Total Depth	3000.5 meters
Type	EX
Status	ABD
Operator	O.G.D.C.L
Concession	BITRISIM (2568-4)

3.4.2 Formation Tops

Formation tops data was issued by DGPC in the txt format. Formation tops detail is given below in the Table 3. Among these formations the interest zone lies in the reservoir rocks which is discussed with detail in Chapter 2.

Table 3 Formation tops of Fateh_01.

Formations	Depth (m)
ALLUVIUM	0
KIRTHAR	654
LAKI	885
SUI MAIN LIMESTONE	1085
UPPER RANIKOT	1196
LOWER RANIKOT	1365
UPPER GORU	1810
LOWER GORU	2083

3.5 Interpreted Seismic Sections

The time section provides the position and configuration of reflectors in the time domain. Six reflectors along with faults have been marked by different colors as shown in Fig 3.2. The Horst structure present on the seismic section (20017-BTM-02) may be a suitable place for the accumulation of hydrocarbons.

Reflector	Color
Kirthar	Brown
Laki	Red
Lower Ranikot	Blue
Upper Goru	Green
Lower Goru	Yellow
Chiltan	Pink
Faults	Black

The aim is to mark the potential source, reservoir and seal rock formations. The interpreted seismic lines 20017-BTM-02, 20017-BTM-09, 20027-BTM-01 and 986-BTM-09 are given in Figures 3.2 to 3.5 respectively.

The seismic sections are in time domain, but the real subsurface structures are in depth domain so we have to convert time sections into depth sections using average velocities. X-Works reads velocity data in IGS Velocity format for time to depth conversion.

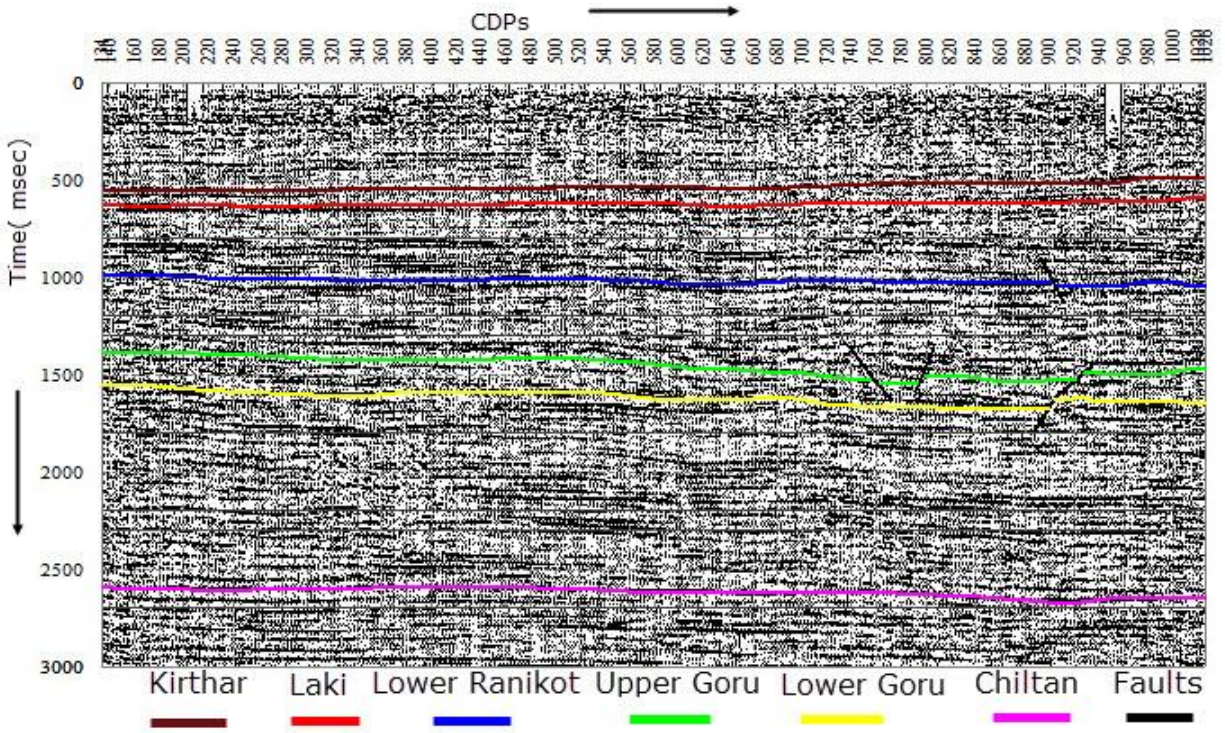

Figure 3.2 Seismic section with marked geological cross section of 20017-BTM-02.

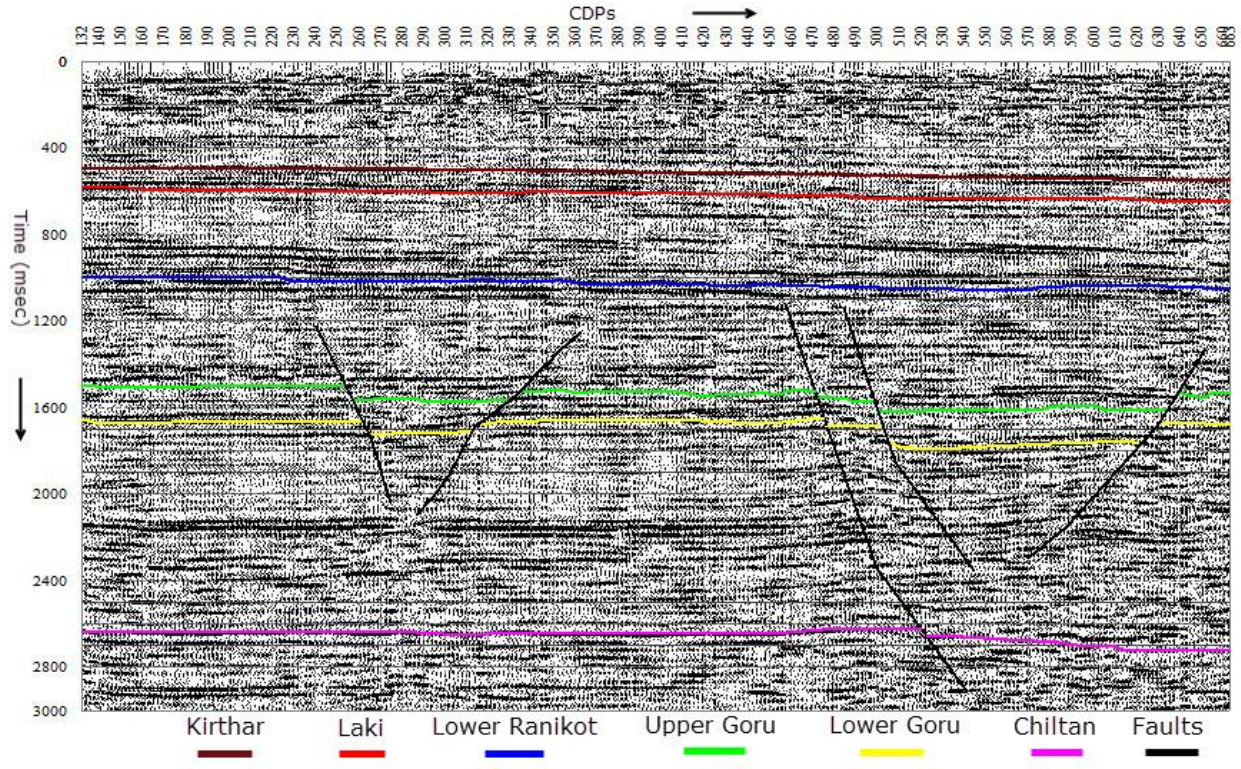

Figure 3.3 Seismic section with marked geological cross section of 20017-BTM-09.

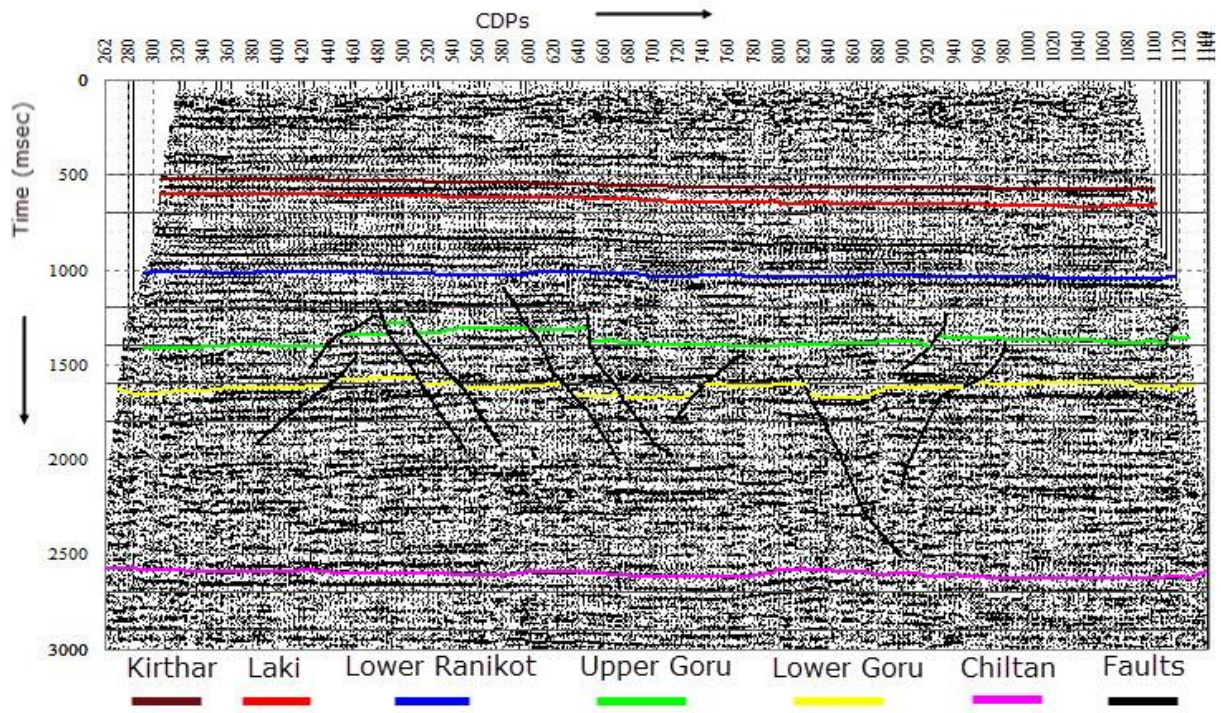

Figure 3.4 Seismic section with marked geological cross section of 20027-BTM-01.

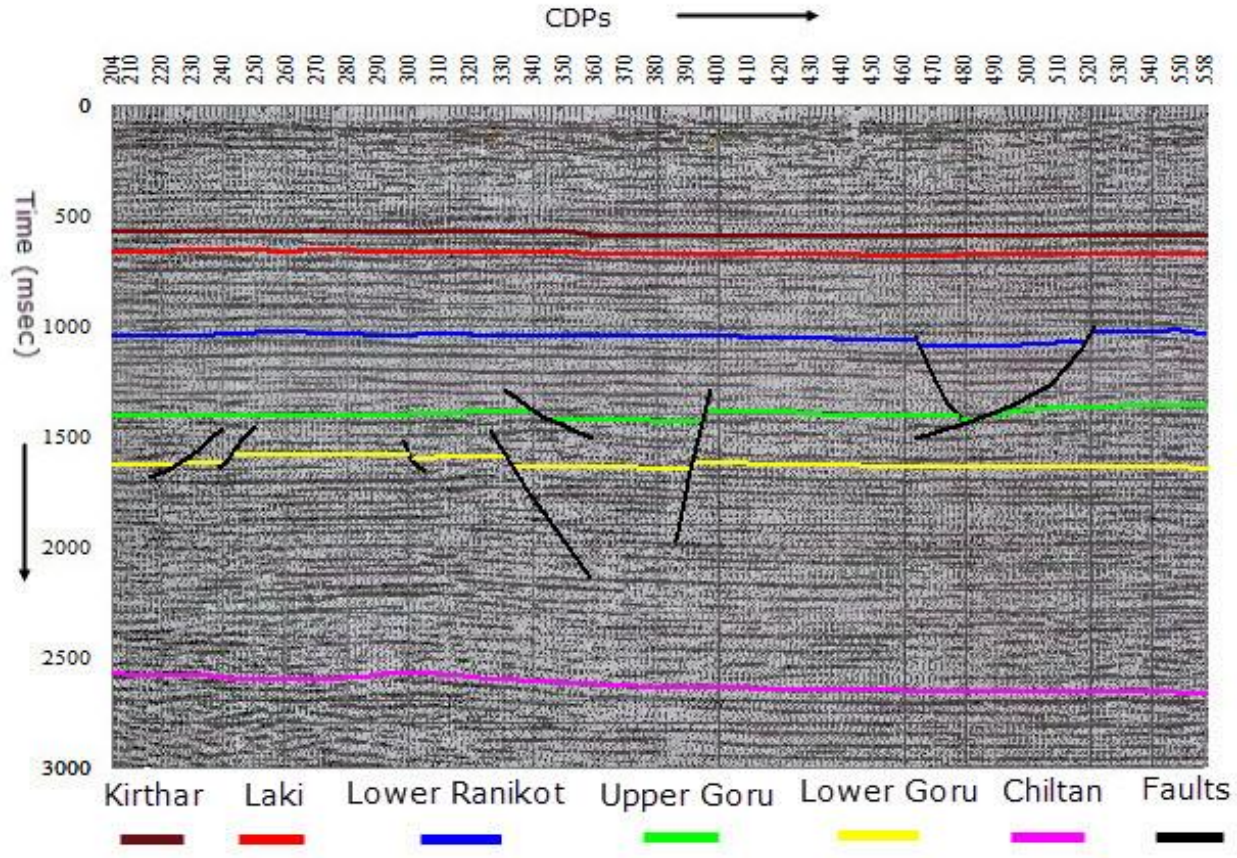

Figure 3.5 Seismic section with marked geological cross section of 986-BTM-09.

3.6 Seismic Velocities Analysis

The seismic velocities determined from velocity analysis are RMS velocity (Vrms). These must be converted into interval (Vint) and finally average (Vavg) velocities for time to depth conversion by using Dix (1955) equation as given;

$$V_{int,n}^2 = \frac{V_{rms,n}^2 T_n - V_{rms,n-1} T_{n-1}}{T_n - T_{n-1}} \qquad \text{(Dix, 1955)}$$

$$V_{avg,n} = \frac{V_{int,n}(T_n - T_{n-1}) + V_{avg,n-1} T_{n-1}}{T_n}$$

X-Works uses a velocity processing engine which automatically converts the input Vrms into Vint and finally Vavg for time to depth conversion. When the velocity data is loaded the velocity functions for all three types are displayed at their corresponding CDP locations i.e. Vrms (Sky Blue) with red nods, Vint (Dark Green) and Vavg (Blue) as shown in Fig 3.10. Later on these velocity functions are interpolated (Time Slice and Horizon Slice) and smoothed for velocity model building. The raw velocities of seismic lines 20017-BTM-02, 20017-BTM-09, 20027-BTM-01 and 986-BTM-09 are shown in Figures 3.6 to 3.9 respectively. The velocity functions are processed and interpolated using X-works, an Integrated Geo Systems (Khan, 2000) application.

RMS velocity has no physical relevance as it can't be used in time to depth conversion. The velocities derived from seismic data are stacking velocities. These are commonly referred to as NMO and RMS velocities. Both of these differ on the basis of spread length and in areas with large lateral variations in velocity. As interval velocity is the average velocity of an interval or layer while average velocity is the interval velocity of an interval that begins at the surface.

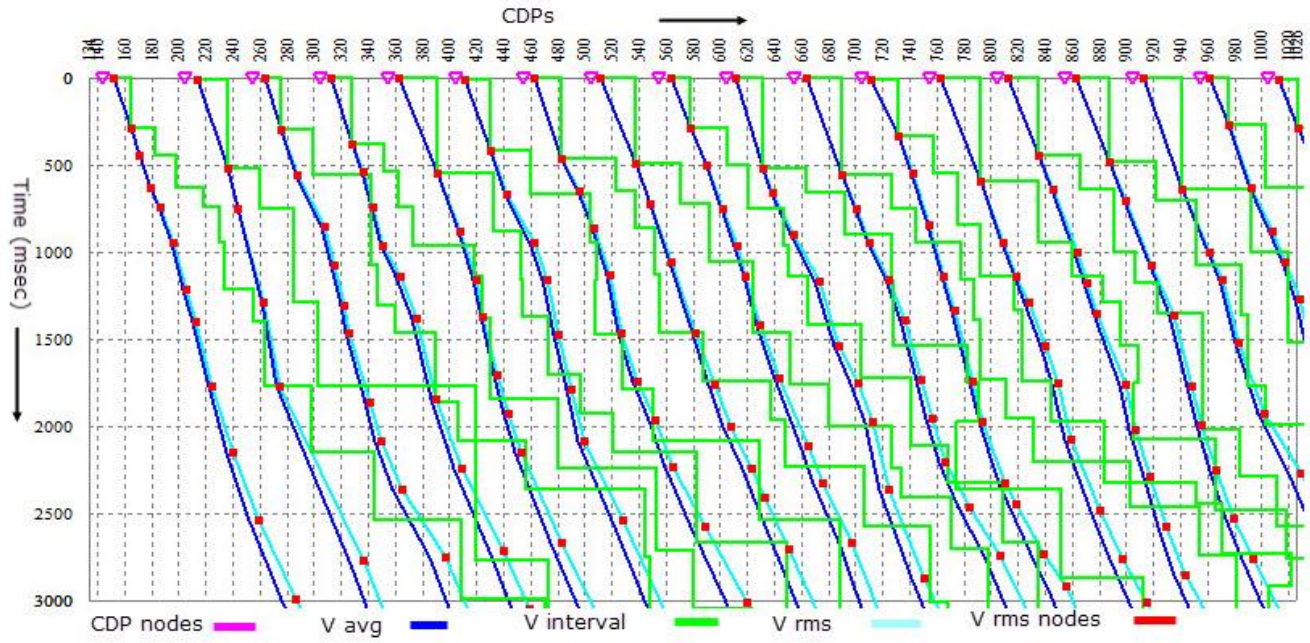

Figure 3.6 Seismic velocities displayed at different CDPs of seismic line 2007-BTM-02 generated using X-works.

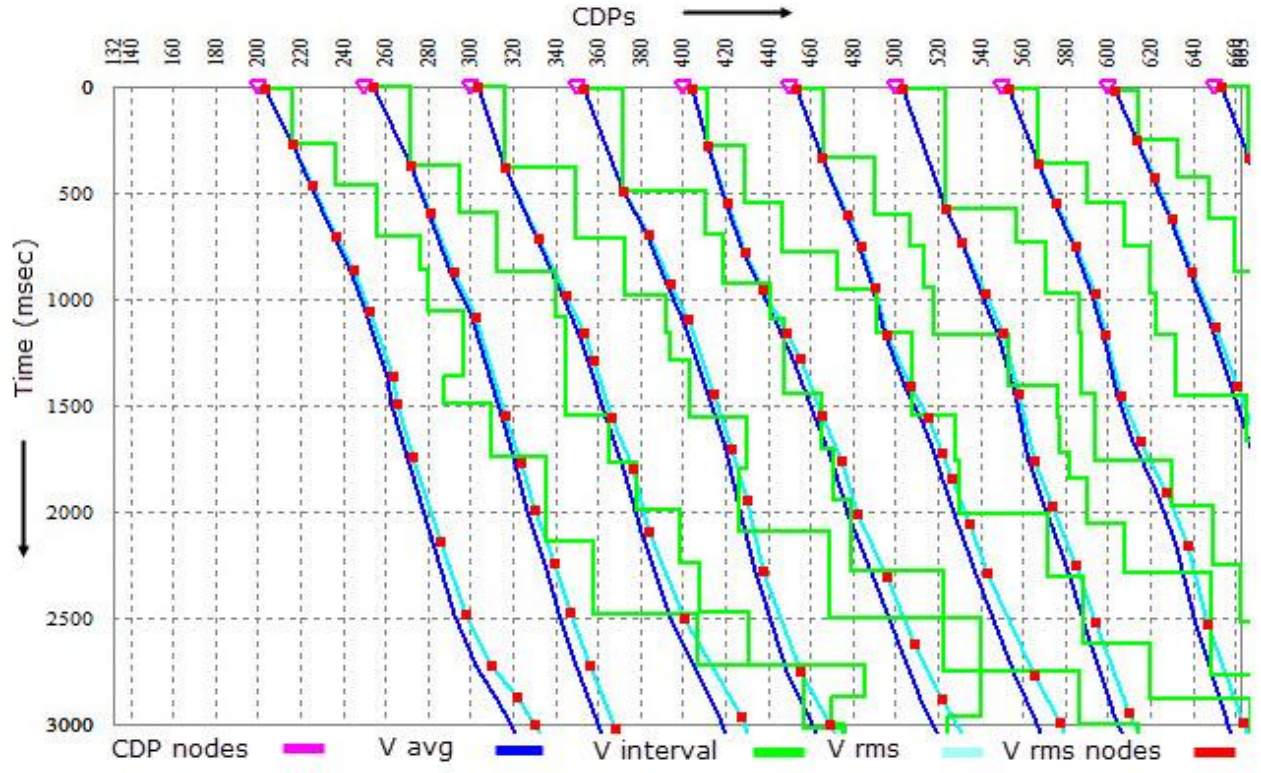

Figure 3.7 Seismic velocities displayed at different CDPs of seismic line 20017-BTM-09.

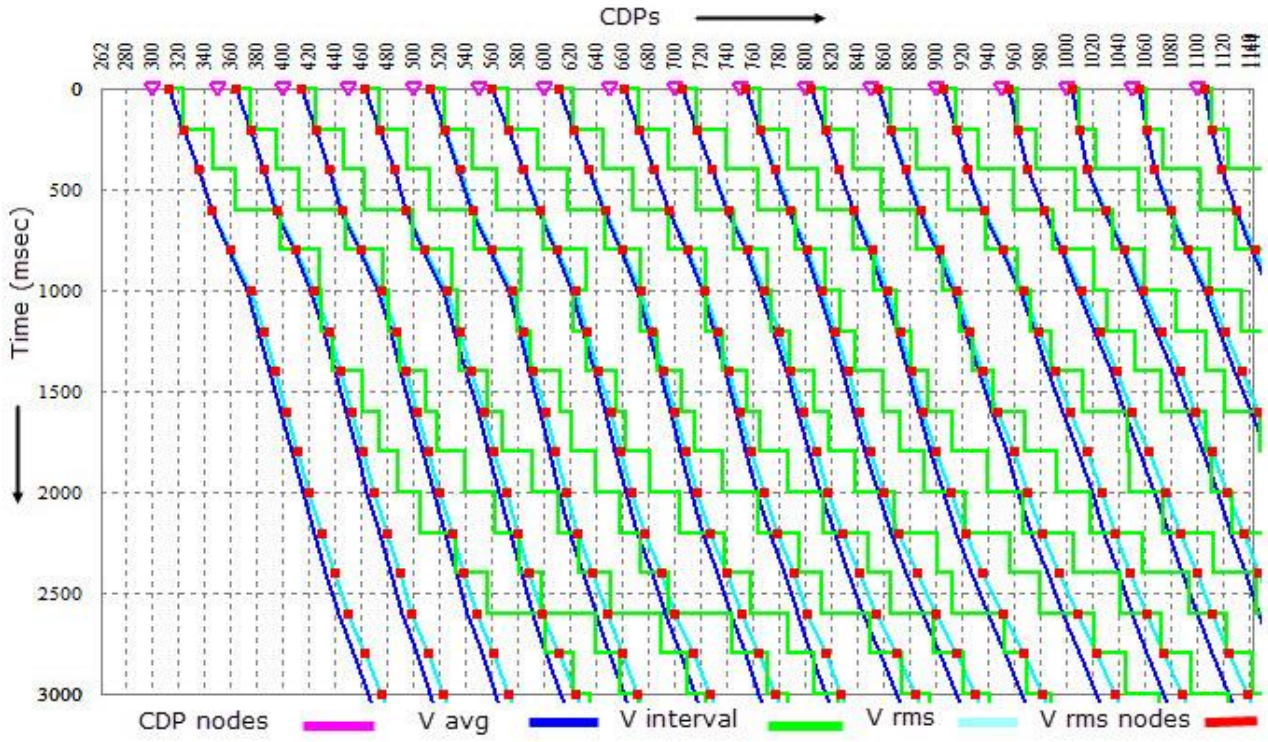

Figure 3.8 Seismic velocities displayed at different CDPs of seismic line 20027-BTM-01.

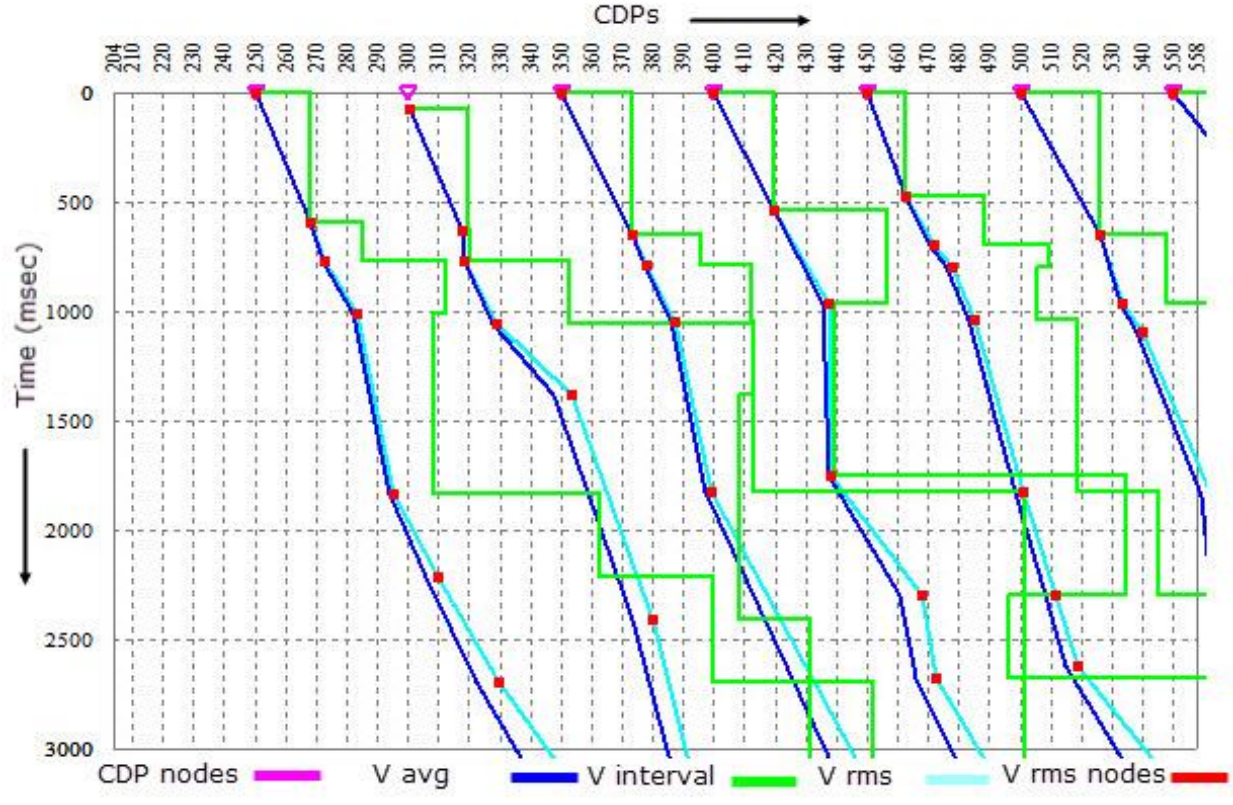

Figure 3.9 Seismic velocities displayed at different CDPs of seismic line 986-BTM-09.

3.6.1 Calibration and Smoothing of Seismic Interpolated Velocities

The seismic velocities of seismic lines 20017-BTM-09, 20027-BTM-01 and 986-BTM-09 were highly fluctuated which were not suitable for time to depth conversion and other applications therefore for their velocities are processed using spatio-temporal interpolation at 200 msec and CDP interval of 10 along with 3 X 3 spatio-temporal smoothing. This provides more precise velocities for time to depth conversion. In addition velocity fluctuations from line to line have been adjusted by calibration of the closest velocity functions of two adjacent lines. The calibrated and smoothened velocities (Vrms) of 20017-BTM-09, 20027-BTM-01 and 986-BTM-09 are shown in Fig 3.10, Fig 3.11 and Fig 3.12 respectively.

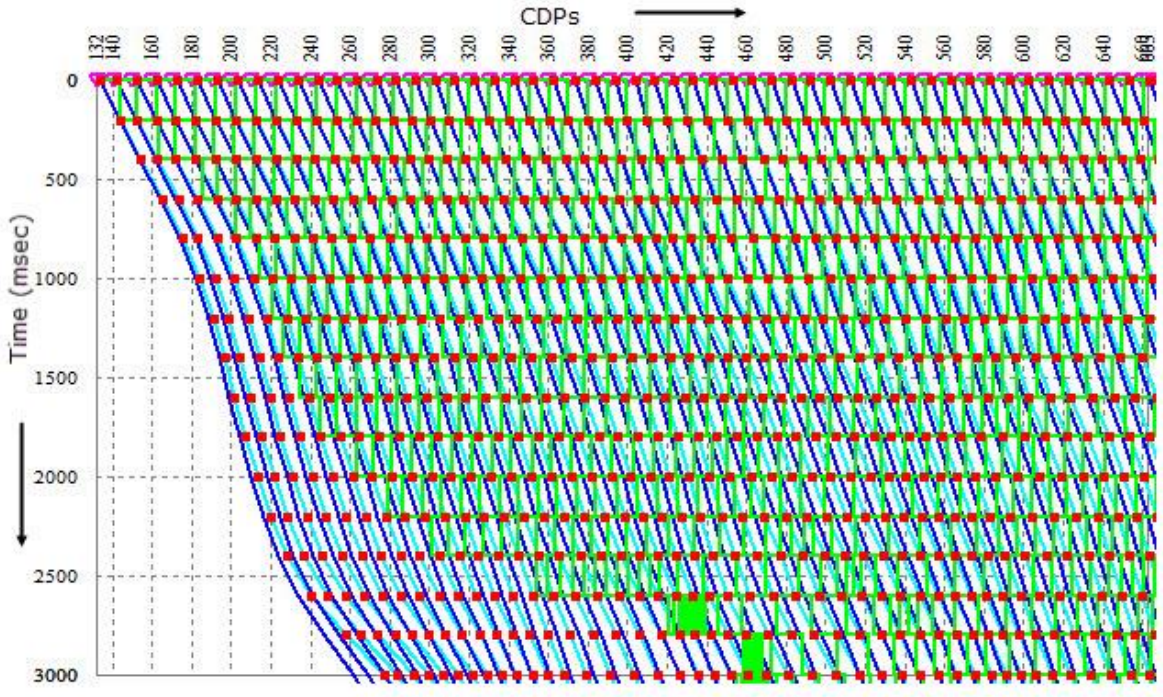

Figure 3.10 Calibrated and smoothened Velocities of seismic line 20017-BTM-09 using spatio-temporal interpolation of every 10th CDP and at 200 msec using Moving average operator of 3x3.

In above figure V average (blue), V interval(green), Vrms(light blue) and Vrms nodes(red) are mentioned which give another view of the variation in the velocities across the cross section of the seismic line.

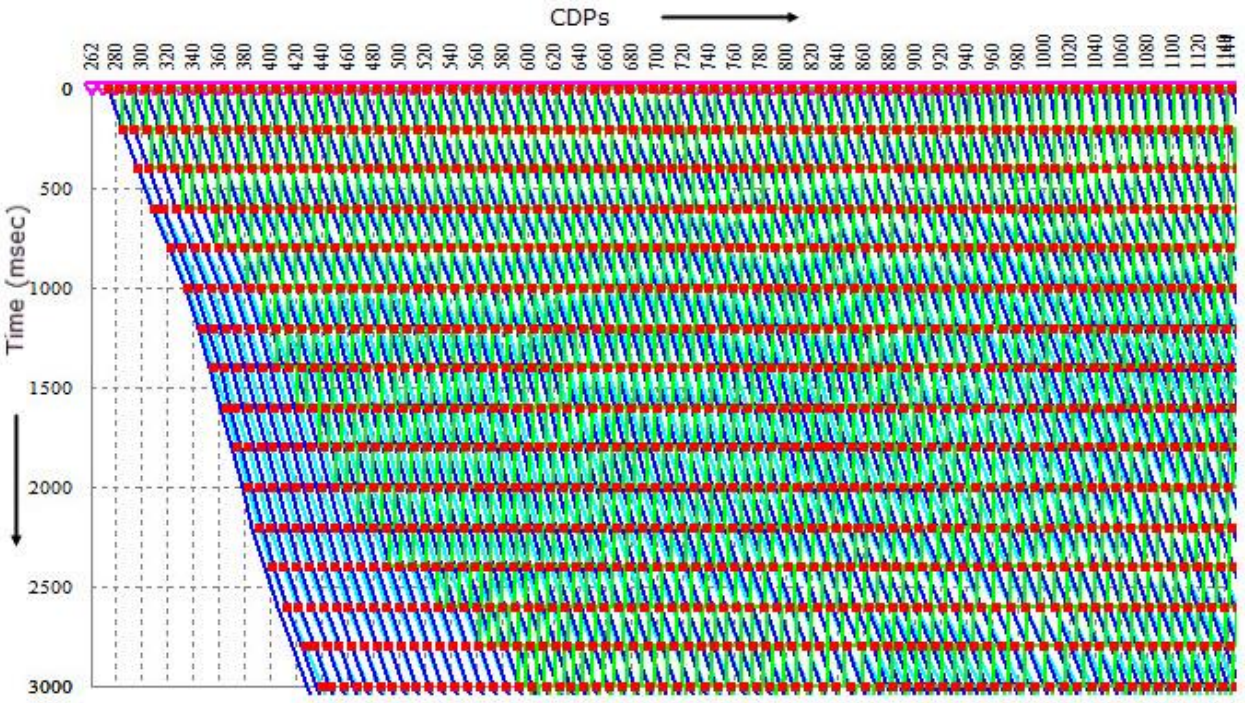

Figure 3.11 Calibrated and smoothened Velocities of seismic line 20027-BTM-01 using spatio-temporal interpolation of every 10th CDP and at 200 msec using Moving average operator of 3x3.

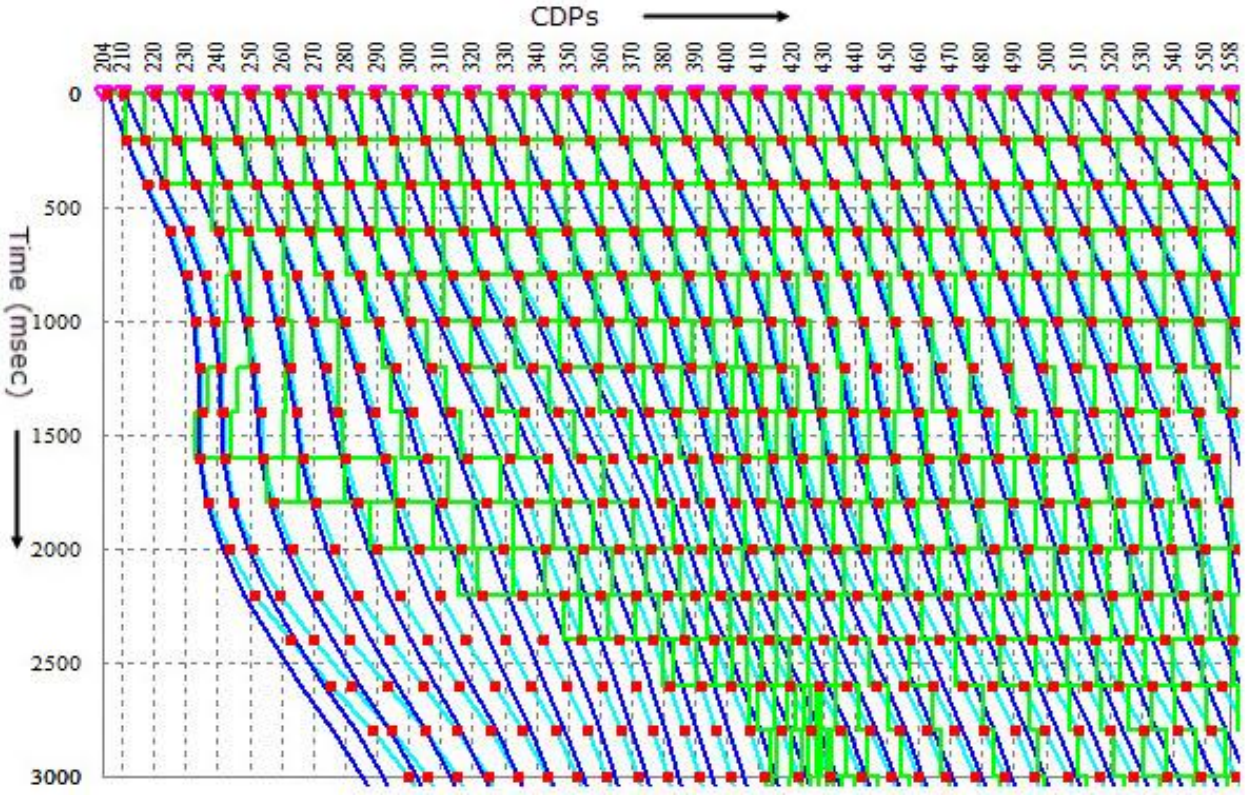

Figure 3.12 Calibrated and smoothened Velocities of seismic line 986-BTM-09 using spatio-temporal interpolation of every 10th CDP and at 200 msec using Moving average operator of 3x3.

3.7 Seismic Depth Sections

Depth sections provide true geologic image of subsurface structures but require a more precise and robust velocity model (Khan and Akhter, 2011). A good seismic image in time domain is not enough for an exploration or field development interpretation. Good well ties and reliable depth conversion are also required.

For time to depth conversion the processed average velocities discussed in the previous section are used. Seismic depth sections of 20017-BTM-02, 20017-BTM-09, 20027-BTM-01 and 986-BTM-09 are shown in Figures 3.13 to 3.16 respectively.

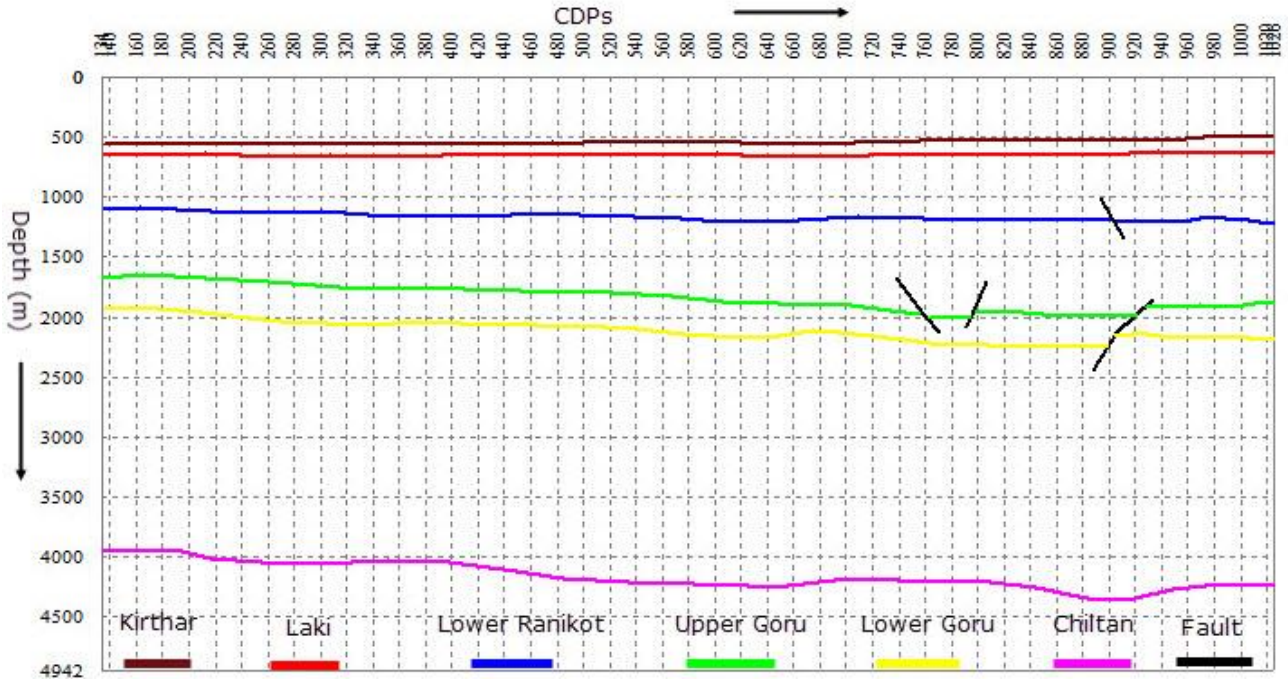

Figure 3.13 Seismic marked depth section of seismic line 20017-BTM-02.

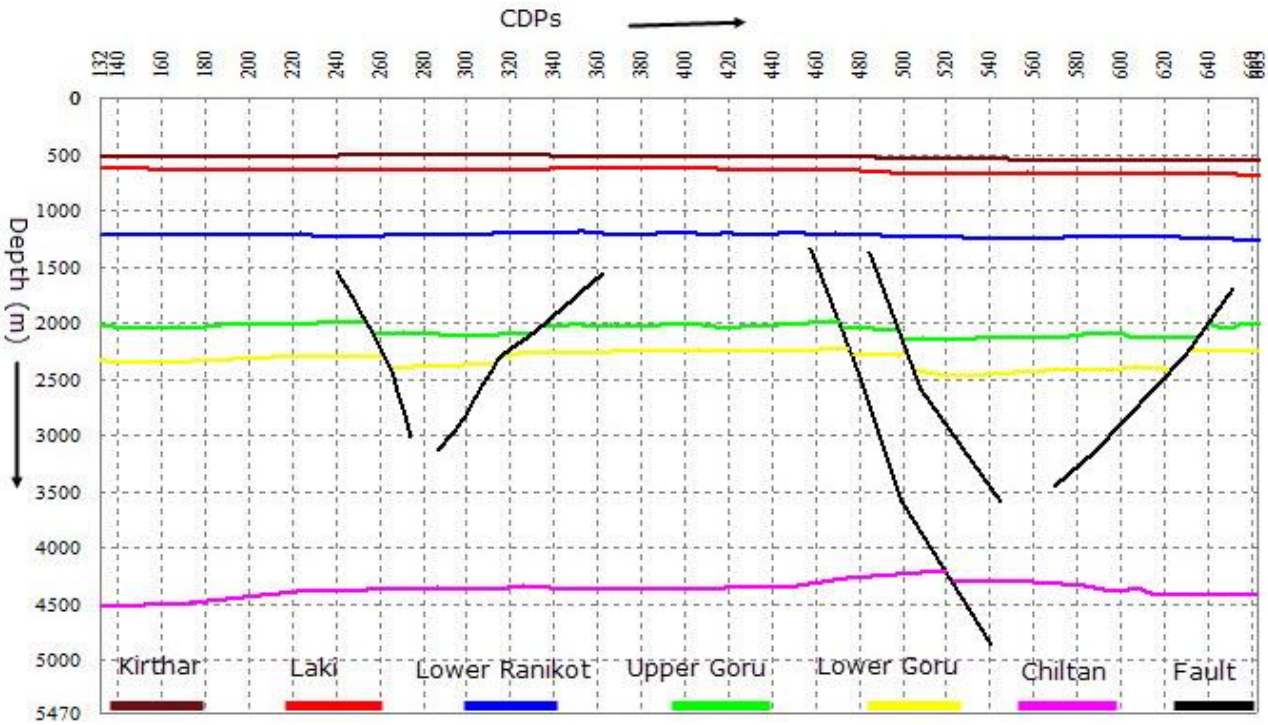

Figure 3.14 Seismic depth section of seismic line 20017-BTM-09.

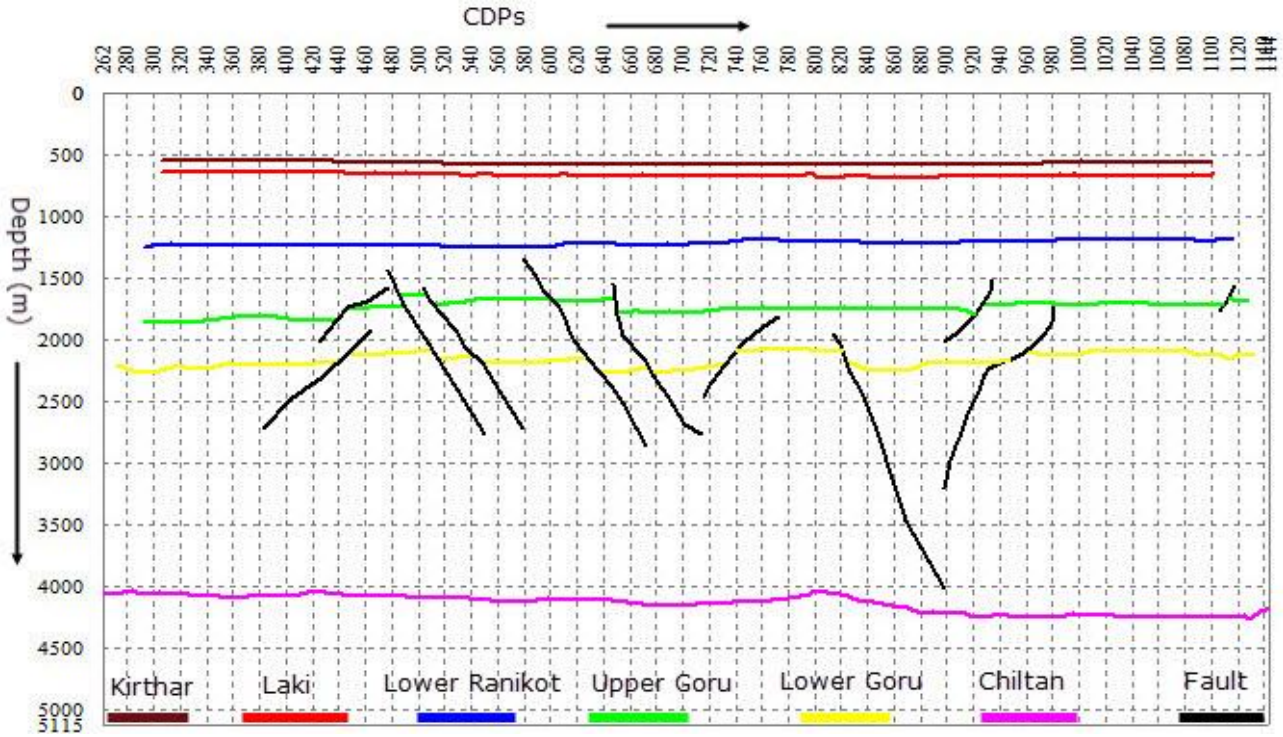

Figure 3.15 Seismic marked depth section of seismic line 20027-BTM-01.

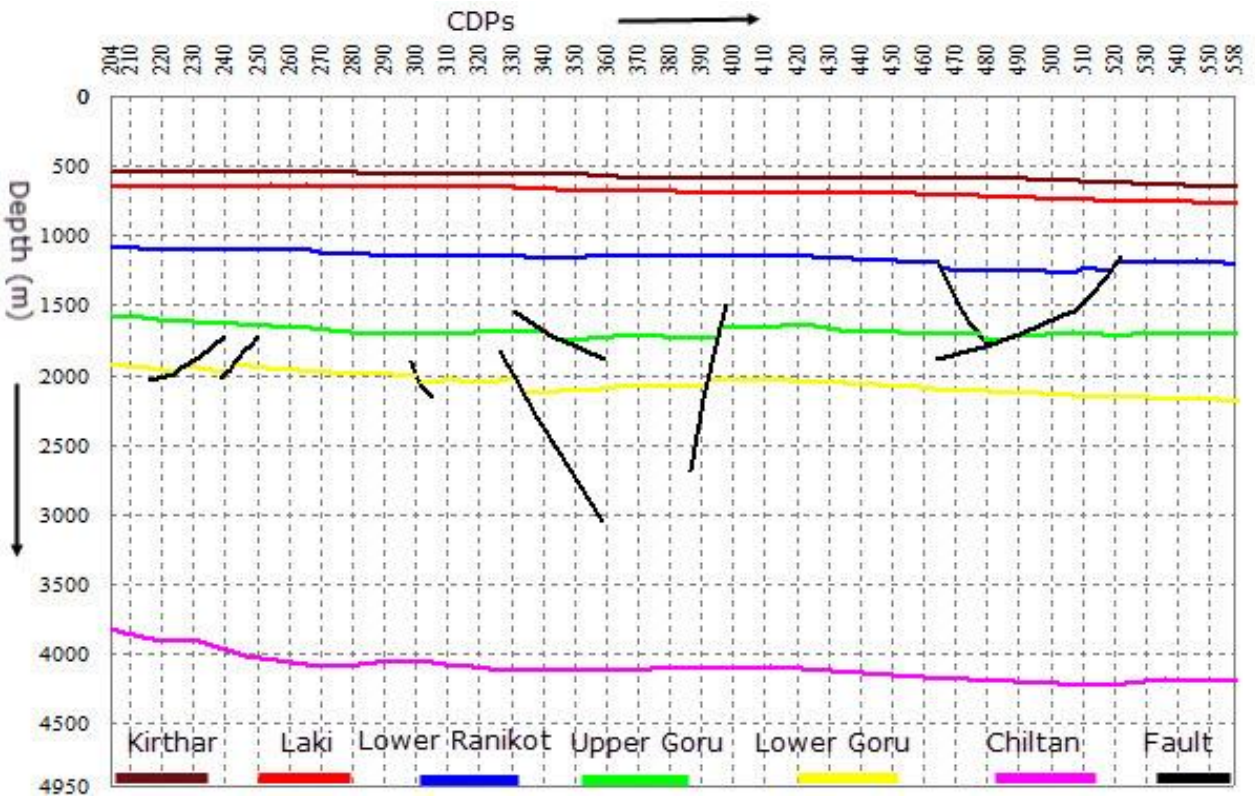

Figure 3.16 Seismic marked depth section of seismic line 986-BTM-09.

3.7.1 Seismic Depth Sections Comparison

The seismic time sections are provided in digital format and their marked horizons are finally converted into depth sections using velocity data. Depth sections can be generated using the raw velocities as well as processed velocities. This section shows the comparison of depth sections generated by both raw and processed velocities as shown in Figs 3.17 and Fig 3.18 respectively. It can be observed that the depth section generated using processed velocities is geologically realistic and reliable as compared to the one generated from raw velocities. K-tron X-works has a powerful velocity processing and depth conversion engine and provides on-the-fly time to depth conversion facility.

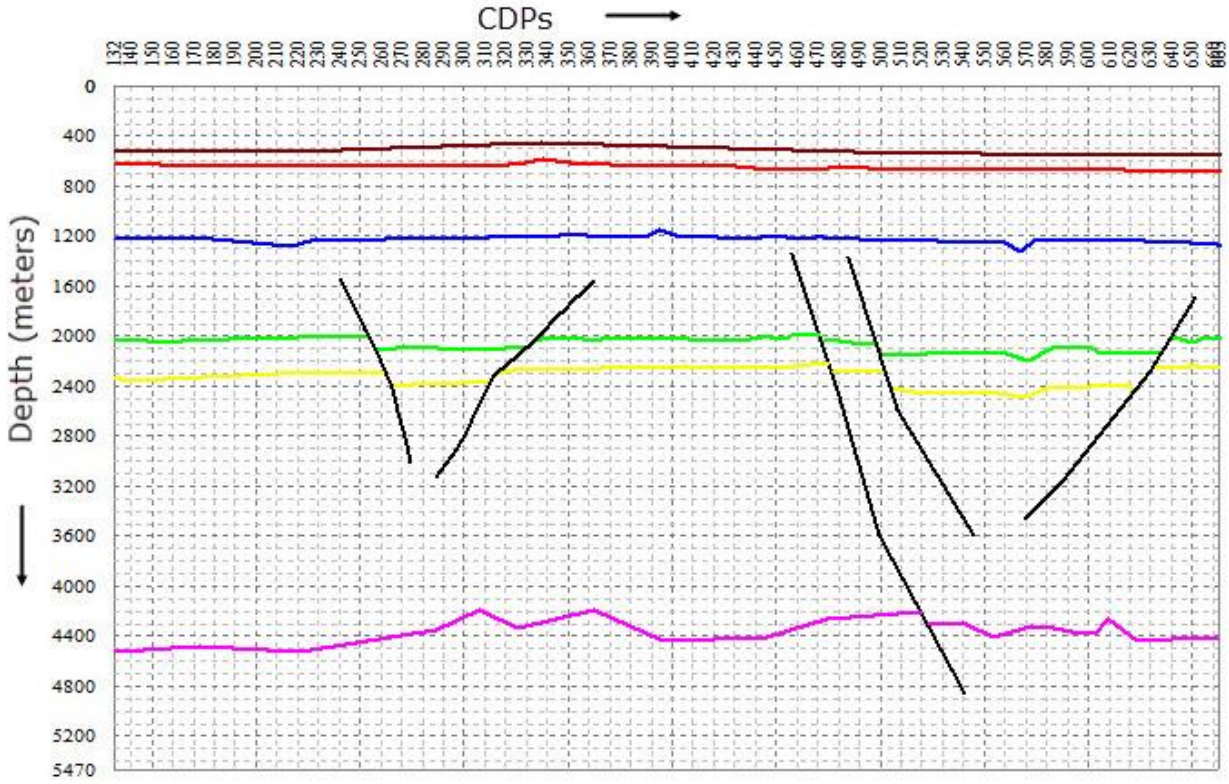

Figure 3.17 Depth section of seismic line 20017-BTM-09 generated using the raw velocities.

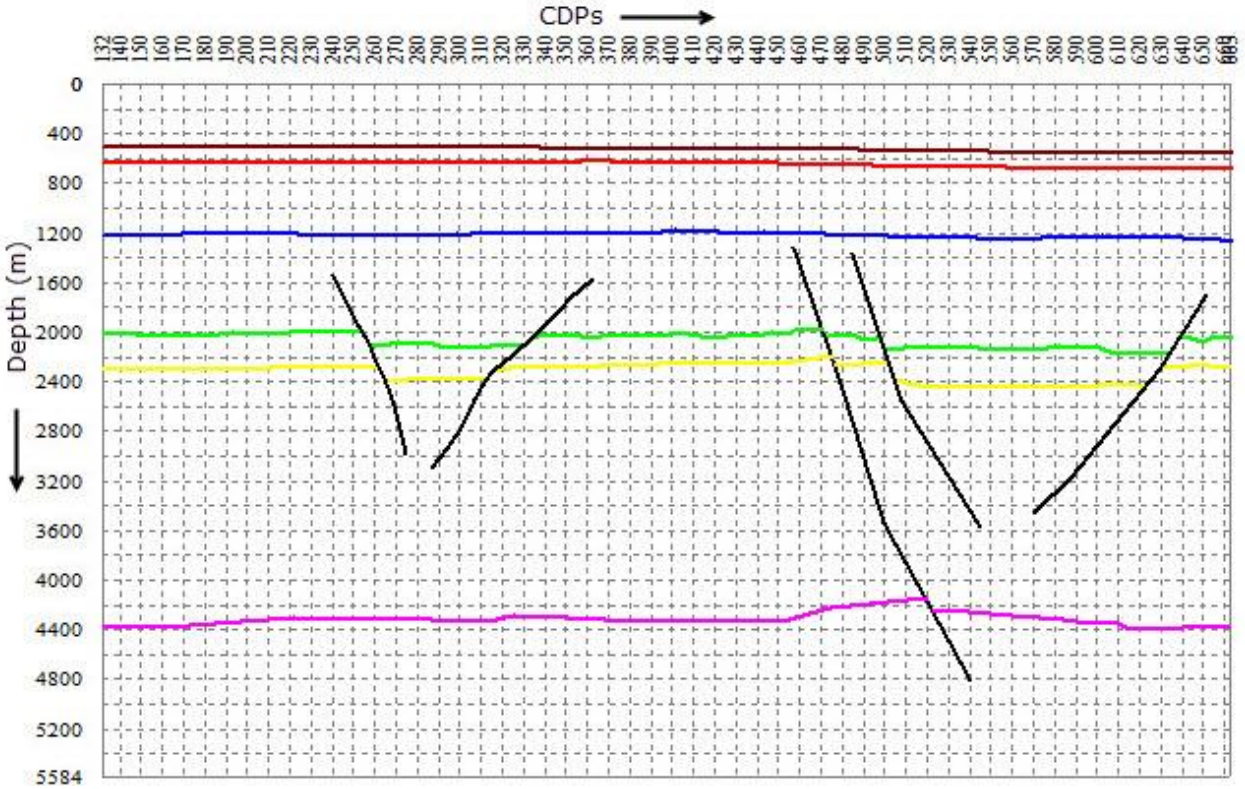

Figure 3.18 Depth section of 20017-BTM-09 generated using the interpolated velocities for CDP interval 10 and temporal interval 100 msec. Smoothing operator coefficient 7x7.

3.8 Contour Maps

Contouring map is an important part of the interpretation of the seismic data. Seismic interpretation leads to the display of the essential information that is extracted during interpretation in the form of time and depth contour maps. The contours are the lines of equal time or depth wandering around the map as dictated by the data (Coffeen, 1986).

To construct a subsurface map from seismic data, first a reference is selected. The datum may be sea level or any other above or below the sea level according to the topography (elevation) and thickness of weathering layer (Gadallah and Fisher, 2009).

Contouring is the representation of three-dimensional earth on a two dimensional surface. The spacing between the contour line represents the steepness of the slope; the closer the spacing the steeper the slope and vice versa.

3.8.1 Time, Velocity and Depth Contour Maps of Kirthar Formation

The time and depth contour maps of Kirthar formation are shown in Fig 3.19 and Fig 3.21 respectively. The depth contour map is generated by multiplying time contours and velocity contours. The pattern of both contour maps confirms the sub-surface shape of the structure present. The hydrocarbon may accumulate where the contour values are low because hydrocarbon accumulates at those places where there is low pressure and there is low value of time and depth contours. The closed contour part can be considered as structural trap. The closed time and depth contours indicated steep sloppy portion which is near the location of wells which confirmed the interpretation that can be seen in Fig 3.19 and Fig3.21 respectively.

A horizon interpolated average velocity contour map for this formation is also generated to understand the spatial variations in velocity which can be seen in Fig 3.20.

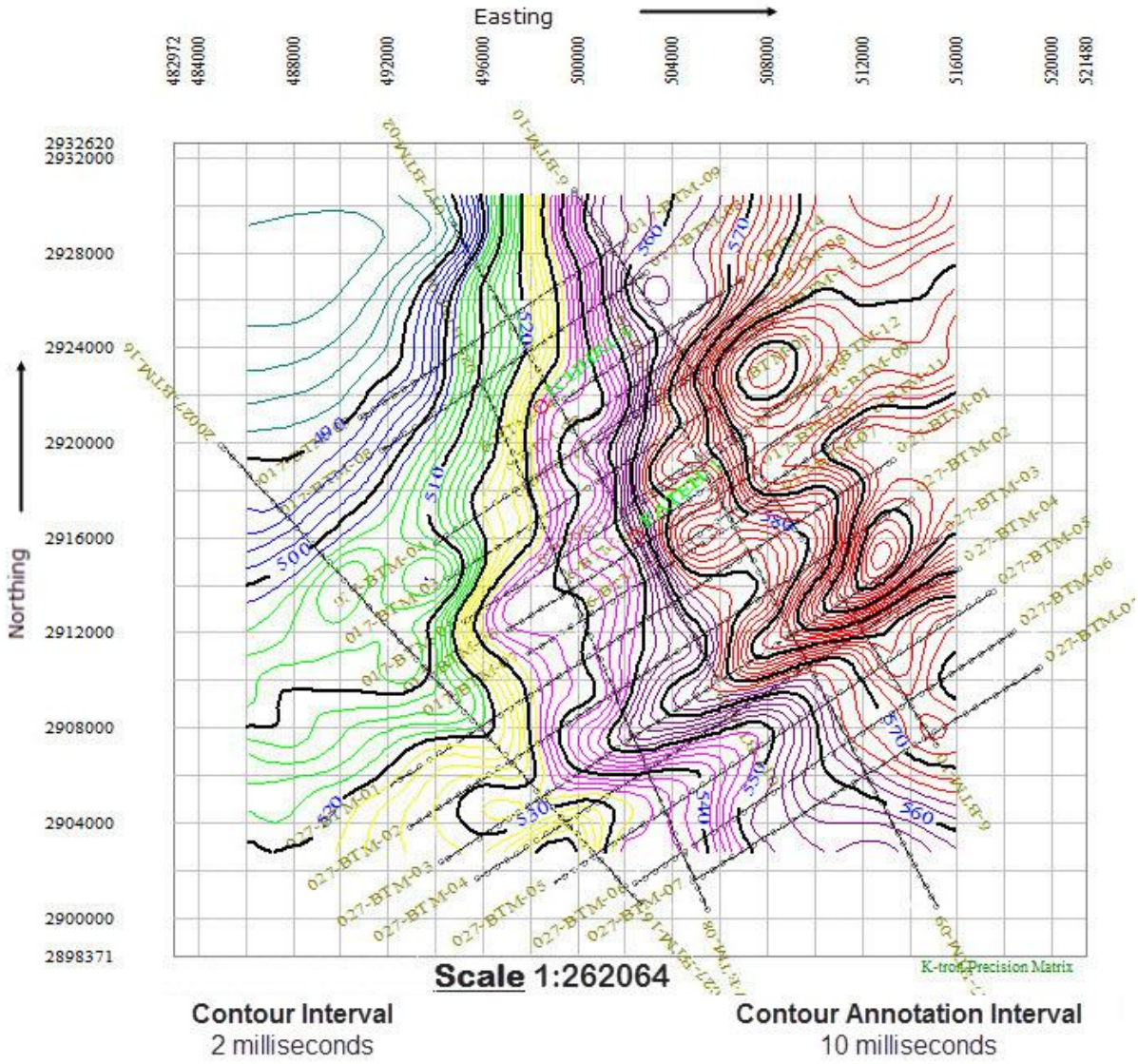

Figure 3.19 Time contour map of Kirthar formation.

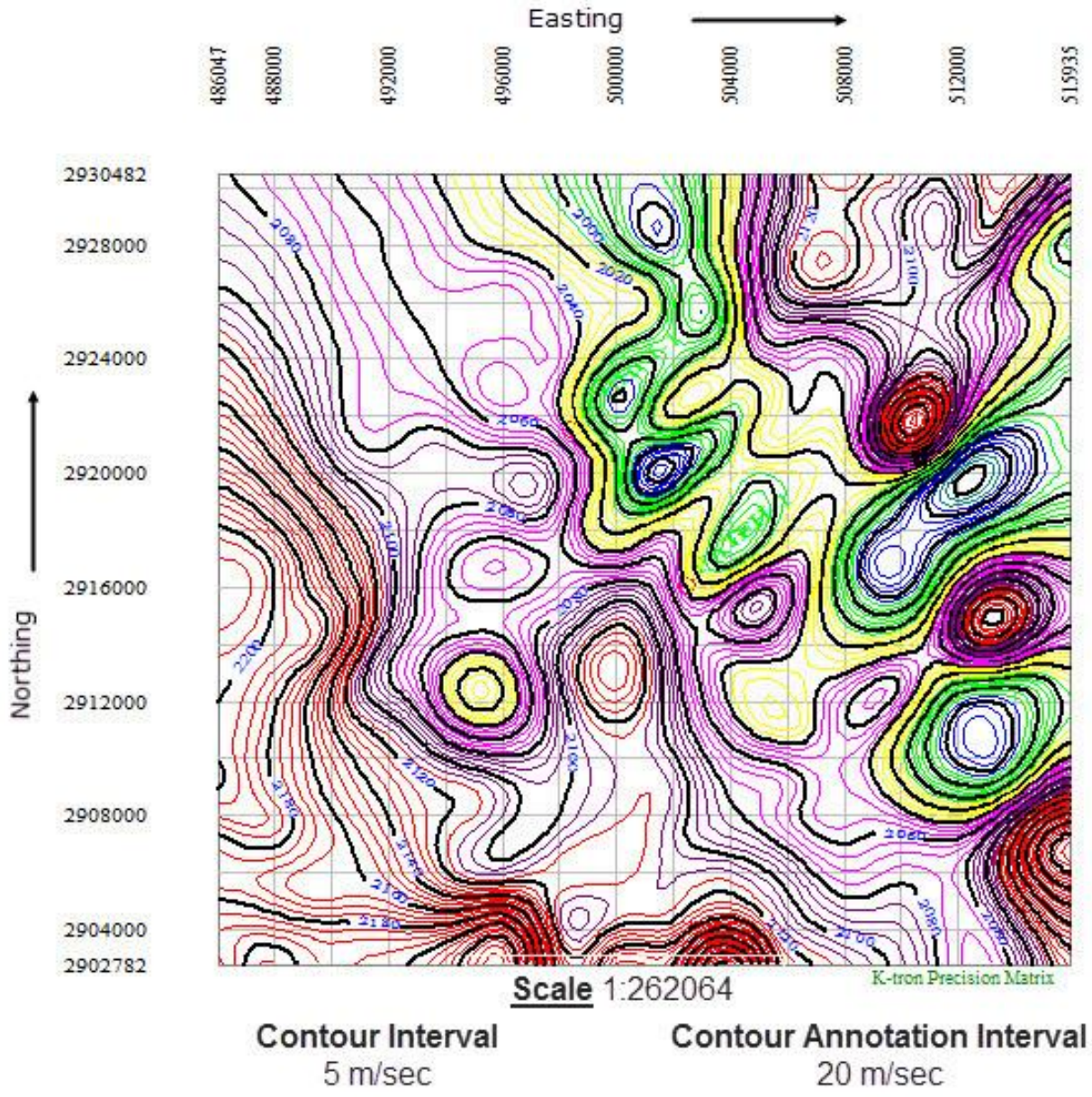

Figure 3.20 Velocity contour map of Kirthar formation.

Velocity contour map showing the variation of velocity in the Kirthar formation which lies in the range of 2000 m/sec to 2200 m/sec. Red contour lines showing the maximum range of velocity variation in the figure. South western part of the study area has a large zone of high velocity data with close contours.

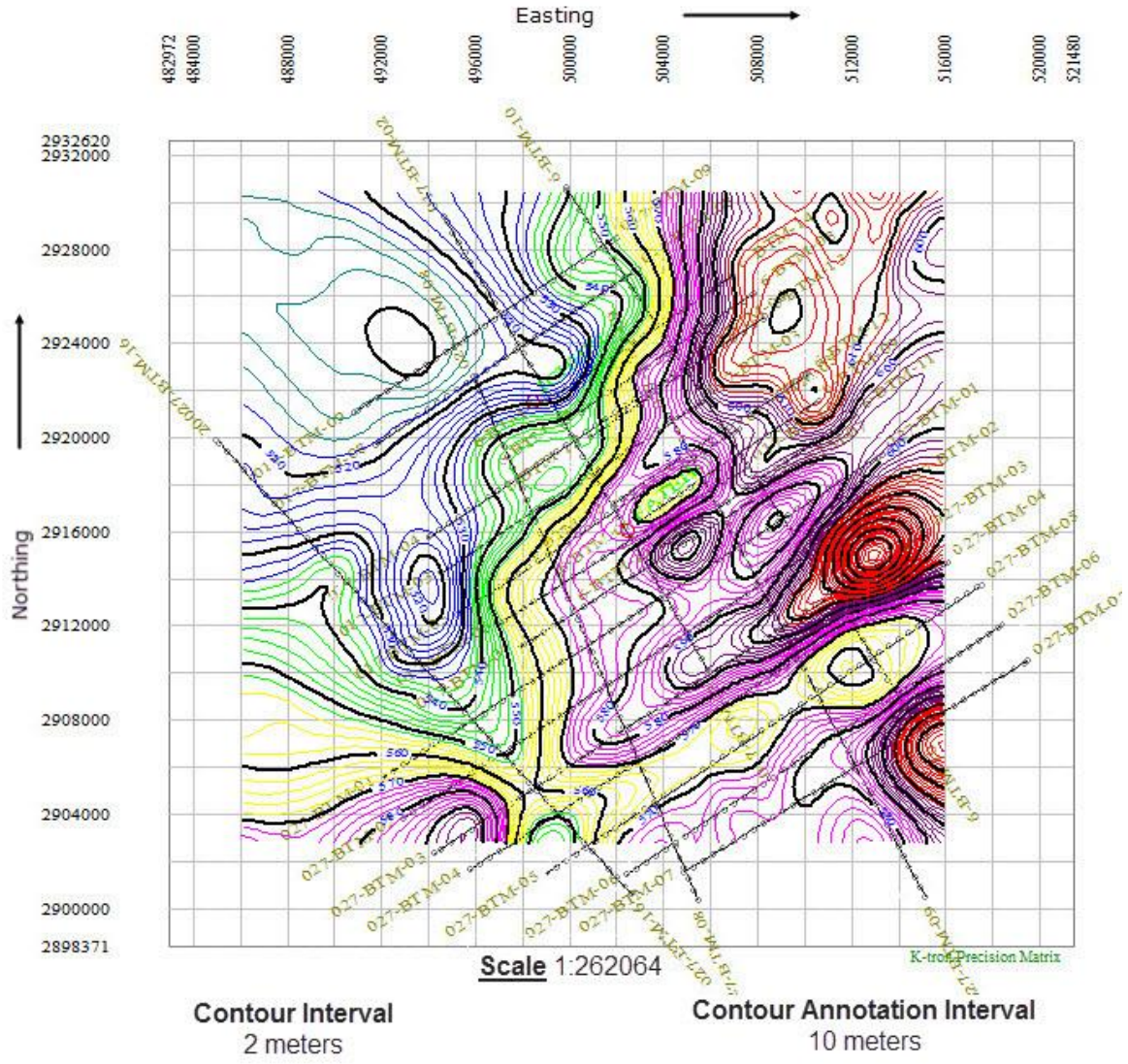

Figure 3.21 Depth contour map of Kirthar formation.

Fig 3.21 confirming the subsurface as the region where the well have been drilled is the area of very close contours. It indicates the presence of steep curvatures in the Kirthar formation over the study area.

3.8.2 Time, Velocity and Depth Contour Maps of Upper Goru Formation

Upper Goru formation is the seal rock of our area showing fluctuations in contours confirming the disturbance of the horizon in the form of horst and graben structure. Time and depth contours map confirming the structure of the area with the contour interval of 4 msec and 5 meters as shown in Fig 3.22 and Fig 3.24 respectively. The interpolated velocities which are important in generating the depth contours are used of the seismic data to study the variation in the Upper Goru formation as well as shown in Fig 3.23.

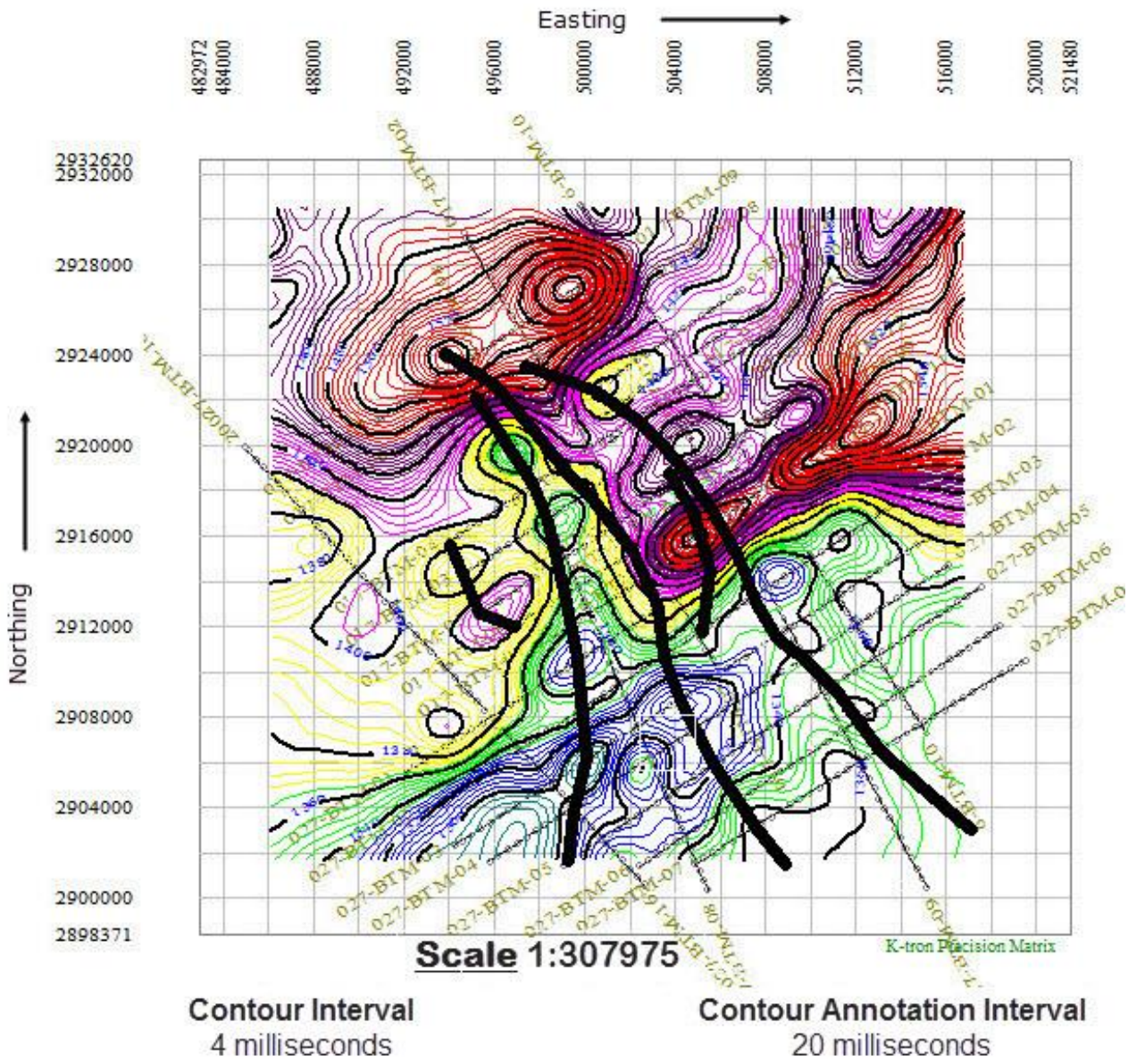

Figure 3.22 Time contour map of Upper Goru formation.

Upper Goru the seal rock of the study area as shown in Fig 3.22 along with fault polygon over the formation. This formation ranges for the time of 1350 msec to 1540 msec. Contours showing the increasing trend from green (lowest) to red (highest) value of the time. Eastern portion with red contours explaining the Graben present in the subsurface.

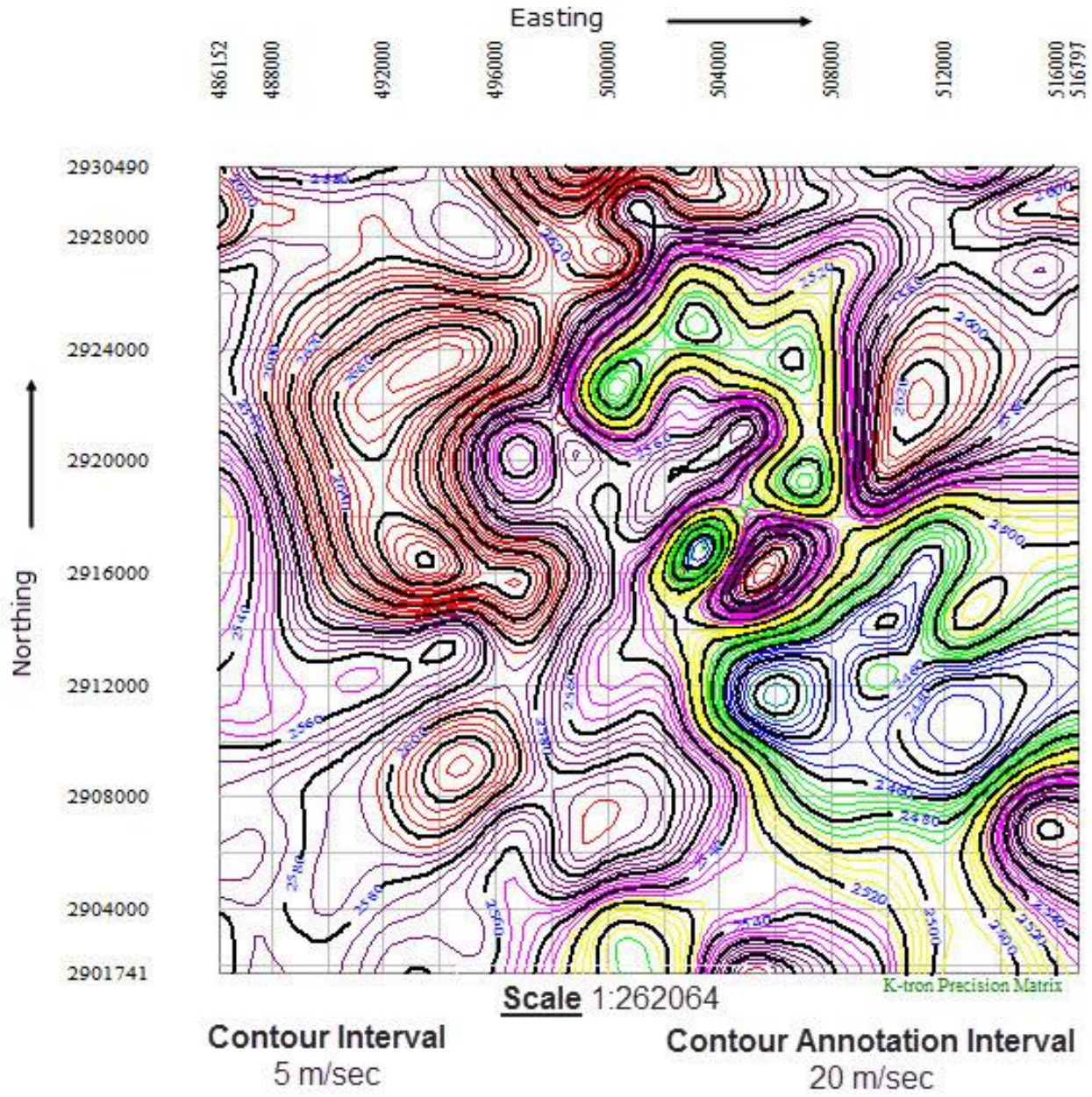

Figure 3.23 Velocity contour map of Upper Goru formation.

Fig 3.23 showing the quite detail variation of velocity ranging from 2400 m/sec to 2660 m/sec. Red coloured contours showing the highest value of the velocity. In this formation the moderate range velocity is dominating over the area.

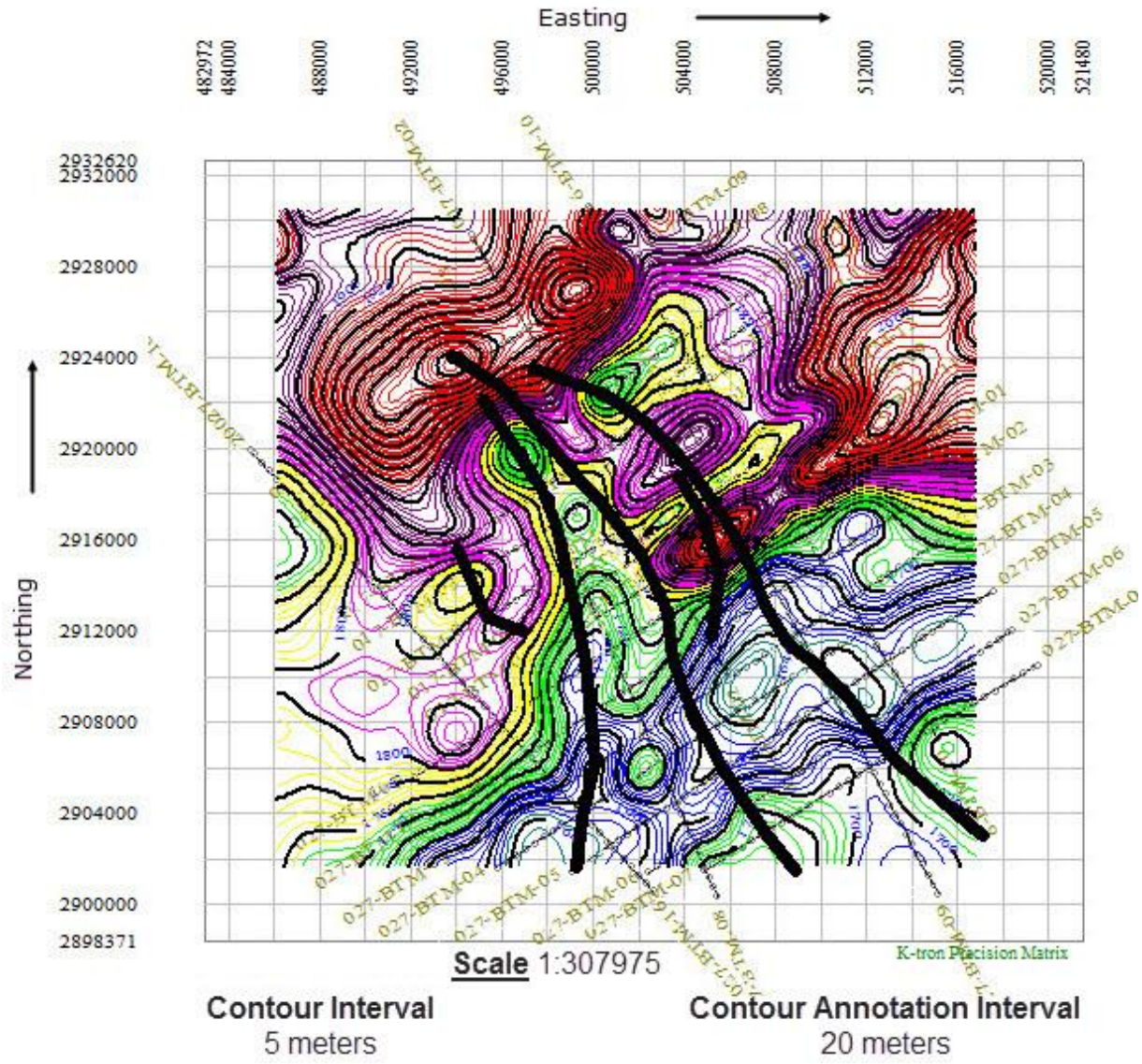

Figure 3.24 Depth Contour map of Upper Goru Formation.

Fig 3.24 confirmed the subsurface structure and the presence of the faults. Red coloured contours showing the relative low lying area which is basically Graben while Yellow coloured contours showing the relative high lying zone of Upper Goru in the subsurface.

3.8.3 Time, Velocity and Depth Contour Maps of Lower Goru Formation

Lower Goru is the main zone of interest of the study area from the hydrocarbon exploration point of view. Time and depth contour maps of Lower Goru formation having contour interval of 4 msec and 4 meters are shown in Fig 3.25 and Fig 3.27 respectively to understand the structural trap present in the reservoir. These are important in case of allocation of new well point to get the economical hydrocarbon which is not for Fateh-01. A horizon interpolated average velocity contour map for this formation with contour interval of 5 m/sec

is also generated to get acknowledge with the spatial variations in velocity as shown in Fig 3.26.

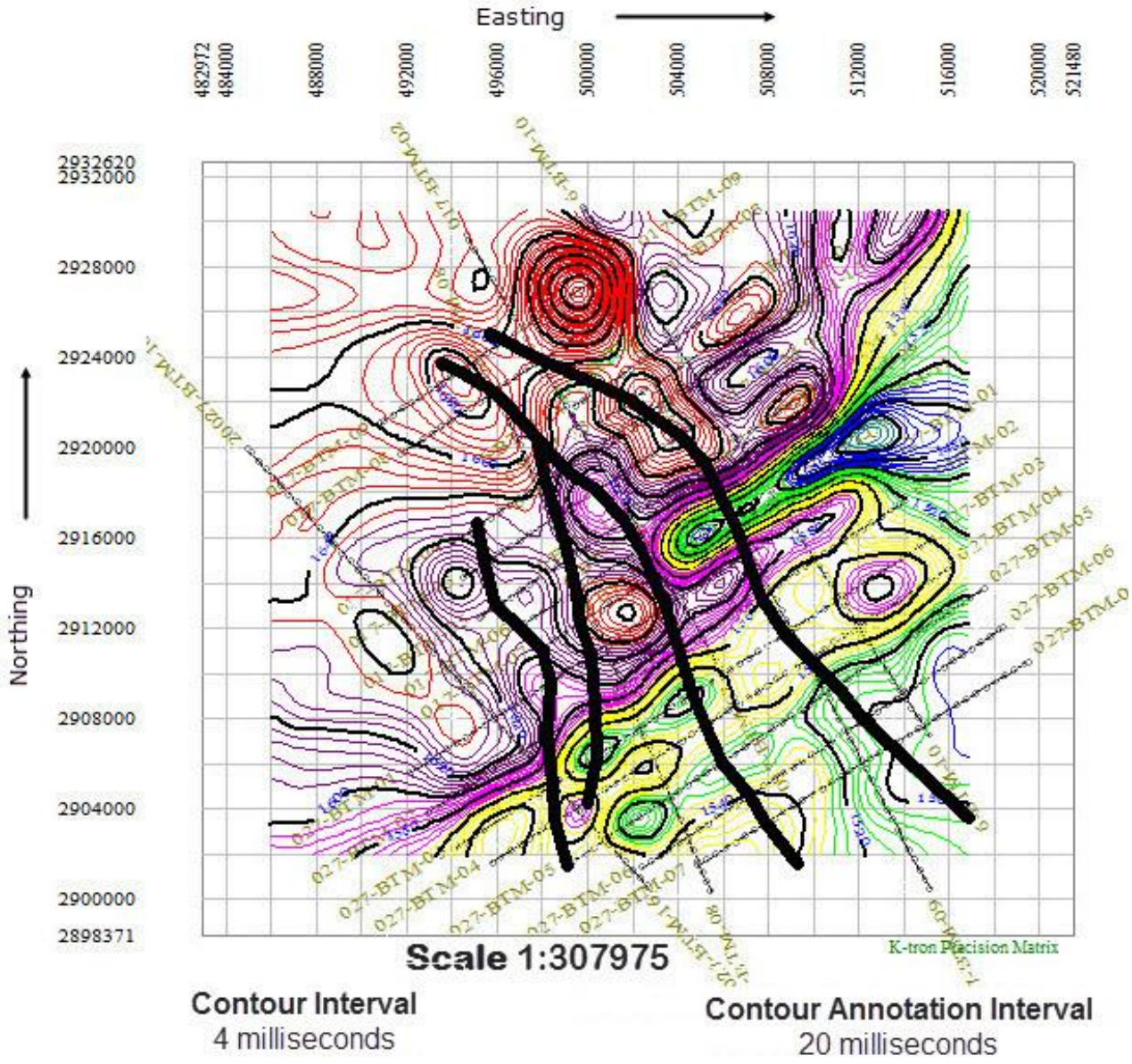

Figure 3.25 Time contour map of Lower Goru formation.

Fig 3.25 explaining the structure quite well as Lower Goru is the main scope of Explorationists in the study area. Both of the wells Fateh_01 and Ichhri_01 are drilled in the zone of steep slopes which confirmed our interpretation. But these both wells are not so economical may be as it lies on the Horst or may be because of fault seal is being disturbed.

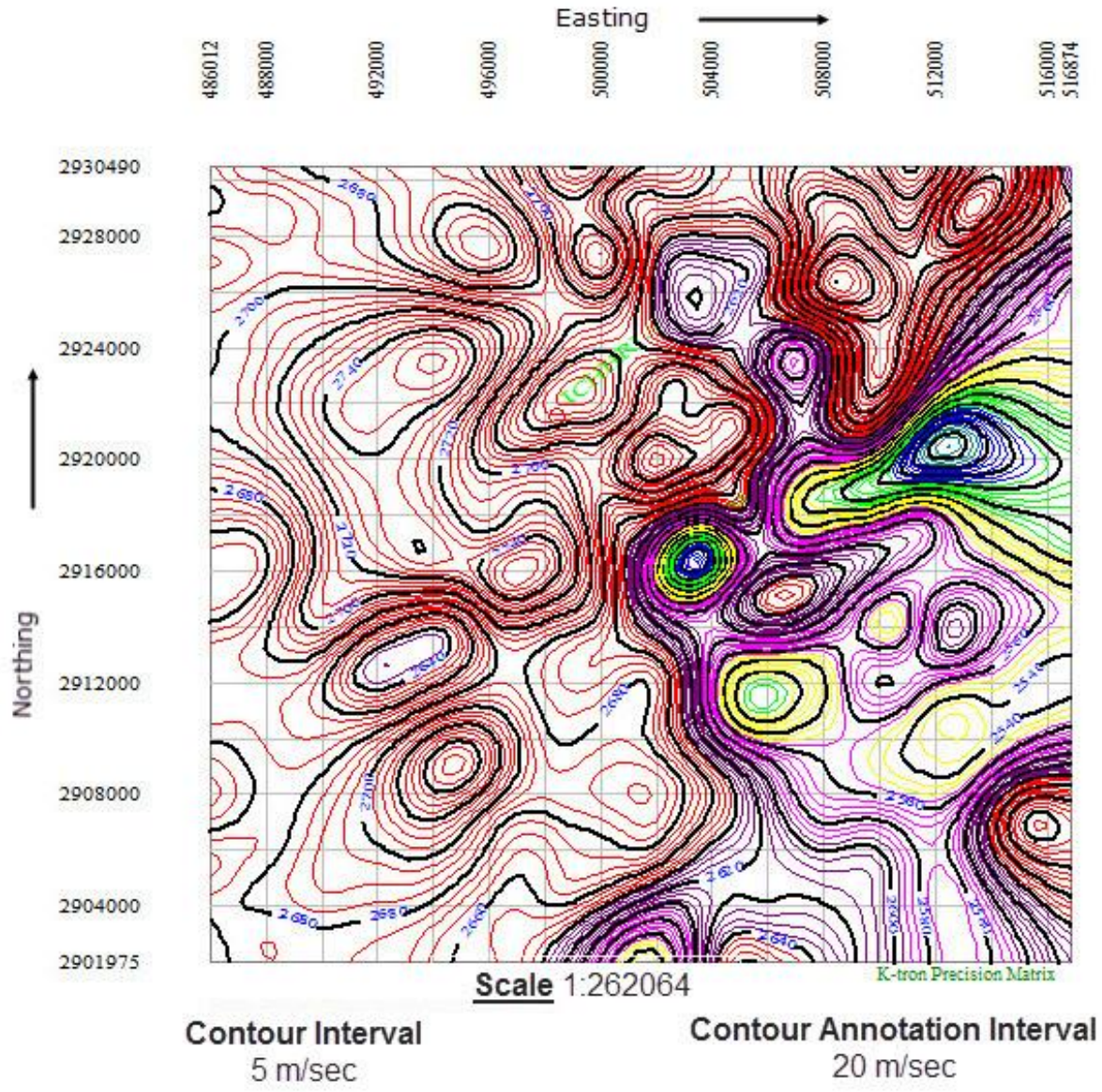

Figure 3.26 Velocity contour map of Lower Goru formation.

Velocity contour map of Lower Goru formation showing a large zone of relative high velocities almost covering the 1/3rd portion of the formation area. It is ranging from 2500 m/sec (blue) to 2740 m/sec (red).

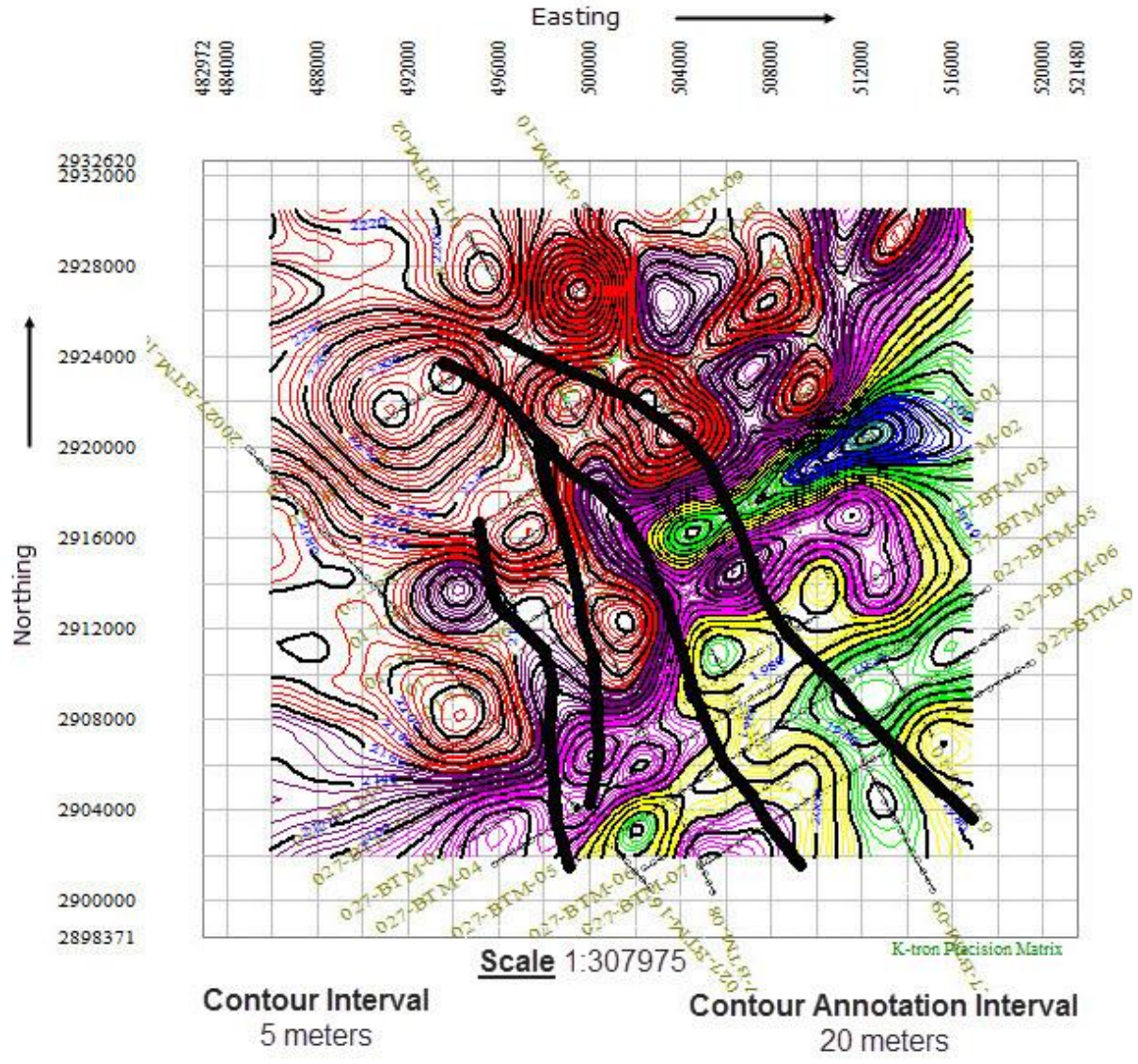

Figure 3.27 Depth contour map of Lower Goru formation.

3.9 1D Forward Modeling

The synthetic seismogram can be of great value to the interpreter and it is best presented by splicing it to an interpreted seismic depth section through the well location (Peterson et al., 1955).

Synthetic seismogram of Fateh-01 well is generated using Wavelets software (Khan et al., 2006). In this procedure the petrophysical logs; Sonic (DT) and Bulk Density (RHOB), which provide the velocity and density information of subsurface layers respectively, are used. The DT is a delay time log and its inverse gives the velocity. We use this velocity and density data to compute a series of reflection coefficients called reflectivity series.

Source Ricker wavelet with a dominant frequency of 35 Hz is generated. The reflectivity series is then convolved with the source wavelet to get a synthetic seismogram as shown in Fig 3.28. Synthetic seismogram is matched with the interpreted seismic depth section at the well point to correlate the succession of reflectors as shown in Fig 3.29. It may also be used to calibrate our seismic velocities.

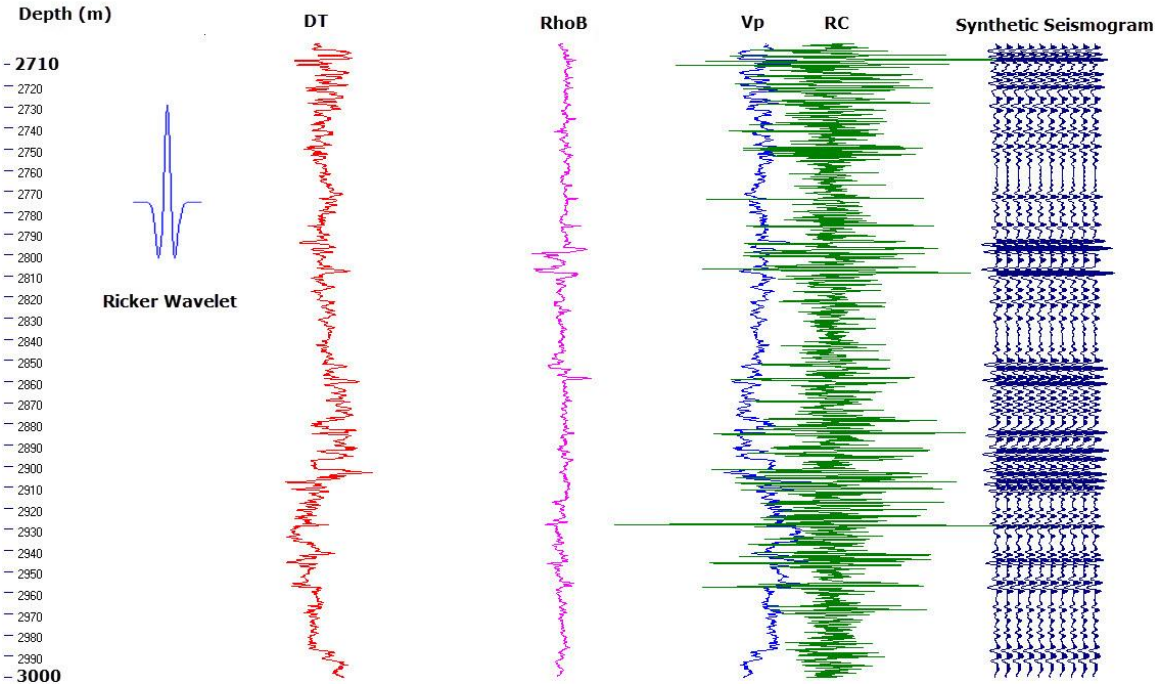

Figure 3.28 Synthetic seismogram of Fateh_01 generated in Wavelets software (Khan et al.,2006).

It may also be used to calibrate the velocity.

Synthetic Seismogram = RC* Ricker Wavelet

Where $$RC = \frac{V_2D_2 - V_1D_1}{V_2D_2 + V_1D_1}$$

D_1 and D_2 are the densities while V_1 and V_2 are the velocities of 1st and 2nd formation respectively. Synthetic Seismogram is generated using following parameters:

- Type of wavelet: Ricker
- Central Dominant Frequency: 35 Hz
- Sampling Rate: 2 milliseconds
- Phase: Minimum phase
- Number of Samples: 53

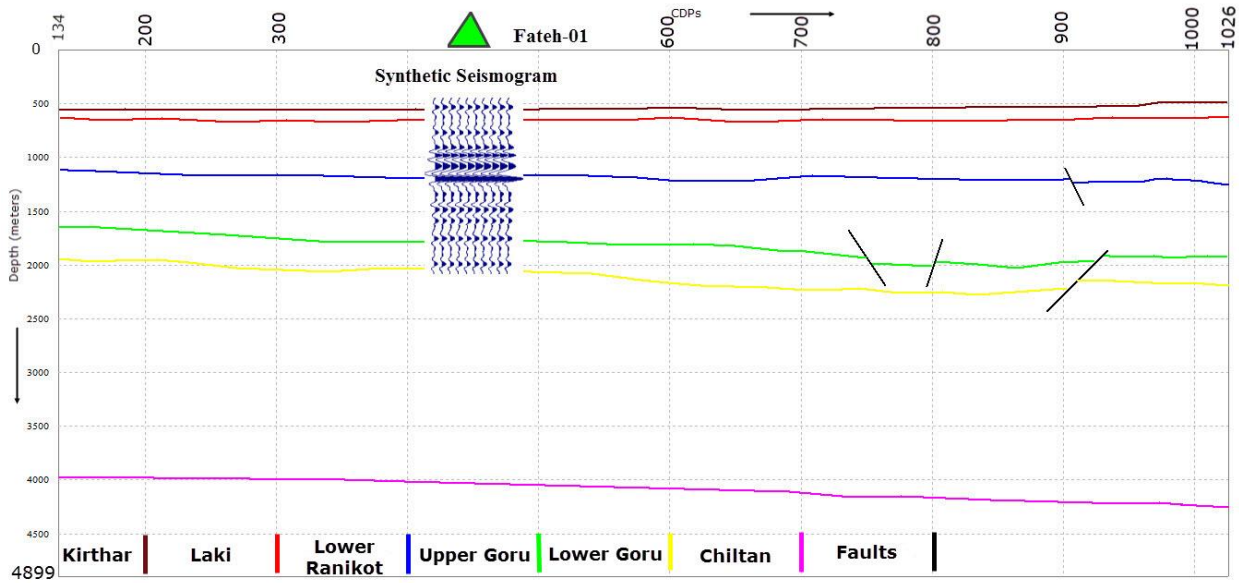

Figure 3.29 Interpreted Seismic depth section of 20017-BTM-02 correlated with the synthetic seismogram of Fateh-01.

3.10 Integrated 3D Visualization

Depth structural contour maps, resulting from 2D-seismic lines are displayed as 3D surfaces to present the undulations in the structural geometry due to faults. As 3D view provides a better visualization as compared to 2D to analyse the structure in better way. Kirthar, Upper Goru and Lower Goru along with Digital Elevation Model (DEM) are mapped and presented using Golden Software Surfer. SRTM (Shuttle RADAR Topography Mission) 30 DEM shows the variation of elevation from mean sea level (M.S.L) and 3D surface maps of above mentioned formations indicate the variation of depth which can be seen from scale in Fig 3.30. From the figure horst and graben is clearly observed, the region shown curvature indicate the graben while horst is determined by the relatively high lying area. Kirthar depth surface is quite variable from the others. As there encountered an unconformity and the formations; Laki, Sui Main limestone, Upper Ranikot and Lower Ranikot, in between Kirthar and Upper Goru.

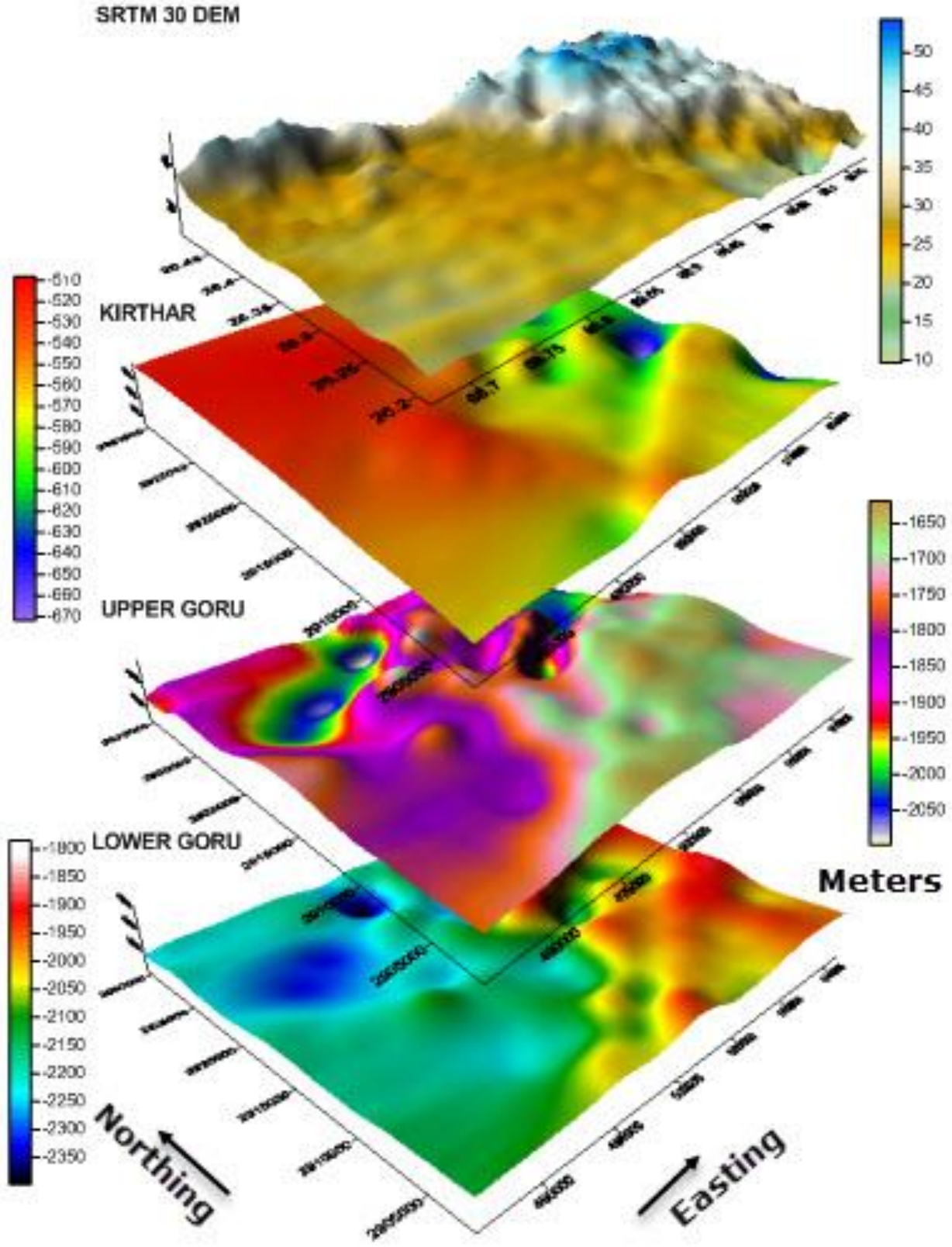

Figure 3.30 3D Visualization of Kirthar, Upper Goru and Lower Goru depth surfaces.

Chapter 4

4. 2D Seismic Modeling, Crustal Extension, Petrophysics and Well correlation

4.1 2D Seismic Modeling

Structural Modeling of the interpreted digital geological cross-section of seismic line 20017-BTM-09 was performed, to generate a synthetic 2D seismic section. It is the reverse process of seismic interpretation. In seismic interpretation we mark geological horizons whereas in seismic modeling we generate the synthetic seismic section. As this modeling is completely based on the structural data the derived synthetic section completely matches the structures. This type of modeling is commonly used to select acquisition parameters for new surveys based on existing geological cross-sections with velocities assigned to each formation. It is also used to get seismic response of stratigraphic models as well as confirmation of seismic interpretation. A synthetic source wavelet (Ricker) was generated using the parameters that were used in the field. The wavelet generation interface along with the input parameters is shown in Fig 4.1.

The geological section was convolved with the Ricker wavelet at CDP intervals 10 to generate a Zero Offset 2D synthetic seismic section. This section is similar to a migrated seismic section shown in Fig 4.2. All interpreted geological horizons were assigned reflection coefficient attributes.

The interpreted geological cross-section has been modelled using X-Works, a geological cross-sections software application, developed using the Wavelets modelling engine (Khan et al., 2006).

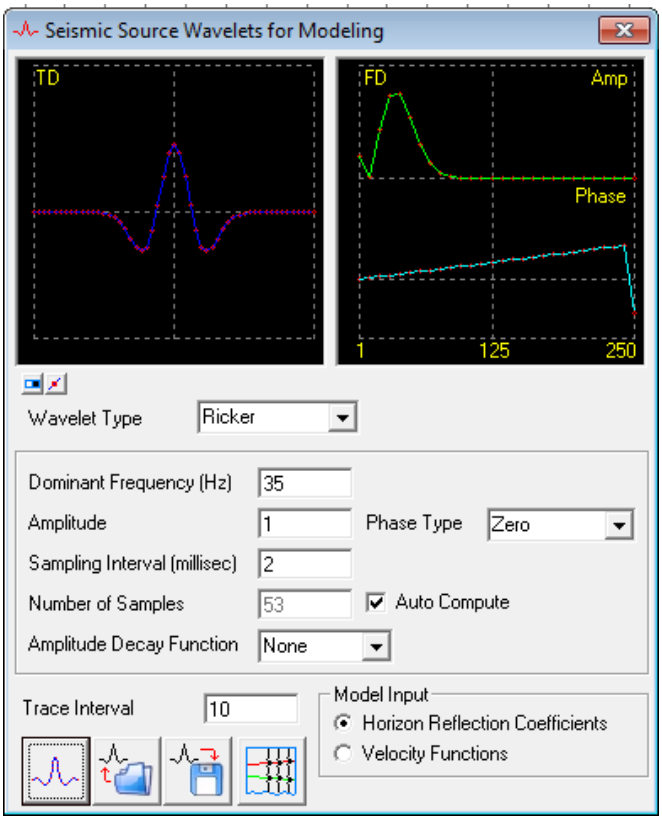

Figure 4.1 Source wavelet generation along with input parameters.

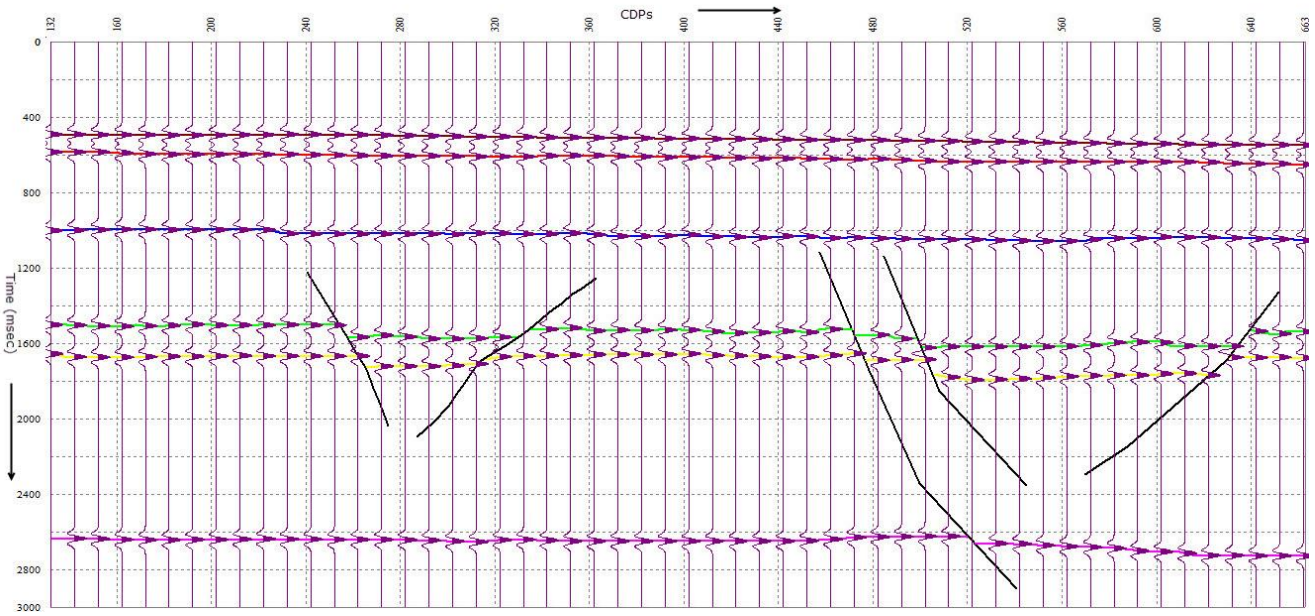

Figure 4.2 Marked geological cross section of seismic line 20017-BTM-09 showing seismic model for each reflector.

4.2 Crustal Extension

Crustal extension is the process of stretching the earth's crust, usually normal faulting and linear folding take place in such case.

Pakistan geographically lies between 60°E to78°E and 24°N to 37°N. It has high density of active faults and is seismically one of the most active area of the Asia. Tectonically it is located in the region of intersection of three plates, Indian, Eurasian and Arabian sea plate. The study area lies in the subduction zone known as Makran Subduction Zone.

To quantify the effect of the tectonic regime in the study area crustal extension of seismic line 20017-BTM-09 has been computed using X-Works software tool.

4.2.1 Procedure

The interpreted seismic line 20017-BTM-09, after time to depth conversion is basically a geological cross-section which shows the deformation in the horizons (formations) due to normal faulting. The length of the section (Lo) is calculated by the multiplication of the number of CDP with the CDP interval. Similarly the length (L) of the horizon is calculated by adding the lengths of its faulted segments. The crustal extension (CE) is then given by;

$$\mathbf{CE = L - Lo}$$

4.2.2 Crustal Extension of Source, Reservoir and Seal Rocks

The crustal extension is calculated for Upper Goru and Lower Goru formations. The current length of seismic line 20017-BTM-09 is 26,550 meters. After deformation of the structures, the formations are separated into different parts due to normal faulting. The length of each faulted part is given in Fig 4.3.

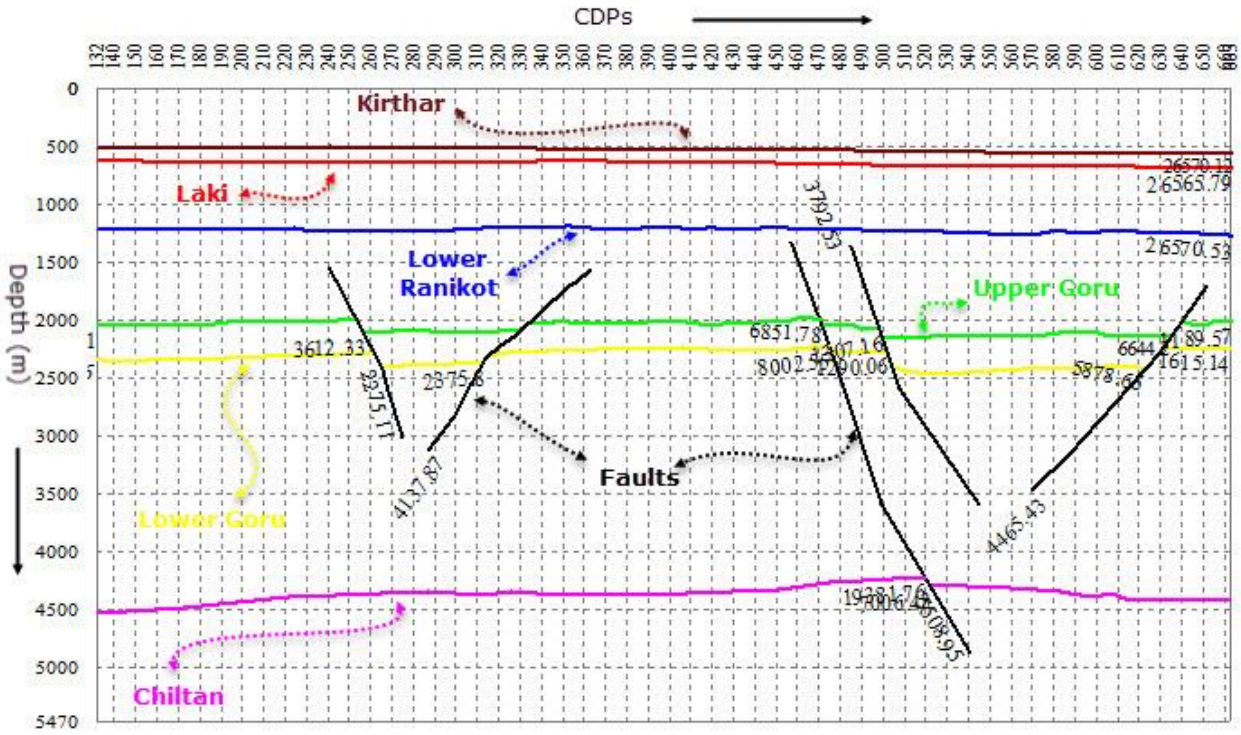

Figure 4.3 Geological depth section of 20017-BTM-09 with calculated length for each horizon and fault segment.

It can be noticed that crustal extension has been taken place along the Upper Goru and Lower Goru formation. The negative sign proved the presence of extensional regime. The average extension take place in the hydrocarbon indicated zone is about 847 m.

Table 4 Horizons length and their corresponding crustal extension.

Horizon Name	Horizon Length L (m)	Section Length Lo (m)	Crustal Extension L-Lo (m)
Upper Goru	25721	26550	- 829
Lower Goru	25684	26550	- 866

4.3 Petrophysics and 1D Rock Physics Analysis

Electrical well logging was introduced to the oil and gas industry over half a century ago and since then, many improved and additional logging tools and devices have been developed and have been put in general use. The technique of interpretation of the data advanced along with the advancements in well logging science. But now, the detailed analysis of a carefully chosen suite of wire-line services provides a method of inferring.

4.3.1 Petrophysical Analysis

The petrophysical analysis was carried out by using the following wireline logs of Fateh_01 issued by DGPC:

- Density log
- Gamma Ray log

4.3.1.1 Log Curves

The log data of Fateh_01 was available in Logging ASCII Standard (LAS) format. The log curves along with some parameters given in the LAS file header are used to calculate all basic and advance parameters. The methodology adopted for this work is given in Fig 4.4 and each analysis step is discussed in the proceeding sub-sections. Using this

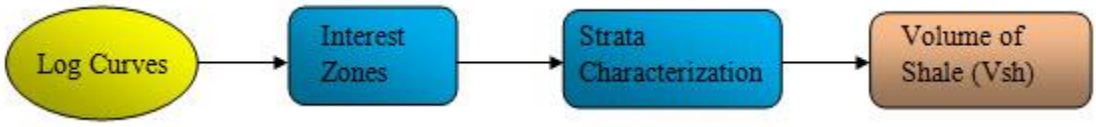

Figure 4.4 Workflow for the computation of volume of shale in the zone of interest.

4.3.1.2 Interest Zones

The zones of interest are defined on the basis of source, reservoir and seal rock formations given in well tops of Fateh_01 well. The zones of interest which are marked are listed in the Table5.

Table 5 Interest Zone of the study area for hydrocarbons.

Zones	Starting Depth (m)	Ending Depth(m)	Thickness(m)
Upper Goru	1810	2083	273
Lower Goru	2083	3000	917

4.3.1.3 Strata Characterization

The lithologies are marked by Gamma Ray log deflections; it is a good indicator of shale. The shale and sand formations are identified by this log, but sometimes calliper and SP log information is also very important for strata characterization. Sand and shale lines are marked at the minimum and maximum values of Gamma Ray in the selected zone of interest, A cut off line is marked in the middle of the two lines which is used to

demarcate sand and shale formations.

4.3.1.4 Calculating Shale Volume

The source formations are commonly shally with higher radioactive content and are therefore indicated by a higher Gamma Ray value. On the other hand, it is also assumed that the radioactive material is not present in other formations which are termed as clean formations. This creates a contrast between shale and other formations. The mathematical formulation used to calculate the Volume of Shale is given below:

$$\text{Volume of Shale (Vsh)} = 0.083[2^{(3.7*IGR)}-1]$$

Where;

$$I_{GR} = \frac{GR_{log} - GR_{min}}{GR_{max} - GR_{min}}$$

The Gamma Ray log along with sand and shale lines as well as linearly computed volume of shale curves for a depth range of 1600 meters to 2900 meters are given in Figure 4.5. It can be observed that both curves are similar to each other when linear computations are used. Volume of shale plot gives the clear picture of reservoir which is not as better because of more shally content in the reservoir. Though the study area is very vital and blessed with hydrocarbons but it is not as such good commercially because of absence of one the main prospect of the petroleum play that is good reservoir. Fig 4.5 demonstrated the range of reservoir is not so much. This is one of the probable reasons of the dryness of well Fateh_01 as it couldn't produce commercial amount of hydrocarbons.

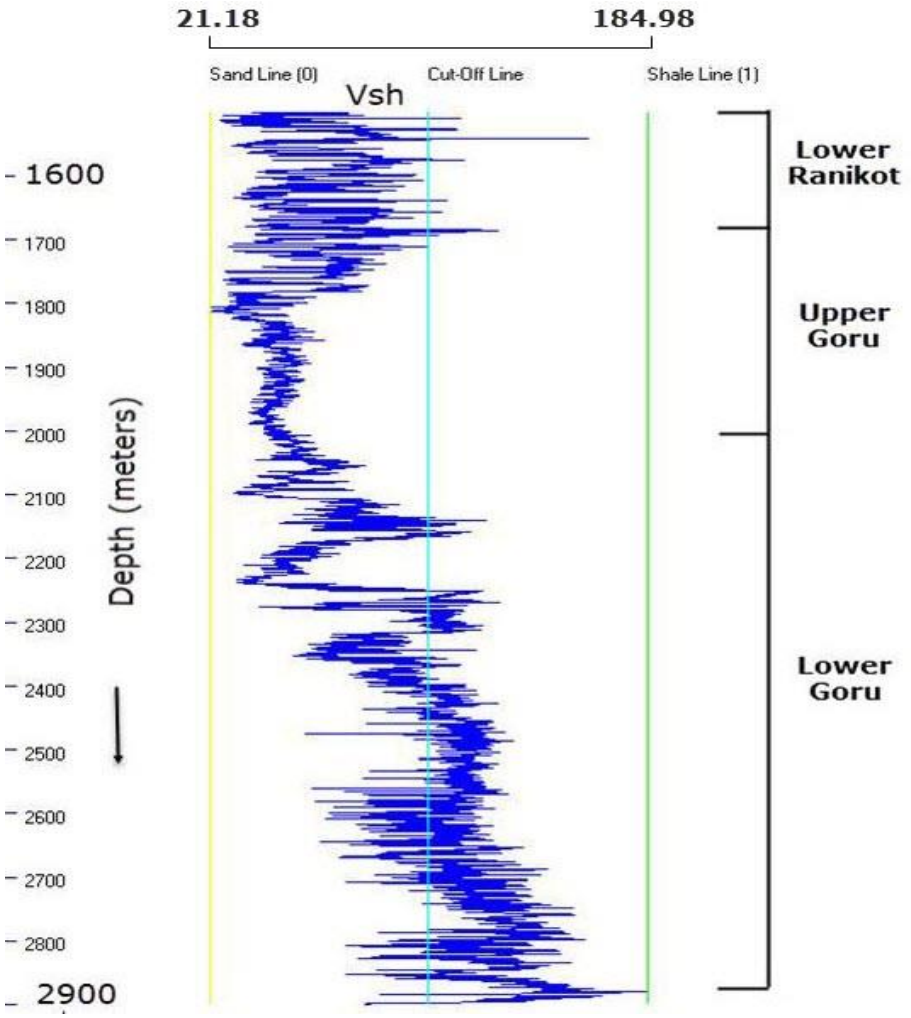

Figure 4.5 Vsh in blue color plotted for well FATEH_01 for the depth range of 1500 to 2900 meters.

4.3.2 Computation Rock Physics Coefficients for the Area

Rock physics contributes particulars about elastic parameters which in turn can be interpreted into useful geologic information. For a trustworthy interpretation at least two among the three input parameters; P-Wave Velocity, S-Wave Velocity and Density must be measured. The two available parameters are correlated to determine the coefficient which better represents the area under study (Khan, 2013).

Well logs for the area contain P Wave Sonic and density, therefore these two parameters have been correlated using K-tron Cleopatra software using the following methodology. Gardner et al. (1974) under a series of empirical studies and determined the following relationship between velocity and density:

$$\rho = aV_p^{1/4}$$

Where *p* is density, *Vp* is P-wave velocity and *a* is the coefficient having a value of 0.31 when *Vp* is in meter per seconds. It is ascertained for an eclectic range of sedimentary rocks. In the current study this parameter is recomputed by fitting a linear least-squares polynomial to the Velocity Density data from well Fateh_01, as shown in Fig 4.6. The computed value for coefficient is 0.297 which remarkably allocates the rocks of the area and therefore is used in computation of all rock physics parameters in 1D as well as 2D.

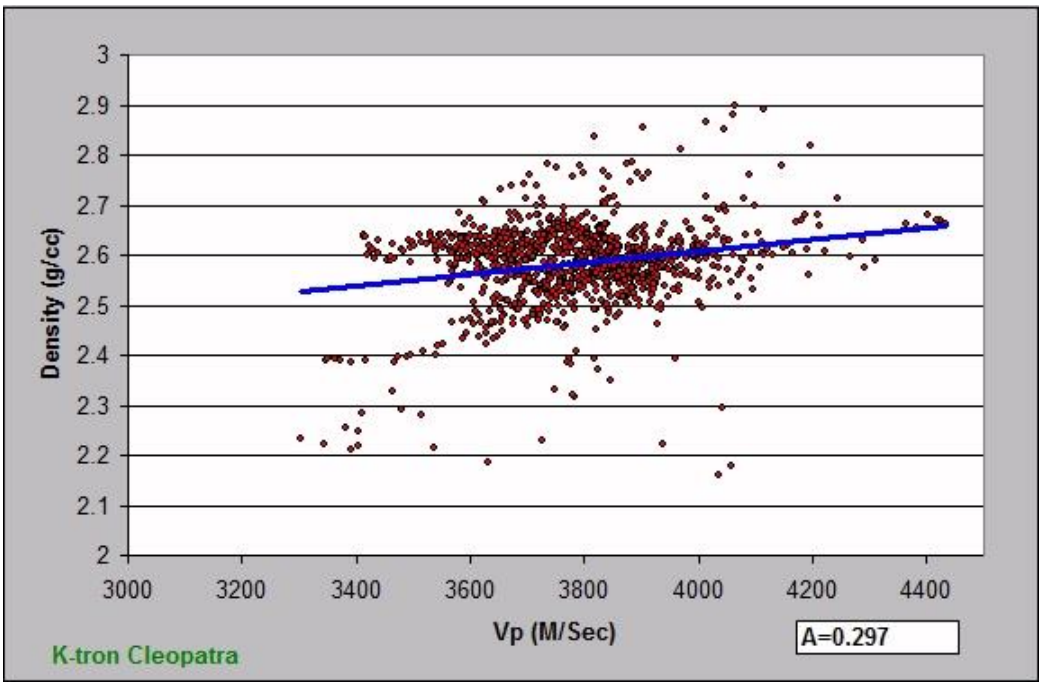

Figure 4.6 Linear least-squares polynomial fitted to the cross-plot of P-Velocity and Density to determine the relational coefficient for the area using K-tron Cleopatra software.

4.3.3 Calculation of 1D Rock Physics Parameters

1D Rock physical analysis has been done to understand the behaviour of different parameters vertically with the depth. Using wavelets software this task has been achieved. Firstly the petro physical log file has been loaded ;which is in LAS (Log ASCII Standard) format, for the specific depth range of the targeted zone. With the help of *DT*(sonic) log *Vp* has been calculated by simply inverting the log value. Then *Vs* will be determined from Vp using mathematical relation. Furthermore rock physics parameters have been computerized by the software using Vp and Vs values. Fig 4.7 is the brief description of the 1D rock physics parameters. Each curve assigned different colour to understand it better. In the figure every parameter has denoted by the symbol which will be explained with more précised detail in 2D in the next Chapter. Fig 4.7 shows DT (Sonic log), Vp (Compressional wave Velocity),

Vs(Shear wave Velocity), phi (porosity), k(Bulk modulus), u(Shear modulus), E(Young's modulus), M(P-wave modulus), l(Lame's constant) and g(Poisson's ratio).

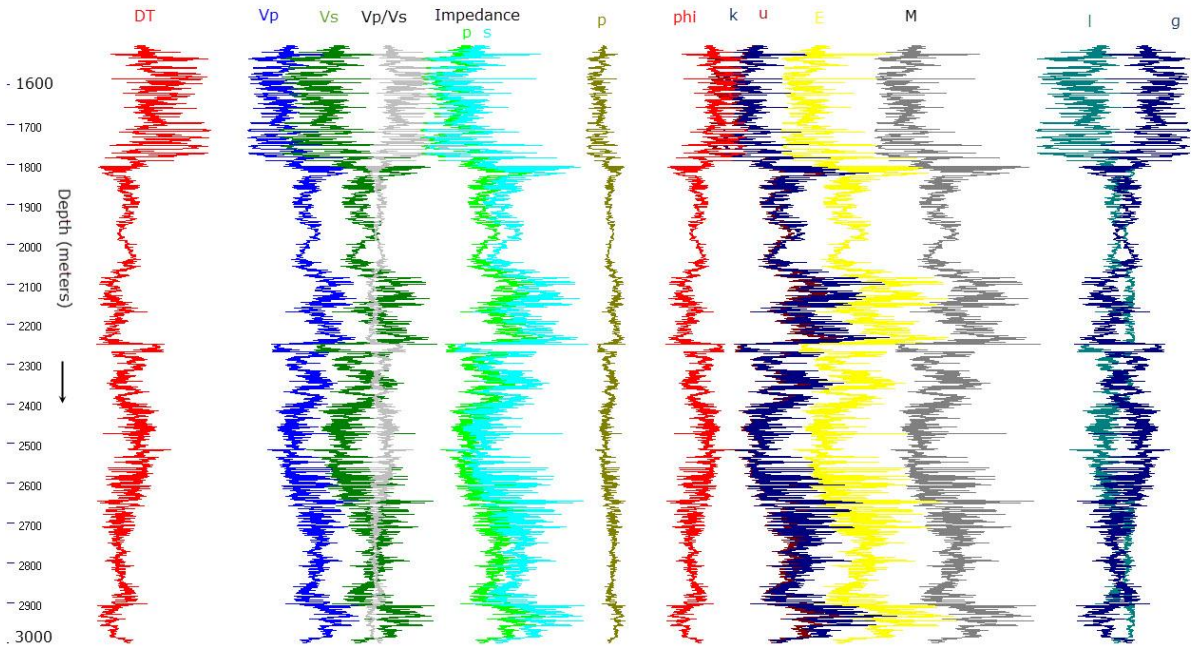

Figure 4.7 Different Rock physics parameters variations with the depth in Fateh_01 using *DT* log.

4.3.4 Poisson's Ratio versus Vp to Vs Ratio Cross-Plot

A common way of looking at the *VP/VS* ratio is to use Poisson's ratio, defined by;

$$\sigma = \frac{0.5(V_p^2 - 2V_s^2)}{V_p^2 - V_s^2}$$

It has been noticed that Gas/Oil lower V_P/V_S and hence Poisson's ratio relative to water filled reservoir. Thus we can also create cross-plots of Poisson's ration and V_P/V_S and identify zones for Oil and Gas, as shown in Fig 4.8. It is the generalized diagram showing relation between above mentioned ratios.

Similarly A cross-plot for Fateh_01 has been designed to understand the extension of the gas, oil and water zones along with the shale region. Fig 4.9 revealed different zones of Fateh_01.

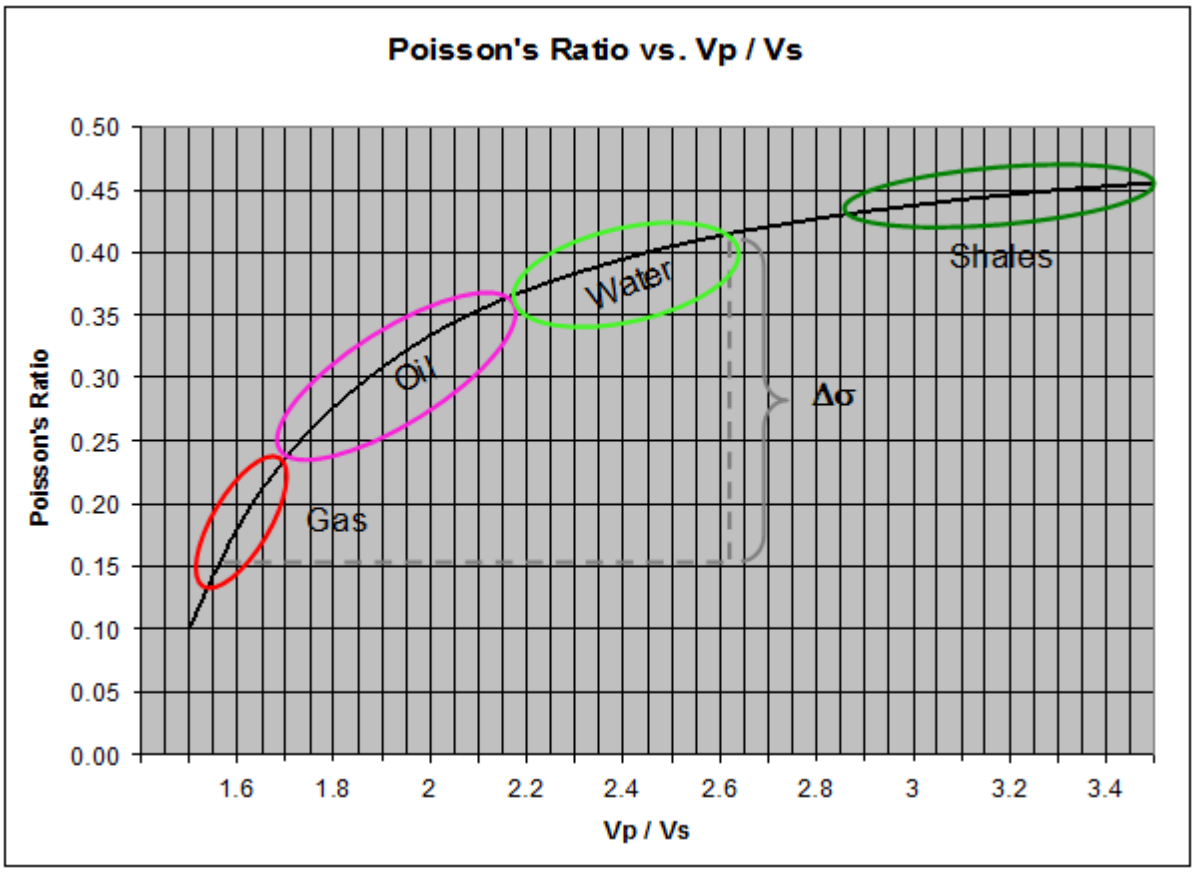

Figure 4.8 Generalized cross-plot between Poisson's Ratio and V_P/V_S showing the marked zone of gas, oil, water and shale in the well.(Khan, 2013)

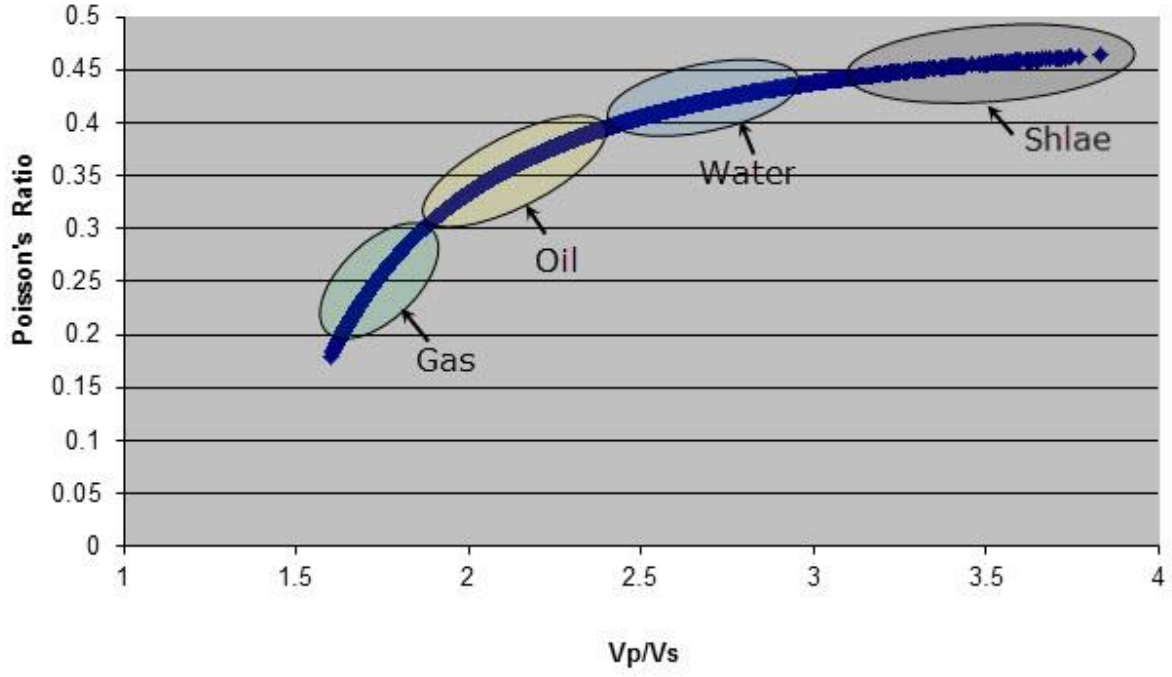

Figure 4.9 Cross-plot of Poisson's Ratio and V_P/V_S for Fateh_01 for the depth (1600 m - 3000m).

4.4 Stratigraphic Well Correlation

Correlation is the determination of equivalence in time-stratigraphic or rock-stratigraphic units of the succession of strata found in two or more different places. The rocks of associated outcrops may be correlated through physical criteria and fossil content. Precise lithological correlations from well to well can be inferred by comparing the tops and bottoms of lithologies in each well, well tops data is used to perform this task. This is normal practice done by geologists.

In addition borehole calibrated seismic velocities in depth domain are interpolated at the correlated lithological contacts along the profile. The interpolated velocity functions are then used to generate a 2D seismic model along the profile. The seismic amplitudes at each contact boundary on this section represent the reflection coefficients between the respective lithologies.

Figure 4.10 shows the complete flow chart for columns, input, embedding, correlation and modeling.

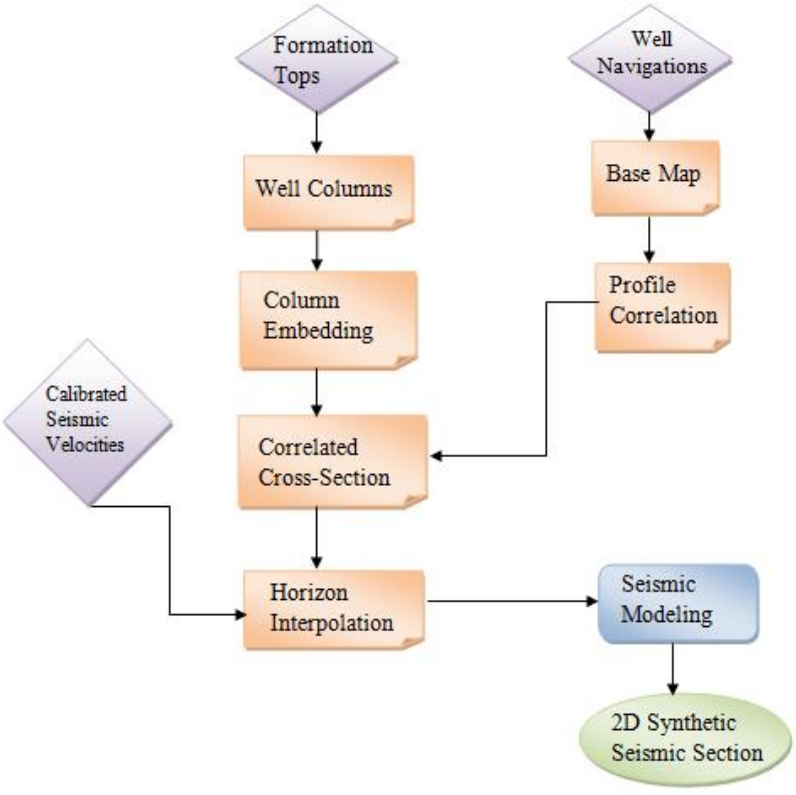

Figure 4.10 Work Flow for Well correlation and Seismic modeling.

4.4.1 Well Correlation Profile

A well correlation map is generated by using the "Measure & Trace" tool in K-tron Precision Matrix mapping software (Khan, 2000). Starting from CHAK 05 DIM SOUTH 01, a profile is passed through all the wells and ended at ICHHRI_01 that are correlated as shown in Figure 4.11. The software also provides the distance between each well along the profile and the total length of the profile. This information is used to create scaled well correlation cross-section by placing the well columns at their appropriate position. Using interpolated velocities along the cross-section a 2D seismic model is generated to match the seismic amplitudes with the lithological contacts.

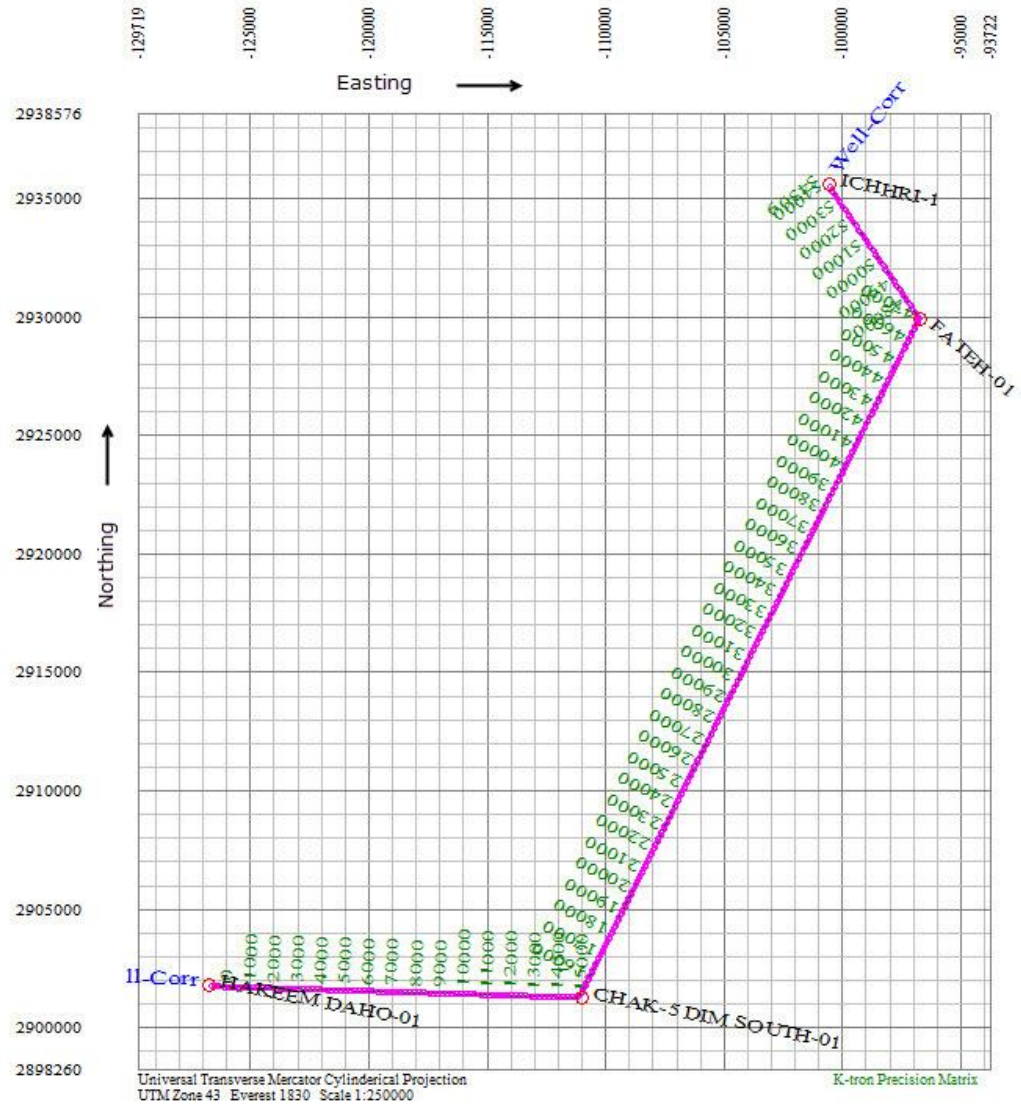

Figure 4.11 Well profile showing the wells location and their lateral distance.

4.4.2 Well Information

The well formation tops are input into the COL format used by K-tron X-Works Geological Sections and Columns software, which provides a highly interactive columns input and editing interface. Using this interface each formation in the column is assigned a name, geologic age, hatching pattern, color and a contact interface. This information is stored in the COL format and can be used to graphically generate the geological column and embed it in the cross-section document according to its position on the correlation profile. In this way columns for each well are input, stored and embedded at their respective position on the cross-section. The formations in these columns are correlated well to well by using interactive section drawing and editing tools. The final correlated section along with embedded columns is saved as a cross-section file. Four wells are used for correlation, information about wells is given in Table 6.

Table 6 Well details which are used for the correlation in the study area.

Well Name	Status	Total Depth(m)	K.B Elevation(m)	Operator
ICHHRI_01	ABD	3300	37.02	O.G.D.C
FATEH_01	ABD	3000.5	35.23	O.G.D.C.L
HAKEEM DAHO_01	OIL&GAS	3210	32.79	O.G.D.C.L
CHAK 05 DIM SOUTH 01	GAS/CON	2908	27.7	O.G.D.C

4.4.3 Well Column Correlation

Interpretation of well log data is the primary method for development of a stratigraphic framework which can be used for mapping and prediction of reservoir intervals. The purpose of it, not only to establish the stratigraphic correlations of different wells in Southern Indus basin but also to clarify the source of sediments and depositional centres during different geological time periods. This helps in identifying the maximum thickness zones of prospective formations in the basin. It also helps in assigning the direction of sediments flow in the basin throughout different geological periods. There occurs the variation in the thickness across the are among these wells which can be visible in Fig 4.12. The probable reasons for these variations are following:

- Erosion.
- Faulting.
- Over burden pressure.

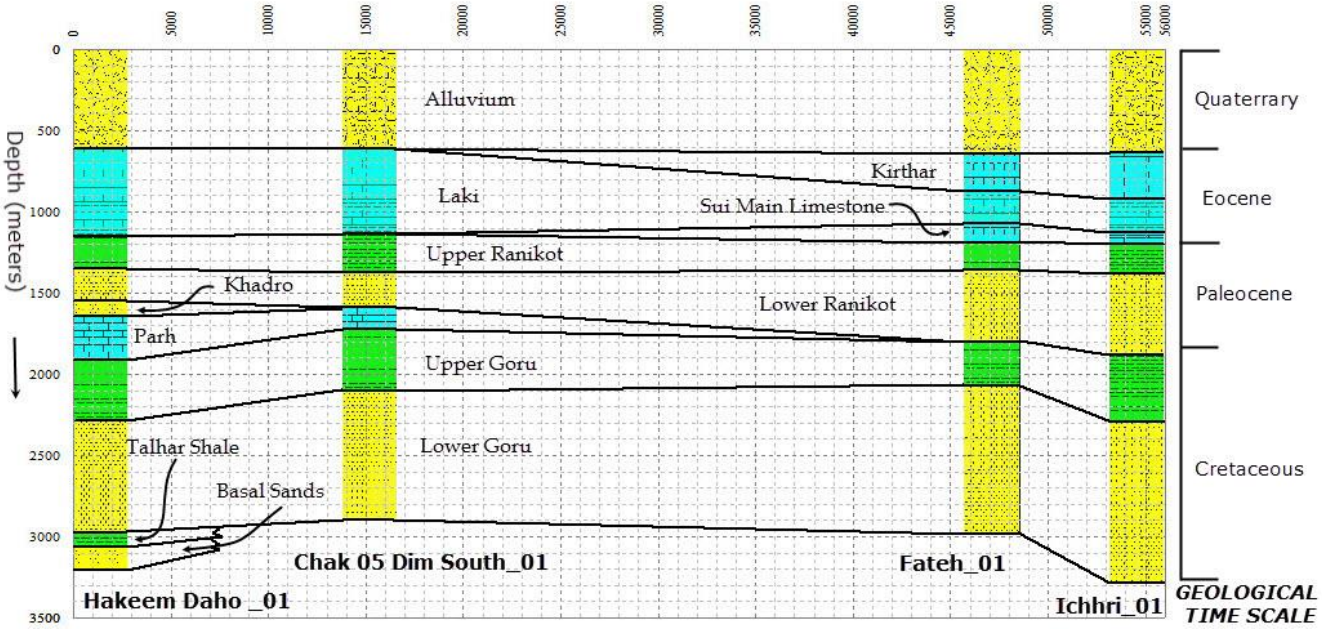

Figure 4.12 Stratigraphic well correlation.

It is obvious from the Fig 4.12 as we move towards southwest Kirthar formation is diminished. By obeying law of lateral continuity its extension is not more towards south of Southern Lower Indus Basin. Thickness of Upper Goru varies towards east, it is going to decrease in the manner while Lower Ranikot a source of gas hydrocarbon in Lower Indus basin is increasing towards the east.

Each boundary assigned a reflection coefficient depending upon its nature. Reflection coefficient varies as because it depends on two factors:

- Density
- Velocity

Using K-tron X-works software 2D seismic modeling has been applied on the boundaries to get better result about lithology in sub surface by using the wells installed the study area which can be observed in Fig 4.13.

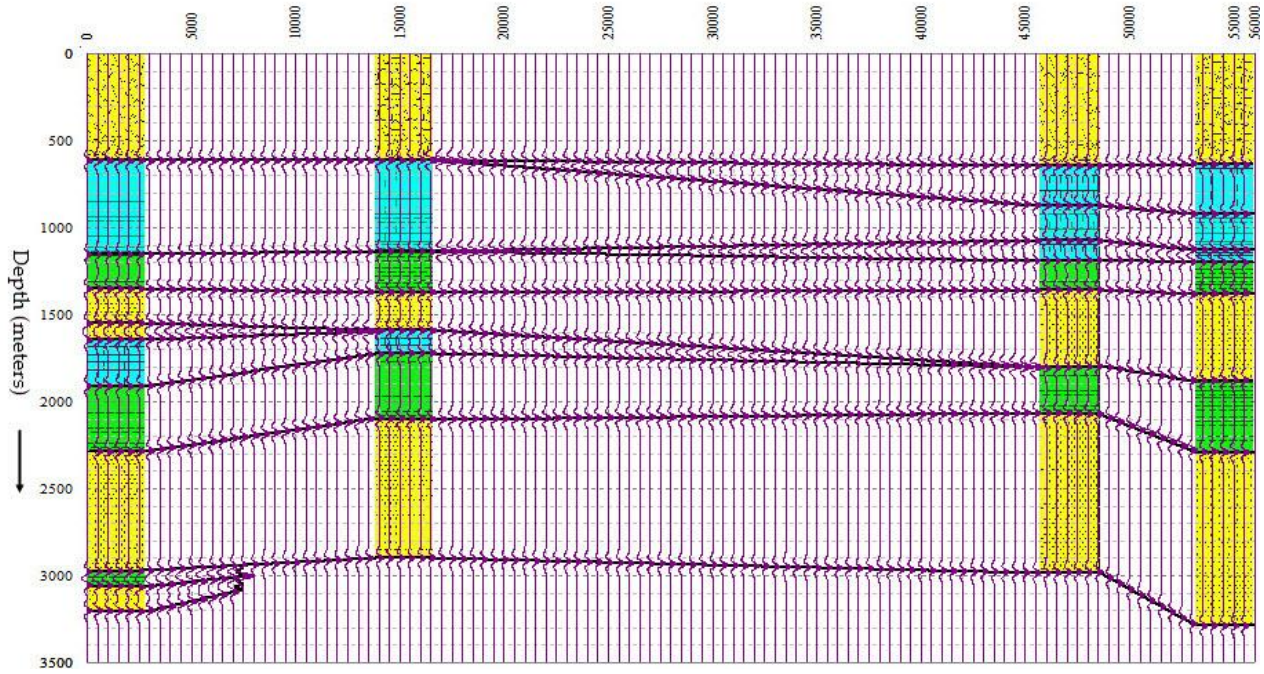

Figure 4.13 Well correlation with help of seismic modeling.

Chapter 5

5. 2D Rock physics and Engineering Properties, Seismic Attribute Analysis and Complex Velocity Model Building

5.1 2D Rock Physics and Engineering Properties

Techniques that relate the geological properties (e.g. porosity, lithology, saturation) of a rock with the corresponding elastic and seismic properties (e.g. elastic modulus, velocity, impedance) at certain physical conditions (e.g. pressure, temperature) termed as Rock Physics.(Dewar & Pickford, 2001).

In Rock physics we usually use Sonic, Density and Dipole logs to establish relationship between P-wave velocity (Vp), S-wave velocity (Vs), Density with Bulk, Rigidity module Porosity, etc. The velocity data is converted into the X-Works format using data formatting scripts available in Visual OIL (Khan et al., 2010).

5.1.1 Approximation of Rock Physics

Accurate relationship between the rock properties and seismic attributes of the targeted area can help the interpreter to put rock properties together with seismic horizons. Rock physics and engineering properties have also been computed using the velocity functions (Vint). In the real earth velocity varies laterally as well as vertically thus we cannot use average velocity (Vavg) and RMS velocity (Vrms) because these are not the true representative of a particular subsurface layer as they provide a vertically summed effect of all overlying layers. Interval velocities (Vint) represent individual rock units therefore they are used for the computation of true lithological properties of the sub-surface layers. The Vint was created and input to Vel2Rock software written in Visual OIL (Khan et al., 2010) shown in Fig 5.1. To determine the rock physics parameters many equations are used as given in Fig 5.2.

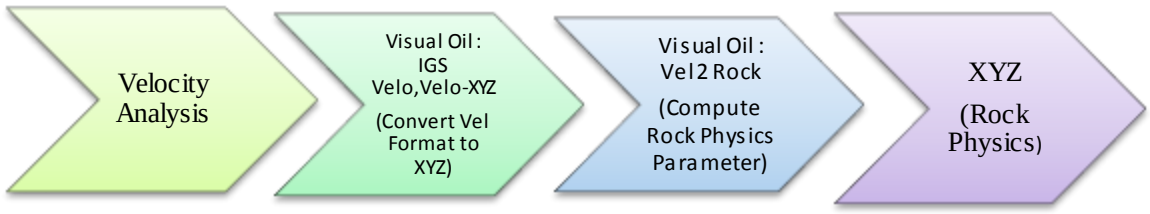

Figure 5.1 Generalized flow chart for the generation of Rock Physics parameters.

$$V_p = 1.16 * V_s + 1.36 \qquad V_p = \sqrt{\frac{K + \frac{4\mu}{3}}{\rho}} \qquad V_s = \sqrt{\frac{\mu}{\rho}}$$

$$V_s = (V_p - 1.36) / 1.16$$

$$\rho = 0.31 * V_p^{.25} \qquad A = V_p * \rho \qquad VpVs_{Ratio} = \sqrt{\frac{K}{\mu}} + \frac{4}{3}$$

$$\mu = \rho V_s^2 \qquad K = \rho(V_p^2 - \tfrac{4}{3} V_s^2) \qquad E = \frac{9K\mu}{3K + \mu}$$

$$M = K + \frac{4\mu}{3} \qquad \sigma = 0.5(V_p^2 - 2V_s^2) / (V_p^2 - V_s^2) \qquad \lambda = K - \frac{2\mu}{3}$$

Figure 5.2 Equations for computation of Rock Physical & Engineering Properties.

5.1.1.1 Iso Velocity Cross Section

Secondary Waves which arrive after the P-Waves are also called transverse or shear waves, as particle motion is perpendicular to the direction of propagation of wave. They travel only through solids, as fluids (liquids & gases) do not support shear stresses.

The Iso-Velocity section of seismic line 20017-BTM-02 is shown in Fig 5.3, the trend of the velocities is tend to be increasing progressively with the depth, it can be seen from the color variation. As S-wave can only travel through solids, so it is essential to calculate the S-wave velocity to study the nature of sub-surface structure. These velocities are further used in the computation of porosity, Vp to Vs ratio and Young's Modulus cross-sections.

Mathematical formula is given for the calculation of S-wave:-

$$Vs = \frac{(Vp\text{-}1.36)}{1.16}$$ (Castagna et al., 1985)

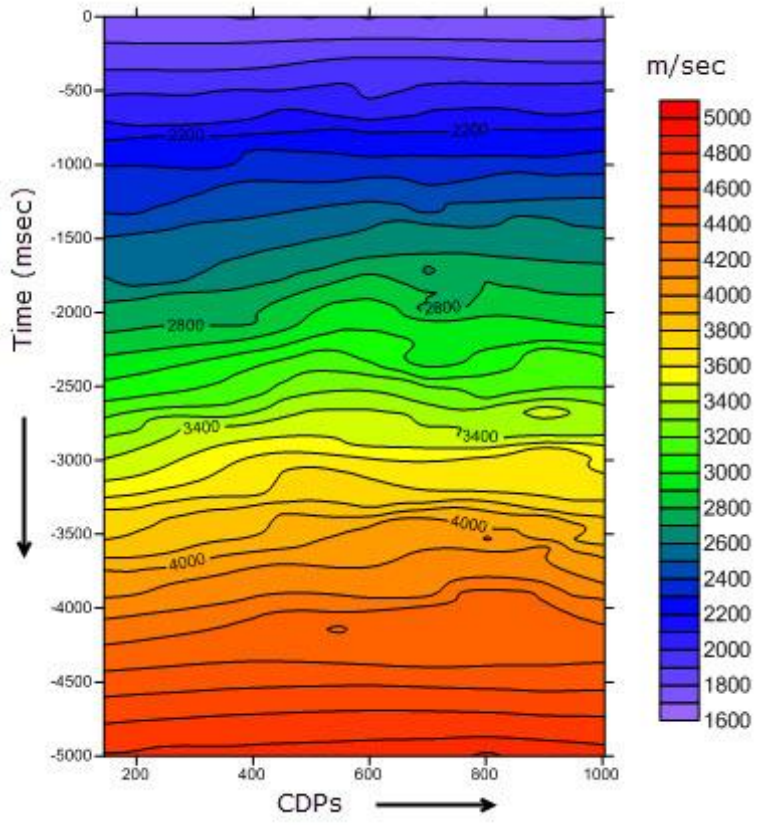

Figure 5.3 Iso-Velocity Cross section of seismic line 20017-BTM-02.

S-wave velocity ranges of different rocks is given in Table 7 from which we can estimate the lithology in the area. It is observed the formations which can hold saturated fluids have low values of S-wave velocity while those which are compact have higher range e.g. limestone.

As Lower Goru containing limestone interbedded with sands whose velocity ranges from 2800 meters per seconds - 3100 meters per seconds lying in the centre of cross section confirming the interpretation. The velocity of the seismic line 20017-BTM-02 is ranging from 1600 meters per seconds to 4760 meters per seconds.

Table 7 S-wave velocities for different lithologies.

Lithology	S-wave value (m/s)
Limestone	2800-3000
Sandstone	700-2800
Clay	400-1000
Glacial deposit	600-1000

5.1.1.2 Density

Density is very important property of rock. P-Wave velocities passing through material is directly depended on density of that material.

It can be seen from Fig 5.4 which shows the general behaviour of density which increases with the depth and also varies as we move laterally. The cross-section of density is then interpreted using known values of different rock units as mentioned Table 8.

Table 8 Densities of different lithologies.

Material	Density (g/cc)
Sandstone	1.90-2.58
Shale	2.0-2.5
Limestone	2.6-2.72
Dolomite	2.2-2.6

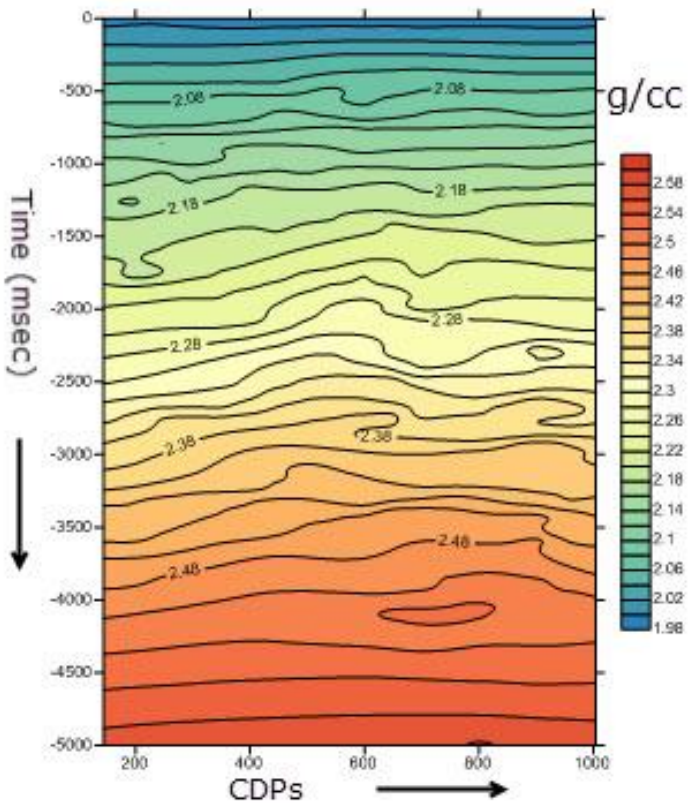

Figure 5.4 Density cross section of seismic line 20017-BTM-02.

An anomalous zone is observed between CDP 400-750 which may probably be the indication of liquid or hydrocarbon etc.

5.1.1.3 Porosity

The ratio of the volume of void to the total volume of the rock is termed as porosity.
Velocities are inversely proportional to the porosity because of the compaction increases with the depth.

Mathematical formula is given for the calculation of Porosity:-

$$\frac{1}{V_{bulk}} = \frac{\Phi}{V_{fluid}} + \frac{1-\Phi}{V_{matrix}}$$

Where Φ = Porosity

V_{bulk} = Wave speed of the rock formation

V_{fluid} = Wave speed through the pore fluid

V_{matrix} = Wave speed through the solid matrix

Table 9 Percentage porosities for different lithologies.

Lithology	Porosity (%)
Gravel	30-40
Sand	20-35
Sandstone	5-30
Limestone	5-30
Shale	10-30
Granite	0.5-1.5

The porosity variation for interval velocity can be observed in the section given in Fig 5.5. The calculation of porosity is helpful to confirm the reservoir; porosity must be high for reservoir rock. At high porosity, velocity in reservoir rocks strongly depends on the position of the inter-granular material.

From Fig 5.5 it can be seen that as we move down the porosity is decreasing with the depth depicting more compact layer is present, the range of porosity throughout the cross section is 0.04 to 0.42. An anomalous zone is observed between CDP 450-700 which may be indication of reservoir which confirmed the interpretation. The lateral variation is also observed in the porosity cross section. The detail of porosity range for some known lithologies is given in Table 9.

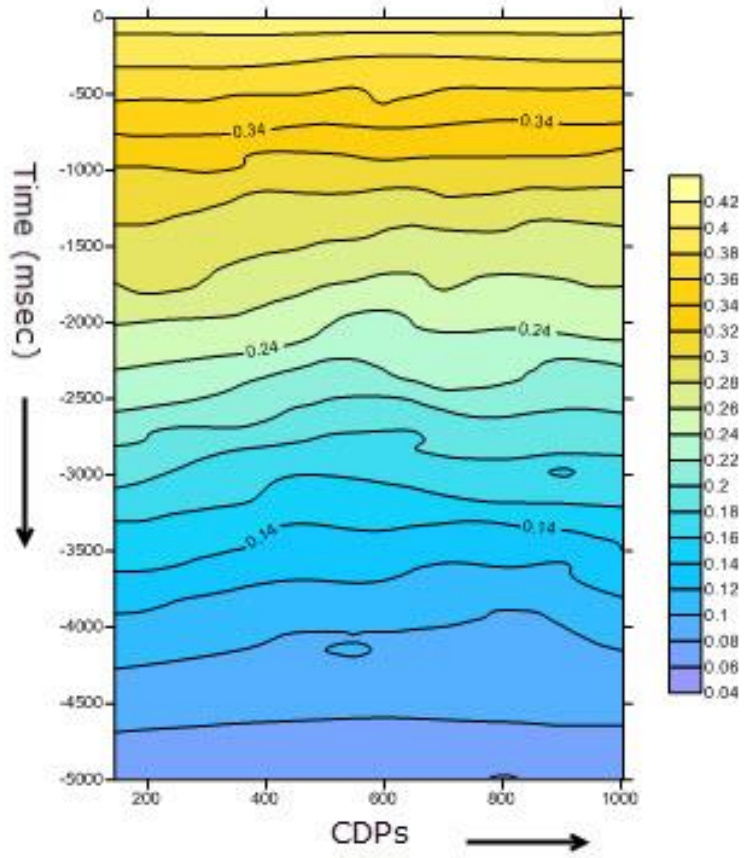

Figure 5.5 Porosity cross section of seismic line 20017-BTM-02.

5.1.2 Engineering Properties

Engineering properties show the strength of the material. We can compute the different engineering properties by analysing the velocities using the same method as that for the rock physics

5.1.2.1 Young's Modulus

It is defined as "the ratio of the uniaxial stress over the uniaxial strain in the range of stress in which Hooke's Law holds". Young's modulus (E) is a measure of stiffness of an isotropic elastic material. Young's modulus, E, can be calculated by dividing the tensile stress by the tensile strain;

$$E = \frac{\sigma}{\epsilon}$$

The cross-section of Young's modulus is given in Fig 5.6. From the cross-section it can be seen that the values of Young's modulus increase progressively with the depth due to

overburden pressure, keeping in view this fact we can believe that reservoir rock has medium range values of the Young's modulus and we can identify them on the cross-section map, on the time scale around interval 2500 msec to 3000msec we could have hydrocarbon which can be estimated by the variation in the values horizontally. The range of Young's modulus is from 0.17 to 56 GPa. Young's modulus for limestone, shale and sandstone is given in Table 10.

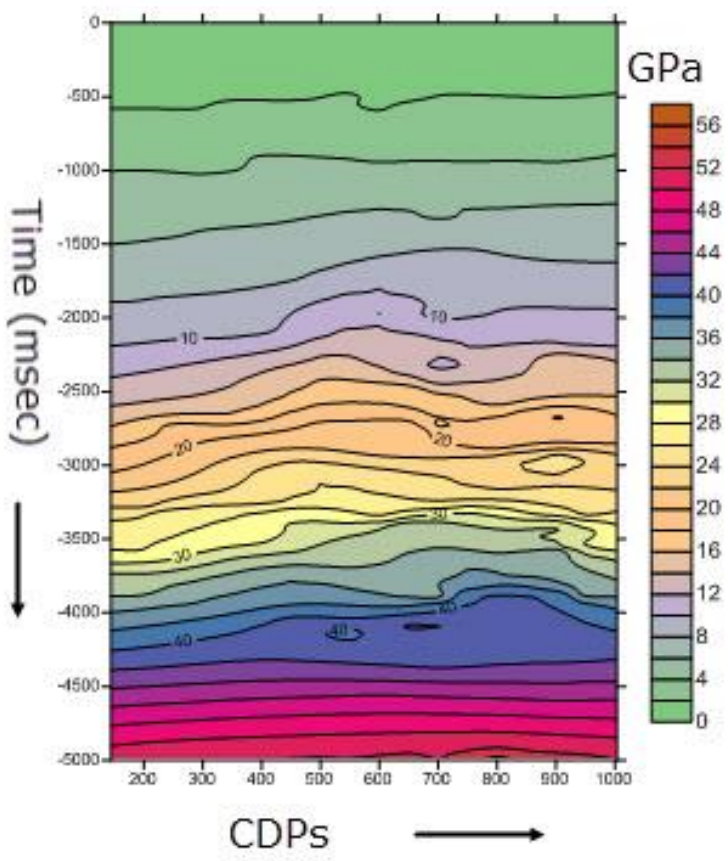

Figure 5.6 Young's Modulus cross section across seismic line 20017-BTM-02.

Table 10 Yong's Modulus for different lithologies.

Lithology	Value of Young's Modulus (GPa)
Limestone	15-55
Shale	1-70
Sandstone	1-20

5.1.2.2 Bulk Modulus

The bulk modulus (K) of a rock can be defined as the measures of the resistance of rock to uniform compression. It is the ratio of volumetric stress to volumetric strain. It describes the material's response to uniform pressure. Bulk modulus for different lithologies are given in Table 11.

Table 11 Bulk Modulus for different lithologies.

Lithology	Value of Bulk Modulus (GPa)
Sandstone	4.7
Shale	10
Limestone	65
Granite	50

The value of bulk modulus increases with the depth as it is followed by the cross section shown in Fig 5.7. An anomalous zone is observed between CDP number 450-750 which may be the indication of presence of hydrocarbon. Cross section of Bulk modulus is not so complex showing the regular deposition and low disturbed region tectonically.

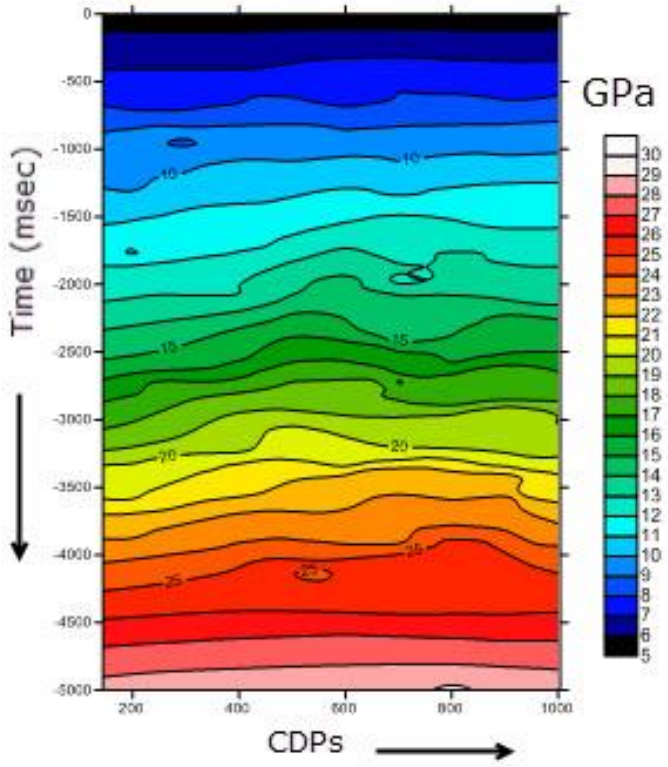

Figure 5.7 Bulk Modulus cross section of seismic line 20017-BTM-02.

5.1.2.3 Shear Modulus

The ratio of shear stress to the shear strain (angle of deformation) is termed as shear modulus. It signifies with the deformation of a solid when it experiences a force parallel to one of its surfaces while its opposite face experiences an opposing force such as friction.

Mathematically it can be calculated by using relation

$$\mu = \rho * Vs$$

μ = Shear modulus

ρ= Density

Vs= S-wave velocity

Table 12 Shear Modulus of different lithologies.

Material	Shear Wave Modulus
Loose sand	4.14-9.66
Medium dense sand	4.41-6.90
Dense sand	6.90-11.04
Silty sand	13.08-22.08

It describes the material's response to shear strain, shear modulus cross section of 20017-BTM-02 is shown in Fig 5.8, and color contrast shows variation in moduli value with time, the value of shear moduli increases as we move deeper due to its dependency upon the density. Shear Modulus for different lithologies are given in Table 12. Shear modulus in Fig 5.8 ranging from 0.20 to 23 GPa (Giga Pascal). An anomalous zone can be seen between CDP number 450-700 below the time 2500 msec which may be indication of hydrocarbon is shown in Fig 5.8.

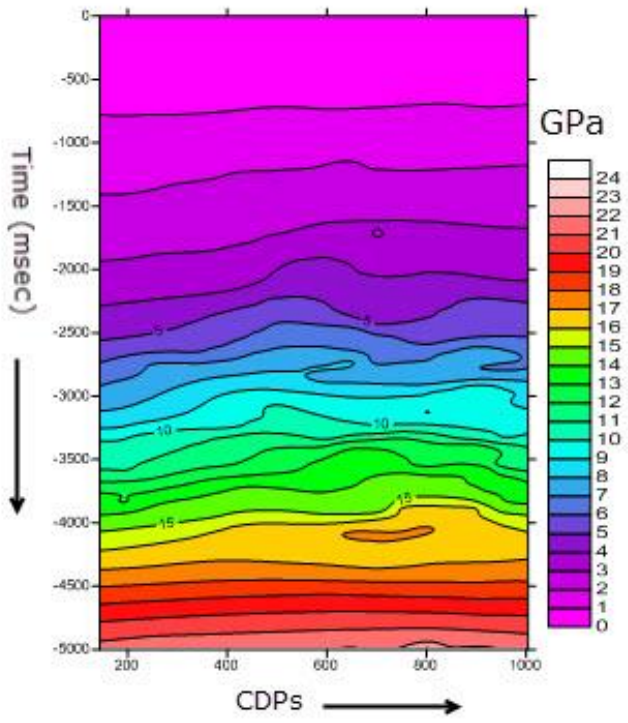

Figure 5.8 Shear Modulus of cross section of seismic line 20017-BTM-02.

5.1.2.4 Poisson's Ratio

This constant signifies the elastic properties of solid its value becomes zero in ideal liquid sand gases. Bulk modulus and Poisson's ratio logs show the opposite character because Poisson ratio can apply only on solids while Bulk modulus can apply on solids, liquids and gasses.

It is calculated by using the following formula:-

$$\sigma = \frac{0.5(Vp^2 - 2Vs^2)}{Vp^2 - Vs^2}$$

The cross section in Fig 5.9 shows that the value of Poisson ratio is decreasing as we move deeper, the case may arise due to the fact that there is less penetration of seismic waves in the deeper layer, thus will have low value of P-wave velocity. Poisson's ratio for different lithologies are given in Table 13. An anomalous zone is observed between CDP numbers 450-750 at the time of 2800 msec - 3200 msec which is the indication of presence of liquid or hydrocarbon.

Table 13 Poisson's Ratio for different lithologies.

Lithology	Poisson's Ratio
Limestone	0.20-0.30
Saturated Clay	0.40-0.50
Clay	0.30-0.45
Loose sand	0.20-0.40
Dense sand	0.25-0.40
Silty sand	0.20-0.40
Sand and gravel	0.15-0.35

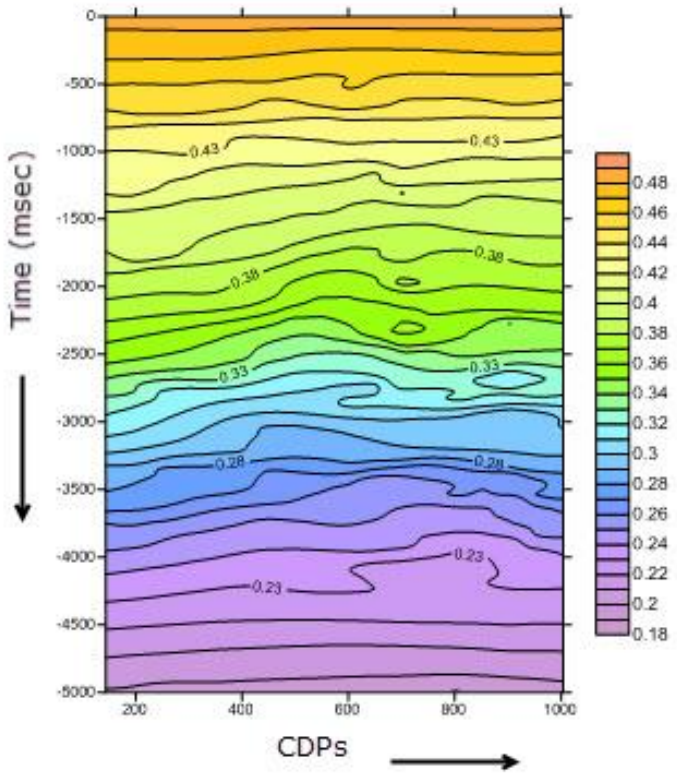

Figure 5.9 Poisson's Ratio cross section of seismic line 20017-BTM-02.

5.2 Seismic Attributes Analysis

Seismic attributes are the set of properties computed from the data which consists of the amplitude. Attributes can be computed on the basis of pre stacked data and post stacked data. The most common types of post stacked attributes are instantaneous attributes which are computed for every sample of the seismic trace.

The seismic energy is basically a mechanical energy which has two components:

- Kinetic
- Potential

Through experiment it has been found that kinetic component of the seismic energy has been measured. We need to measure the imaginary potential component for instantaneous attributes (Khan, 2010).

A measurable property of seismic data, such as amplitude, dip, frequency, phase and polarity. Attributes can be measured at one instant in time or over a time window, and may be measured on a single trace or set of traces from seismic data.

5.2.1 Essential of Seismic Attributes

The increasing reliance on seismic data requires that we gain the most information possible from the seismic reflection data. It empower interpreters to obtain more information from seismic data. Seismic geomorphology uses seismic attributes to extract geomorphologic insight using 3-D datasets. Amplitude is the default attribute of Seismic reflection data for the determination of physical parameters like reflection coefficients, velocities etc. The phase component is the principal factor in determining the shapes of the reflectors and their geometrical configurations. Fig 5.10 explains the true behaviour of complex seismic trace.

Attribute computations decompose seismic data into constituent attributes. There are no rules governing how attributes are computed. They are applicable in checking seismic data quality-identifying artifacts, petroleum prospect identification, hydrocarbon play evaluation and reservoir characterization. Any quantity calculated from seismic data can be considered an attribute. Thus attributes are of many types: pre-stack, post-stack, inversion, velocity, horizon, multicomponent 4-D.

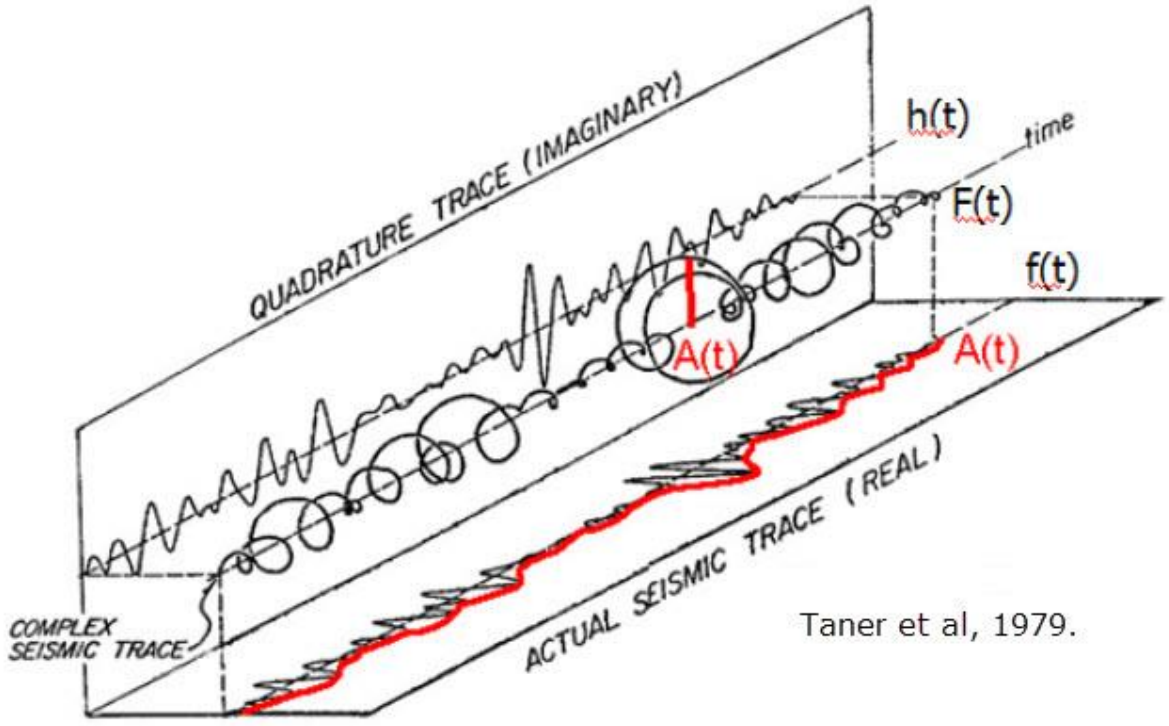

Figure 5.10 Isometric diagram for complex seismic trace showing Real (red) and Imaginary components of complex seismic trace.

5.2.2 Hilbert Transform

Hilbert Transform is introduced by David Hilbert to solve special case of the Riemann-Hilbert problem for holomorphic functions. It is used in seismic attribute analysis and electrical engineering. The Hilbert transform is generally introduced as a convolution between a real signal *f(t)* and *1/πt* as given below;

$$h(t) = \frac{1}{\pi t} * f(t) = \frac{1}{\pi} \int_{-\infty}^{\infty} \frac{f(\tau)}{t-\tau} d\tau$$

The Hilbert transformed signal *h(t)* represents the imaginary part of the real signal *f(t)*.

The imaginary component is basically a 90 degree phase rotated version of real component of seismic trace, therefore can be computed through Hilbert Transform (Taner et al. 1979).The Hilbert Transform of the real seismic trace is generates an imaginary trace and using both these traces the envelope trace is computed. Fig 5.11 shows the real trace and quadrature trace(imaginary) of complex seismic trace along with reflection strength real seismic trace. Reflection strength seismic trace which will always be positive.

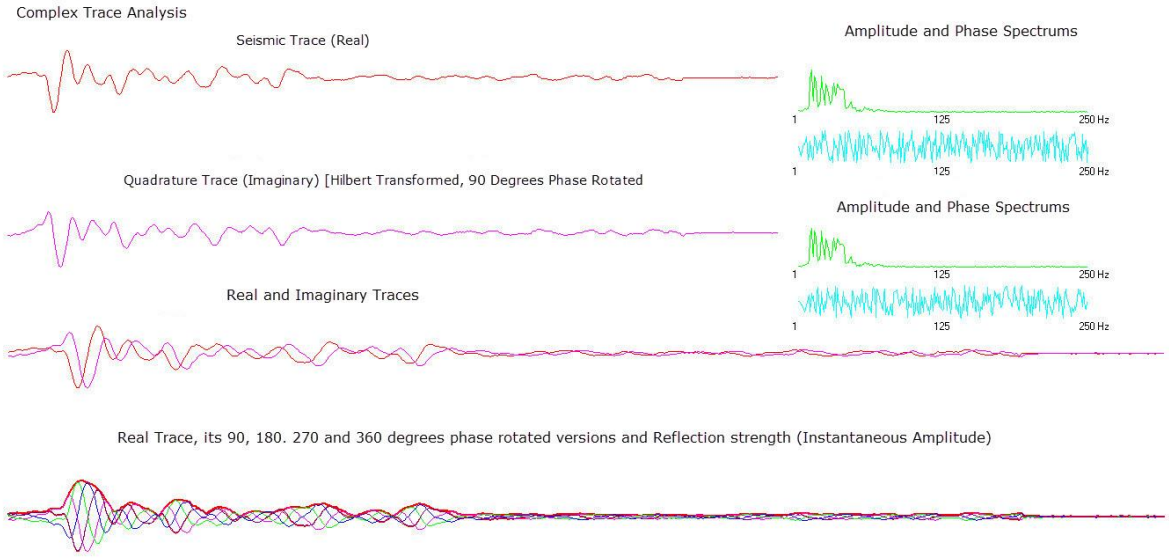

Figure 5.11 Detailed Seismic Complex trace Analysis along with amplitude and phase spectrum.

5.2.3 Reflection Strength Attribute

Reflection strength attribute usually considered as envelop of a trace which represents the total instantaneous energy of the complex seismic trace which is independent of the phase. It is also termed as instantaneous amplitude attribute. First derivative of the envelope shows the

variation of the energy of the reflected events. It is used to detect the possible fracturing and absorption effects. While the second derivative determines the measure of the sharpness of the envelop peak. Mathematically it is computed using the relation given below;

$$A(t) = \sqrt{f^2(t) + h^2(t)} = |F(t)|$$

Where A(t) is amplitude of the seismic trace, f(t) real component, h(t) quadrature component and F(t) is the amplitude of imaginary trace. The behaviour of the instantaneous amplitude wavelet respective to seismic trace is shown in Fig 5.11.The envelope relates directly to the acoustic impedance contrasts. It can be used as an effective tool of distinction for the following characteristics:

- Bright spots, possibly gas accumulation.
- Sequence boundaries.
- Thin bed tuning effects.
- Major changes in depositional environment.
- Spatial correlation to porosity and other lithological variations.

The attribute is computed for seismic line 20017-BTM-02 to see the major changes in lithologies. Even negative reflection coefficients such as limestone formation overlaid on clay formation would generate a positive response in this attribute. Fig 5.12 shows the envelope attribute map of 20017-BTM-02. The thick (yellow) packages indicate the maximum reflection strength corresponding to the source, reservoir and seal rocks. It also shows spatial patterns representing changes in the limestone thickness and breakage due to the faults. In this case not every patch is scattered due to fault these weak reflections may because of interbedded sands or shale.

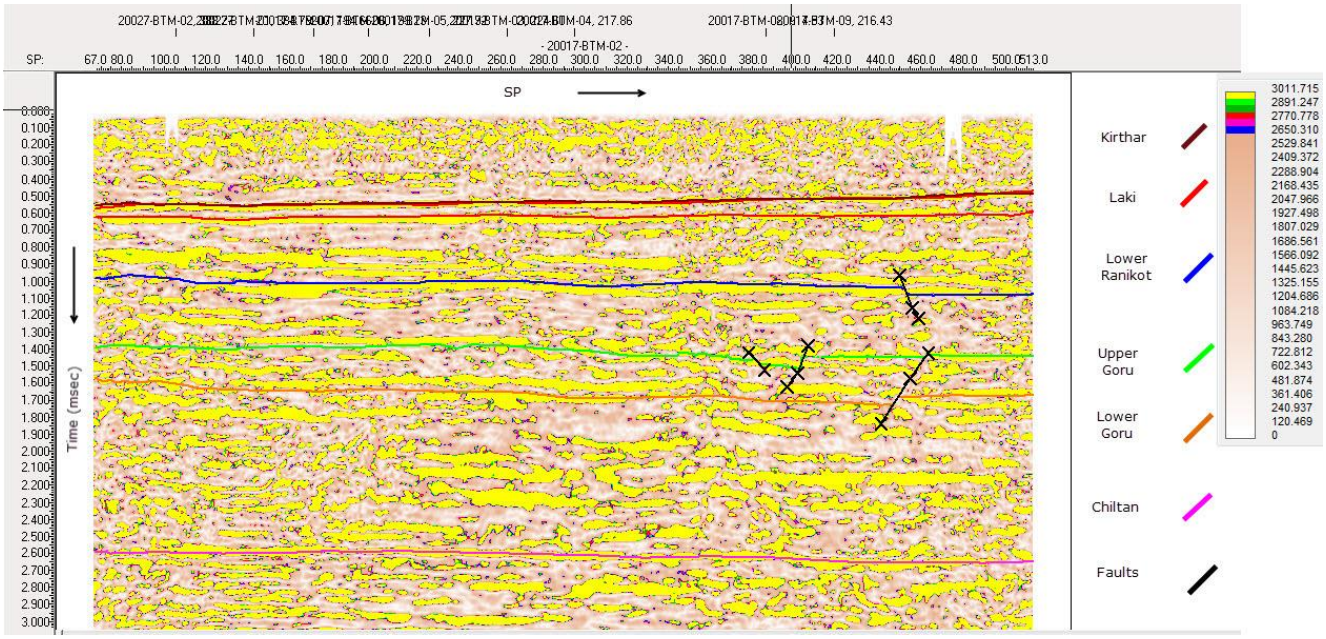

Figure 5.12 The Trace Envelope or Reflection Strength Attribute of seismic line 20017-BTM-02 with marked reflectors and faults.

5.2.4 Instantaneous Phase Attribute

Wave fronts are the lines of constant phase, the phase attribute is one of the physical attribute and can be conveniently used for geometrical shape discrimination. It computes the phase for each seismic trace. It provides the measure of continuity of the reflector. The phase information is independent of seismic trace amplitudes and relates to the propagation of phase of the seismic wave front. It is computed from real and imaginary seismic traces using a mathematical relation as given below;

$$\Theta(t) = \tan^{-1}[h(t) / f(t)]$$

Where h(t) and f(t) are real and imaginary components of the seismic complex trace respectively.

Two different versions of instantaneous phase have been computed; one is for normalized maximum amplitude that is 1 and other is for amplitude 0.2, to clarify the independency of amplitude on phase shown in Fig 5.13 and Fig 5.14 respectively. It can be seen that with the decrease in amplitude the second trace shows very weak events while instantaneous phase remain undisturbed.

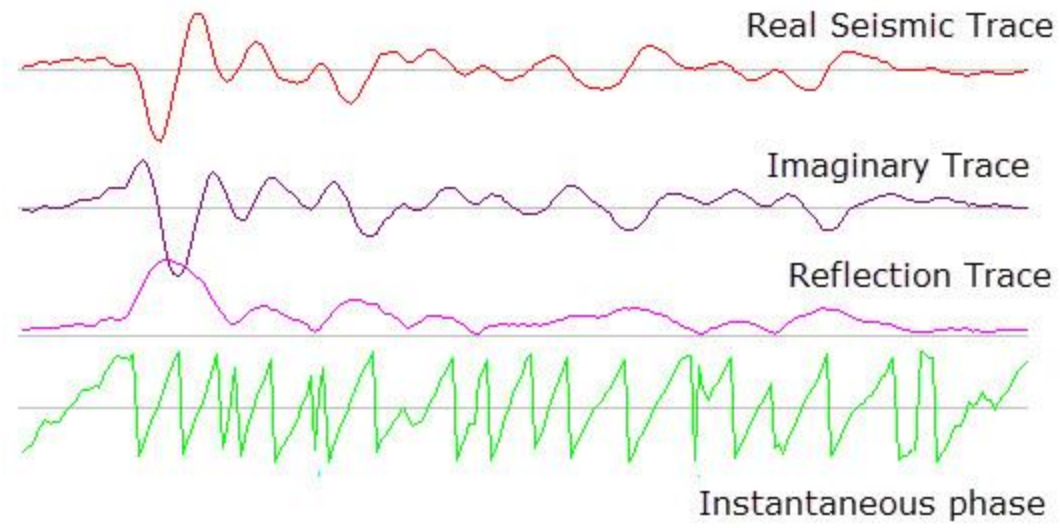

Figure 5.13 Seismic trace generated for amplitude 1 showing instantaneous phase variation respective reflection strength generated using Wavelets.

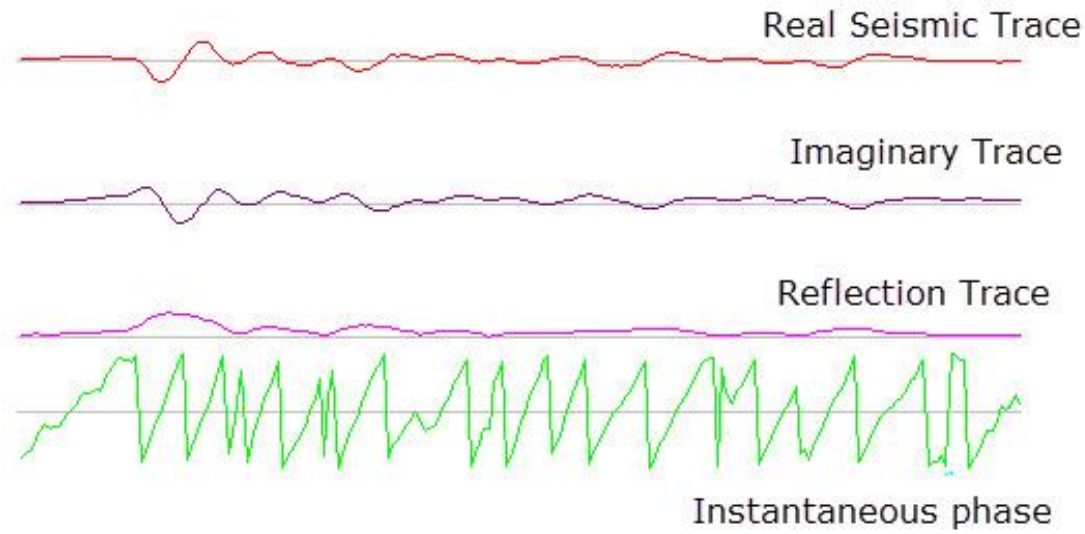

Figure 5.14 Seismic trace generated for amplitude 0.2 showing instantaneous phase variation respective reflection strength generated using Wavelets.

Now it is clear and proved that instantaneous phase is independent of amplitude.

Instantaneous phase used for following purposes:

- Efficient indicator of reflector continuity.
- Relates to the phase component of wave propagation.
- Complete visualization of the stratigraphic events.

Time derivative of the phase attribute give rise to the new attribute termed as instantaneous frequency. In this attribute displays, the phase corresponding to each peak, trough, zero

crossing, etc. of the real trace is assigned the same colour so that any phase angle can be followed from trace to trace. It can be used to highlight interface in sections with high decay of amplitudes and even highlight deeper horizons which are not visible in the normal amplitude sections. Figure 5.15 shows the instantaneous phase attribute which changes from -180^0 to $+180^0$. In this display plus and minus 180 degrees are the same color (purple) because they are the same phase angle. The interpreted horizons lie over the zero phase regions indicated by different colors. In color bar negative value indicating negative phase. It can be observed in comparison to amplitude based sections that the instantaneous phase shows much deeper horizons.

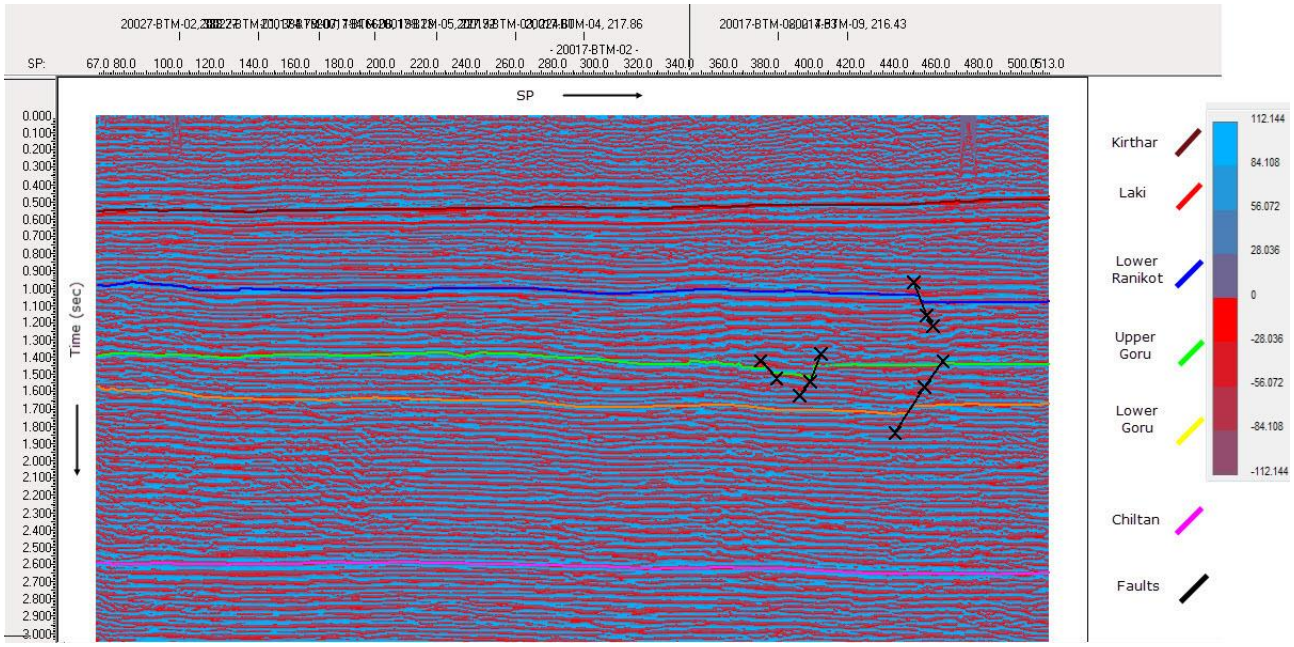

Figure 5.15 Instantaneous Phase Attribute of seismic line 20017-BTM-02 with marked reflectors and faults.

5.2.5 Apparent polarity Attribute

Some of the instantaneous attribute like instantaneous frequency show very sharp and crispy signature therefore are difficult to interpret. Thus wavelet attributes are computed over each cycle of the seismic trace (Khan, 2010).

Apparent polarity shows the blocky nature as it represents the average value over each cycle in the seismic trace which can be observed in Fig 5.16. Each peak in the reflection indicates the cycle.

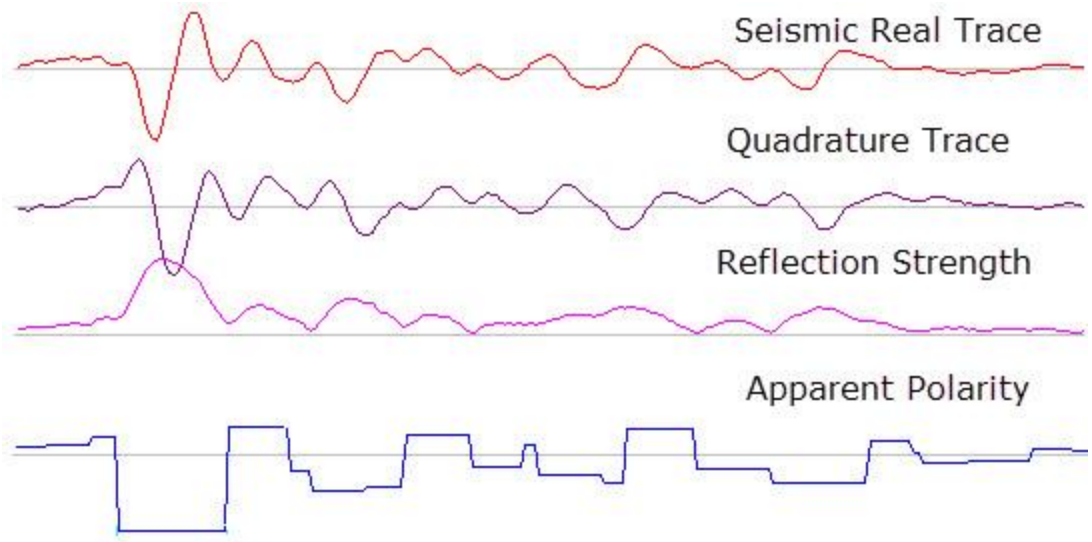

Figure 5.16 Behaviour of Apparent polarity respective to seismic real trace and reflection strength generated using Wavelets.

The procedure of obtaining the blocky behaviour is dependant of:

- Peak value of the reflection strength trace
- Nature either its peak or trough of the real seismic trace.

The wavelet attributes are calculated at the peak of the envelope, which represents the attributes of the wavelets within a zone defined by the trace envelope minima. These attributes indicate spatial variation of the wavelets and therefore relate to the response of the composite group of individual interfaces below the seismic resolution. The attribute individually highlights the seal, reservoir and source rocks as shown in Figure 5.17. Negative value in the colour bar indicating trough region of the seismic trace.

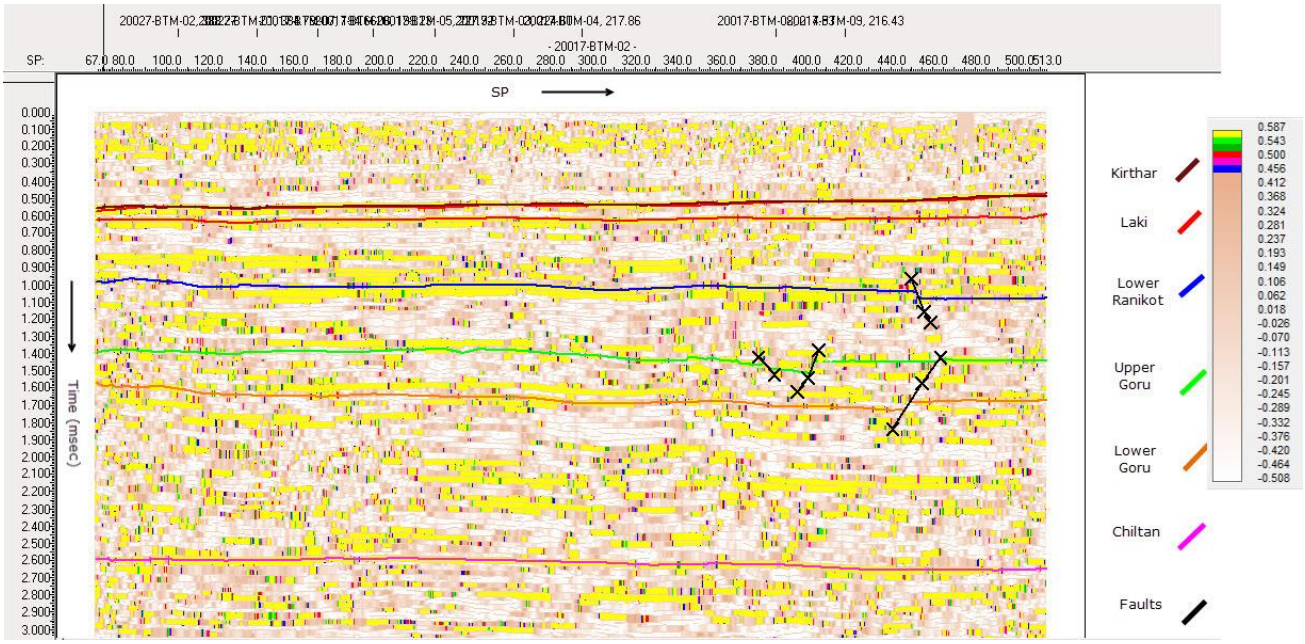

Figure 5.17 Apparent Polarity Attribute for seismic line 20017-BTM-02 showing the reflectors and faults.

5.2.6 Basic Principles for Seismic Attributes

Using too many attributes will create problems instead of solving the issues. Unnecessary attributes are thus duplicates, or they are obscure or unreliable. Review the attributes in light of these following principles:

- Seismic attributes should be unique. When multiple attributes measure the same property, choose the one that works best.
- Never use seismic attribute without having knowledge about it.
- Seismic attributes represents subsets of the information in the seismic data. Quantities that are not the subsets are not the attributes.
- Attributes that differ only in resolution are the same attribute.
- Avoid overlay sensitive attributes.

5.3 Complex Velocity Model Building

The seismic method is controlled by velocities, which is dependant of density and elastic moduli of rocks. In 1968, Penne baker was one of the first who used velocities as a tool of interpretation. Being a drilling professional and not a geoscientist, he was interested in technological innovation problems such as drill-bit use and irregular pressure.

Velocity is a macroscopic (wavelength-scale average) property of the rock depending upon the density and elastic properties of the minerals making up the lithology. Velocities are generally required for:

- Dynamic corrections
- Migration
- Time to depth conversion
- Rock physics analysis (porosity determination, fluid type and it's saturation)

The velocities measured from any source are eventually turned into interval velocities which in turn are associated with particular lithologies. A velocity model is generated when interval velocities are properly associated with their corresponding lithologies. This model is further used for different applications.

We usually use velocities to stack and migration of seismic data, time to depth conversion of seismic section and time contour maps to depth contour maps. Mostly the velocities are measured from velocity analysis where stacking velocities are directly calculated from common depth point (CDP) stacks and common velocity analysis method are constant velocity stack (CVS), vertical seismic profiling (VSP) and check shot survey. (Taner & Koehler, 1969)

However, borehole velocities provide efficient correlation and control for calibrating the seismic velocities (Khan & Akhter, 2011). Thus the development of a velocity model includes more accurate processing interpolation and calibration method.

5.3.1 Seismic Velocity Calibration

Seismic is the main source of velocity distribution and therefore the seismic velocities need to be strengthened through calibration using more accurately calculated borehole velocities. Calibration needs both seismic and borehole velocities to be unique regarding resolution, sampling interval and nature of velocity. The borehole velocities of Fateh_01 are processed, smoothed and sub-sampled to calculate the velocities of seismic line 20017-BTM-09 with regards to resolution. The final log based velocities are then used to adjust the seismic velocities.

A flow chart shown in Fig 5.18 originally contrived by (Khan & Akhter, 2011) reveals the whole process for the calibration of velocities and modeling. It is the best explaining diagram which determines the every single step of velocity modeling.

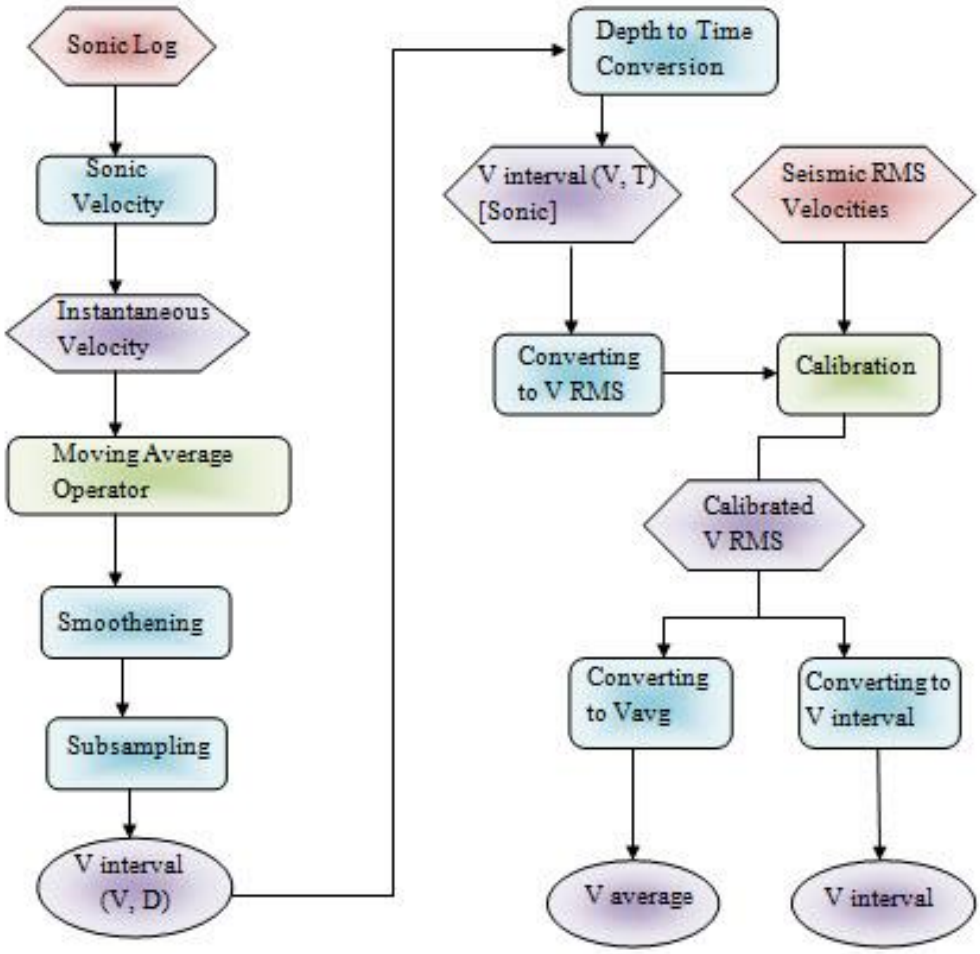

Figure 5.18 Flow chart of velocity data management, analysis and presentation.

5.3.2 Velocity Interpolation and Modeling

The seismic velocity provides the base for seismic time to geological depth techniques. The first step towards the depth conversion is acquiring the best reliable velocity information. The velocity needs to be developed which can be used in many applications. This development is based on interpolation and smoothening of calibrated velocity functions. Work flow of velocity modeling using two interpolation techniques and their applications is described in Fig 5.19.

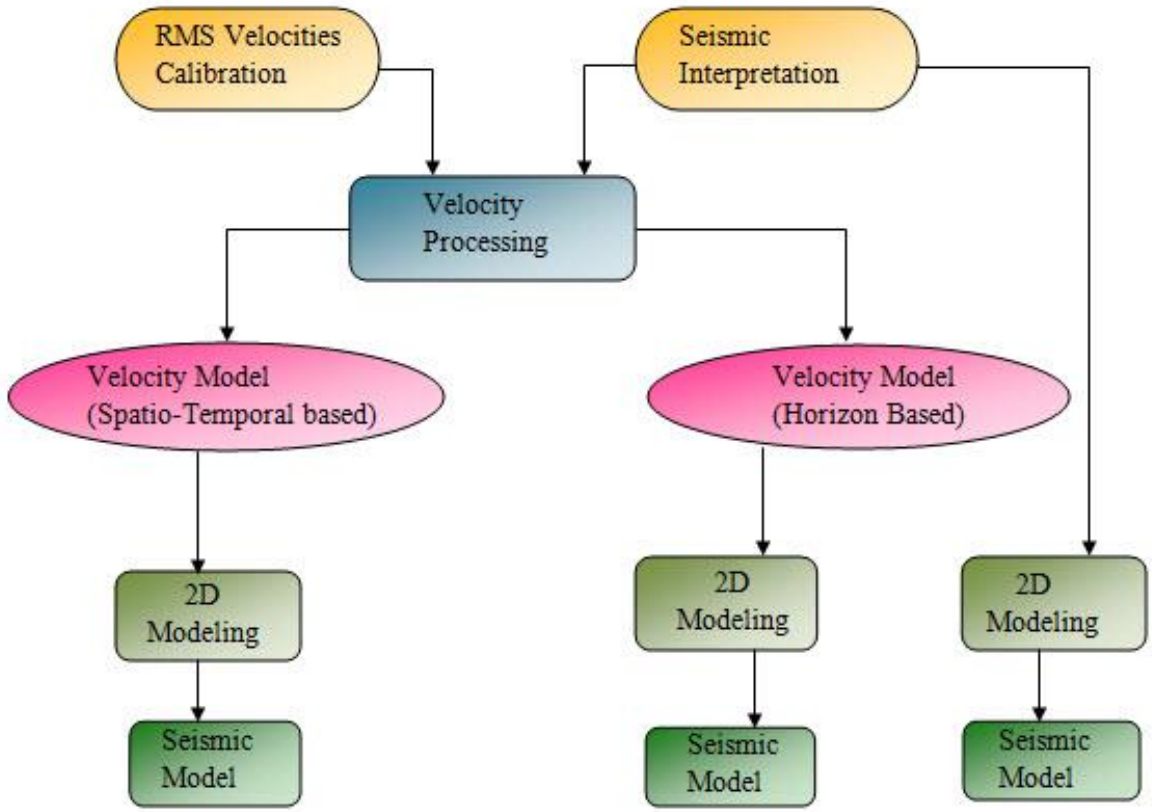

Figure 5.19 Complete workflow for velocity techniques and their applications in generating Seismic Model.

5.3.2.1 Spatio-Temporal Interpolation

The input RMS velocity functions are customarily velocity-time pairs (VT-Pairs) without fixed time intervals. The temporal (vertical) interpolation at 100 milliseconds is used to get velocity functions with VT-Pairs after regular time interval. The spatial (horizontal) interpolation is used to create at desired CDP for every 10^{th}. The moving regular operator of 3 or 5 is used along each function for smoothing. This generates the spatio-temporal inserted Vrms. These Vrms (Sky-Blue) are then converted into Vint (Dark Green), Vavg (Dark Blue) velocities and Vrms nodes(Red) are shown in Figure 5.20.

5.3.2.2 Horizon Interpolation

The horizon interpolation is more complex criteria because it requires input of interpreted reflectors along with the velocity data. The velocity is interpolated along these reflectors. It requires computation of nodes for each reflector at the particular CDP interval. VT pairs are then interpolated at these nodes to create velocity functions. This type of velocity models are widely used for velocity modeling and Pre-Stack Depth Migration (PSDM). The velocity

model established by this strategy closely matches the subsurface structure as shown in Fig 5.21.

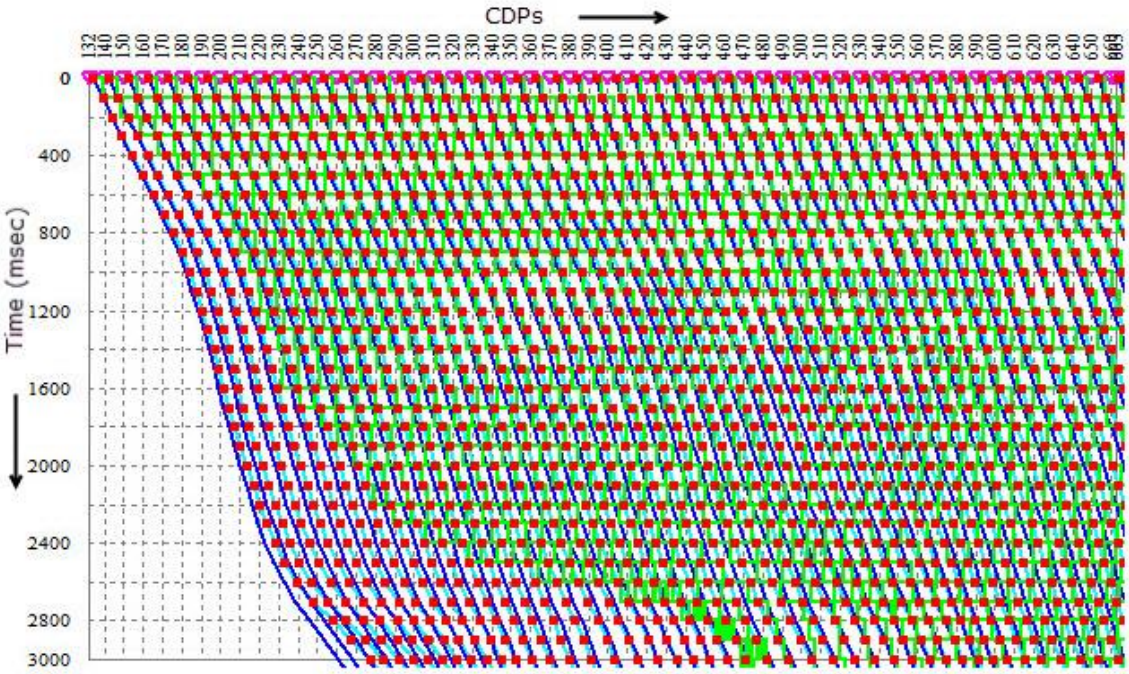

Figure 5.20 Spatio-temporal Velocity Model at temporal interpolation every 100 milliseconds and spatial interpolation at CDP interval 10 of seismic line 20017-BTM-09.

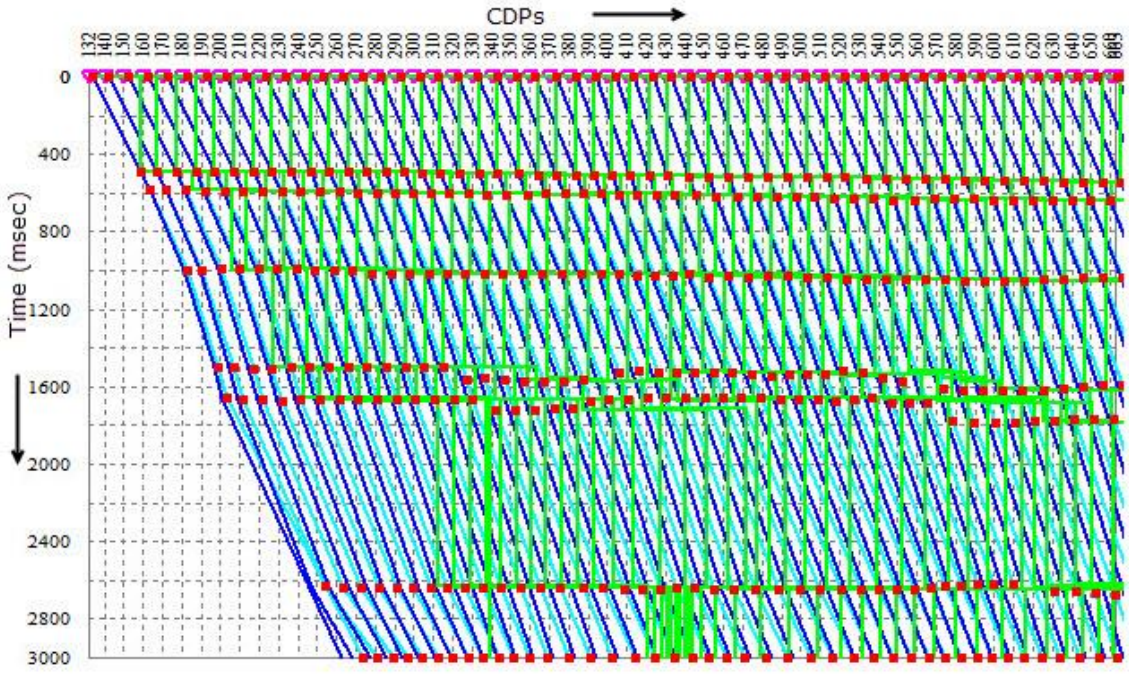

Figure 5.21 Velocity Model interpolated for velocity functions at every 10th CDP along the interpreted reflectors.

5.3.3 2D Seismic Modeling

2D seismic model is generated for 20017-BTM-09 by using three techniques. Two of them are generated from the velocity model, while the third is produced through interpreted seismic depth section for horizon reflection coefficient based which is explained already in chapter 4 with detail. In all these techniques a Ricker Wavelet of 35 Hz frequency without any amplitude decaying function is used as a source shown in Fig 5.22.

The wavelet is convolved with velocity model on interpreted time sections at every 10 CDP to generate a seismic section. Two of these three seismic modeling techniques are described with detail below.

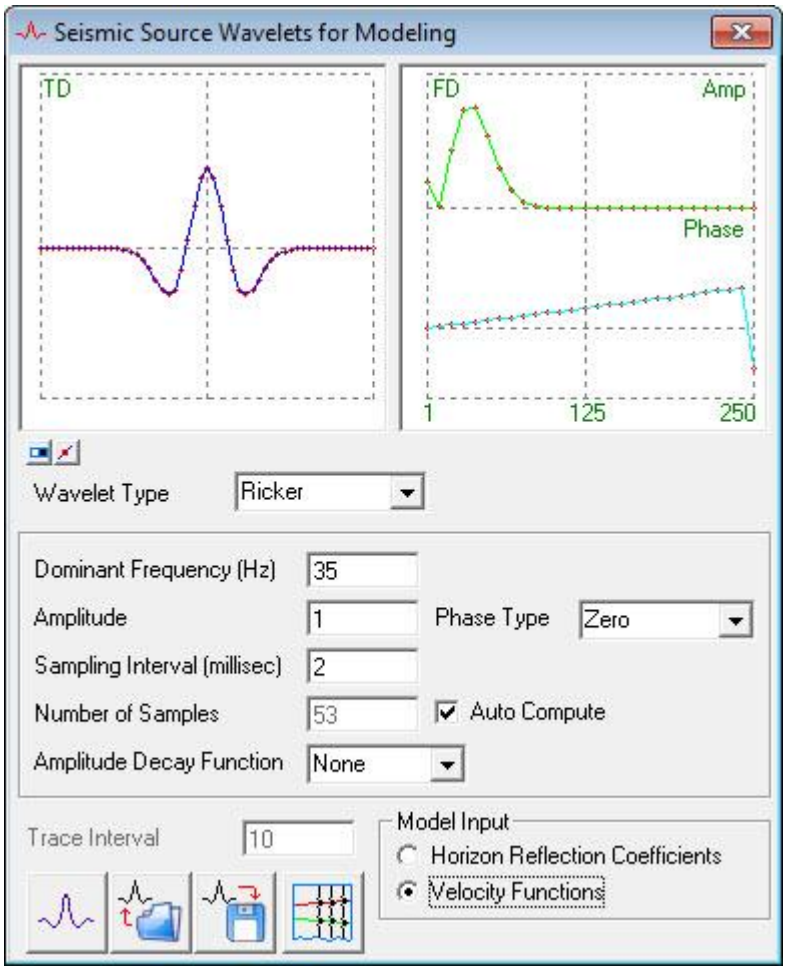

Figure 5.22 Seismic source wavelet generation at zero phase without amplitude decay function.

5.3.3.1 Seismic Model Based on Spatio-Temporal Velocity Interpolation

The spatio-temporal interpolated velocity model is used as input. The RMS velocity functions are converted into interval velocity functions. The interval velocity functions are used to

generate reflectivity sequence which convolved with the source wavelet to generate seismic records developing a 2D seismic model. It can be seen that the seismic section generated from this technique does not display any structural feature as shown in Fig 5.23. This indicates that structural information contained in original velocity functions is missing due to spatio-temporal interpolation. Thus spatio-temporal interpolated velocity model cannot be used in modeling and rock physics applications but can be used in time to depth conversion.

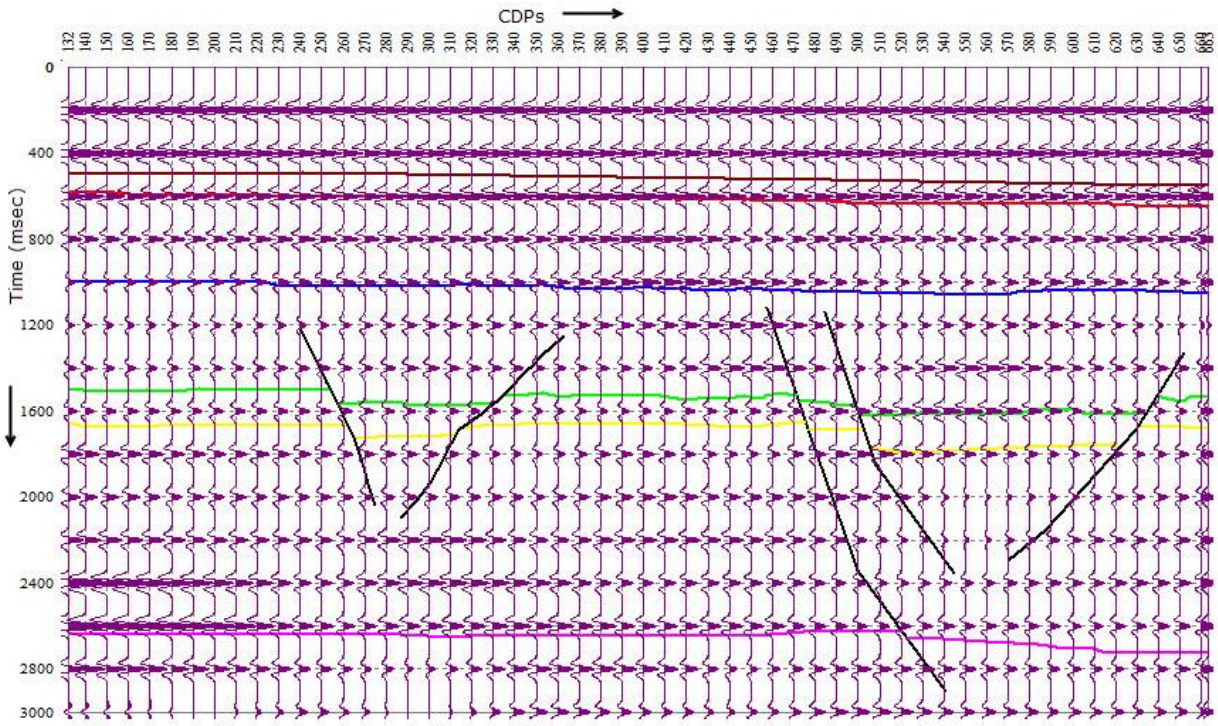

Figure 5.23 2D seismic model generated by using spatio-temporal velocity interpolated model of 20017-BTM-09 are displayed in purple colour while horizons are with different colours and faults (black).

5.3.3.2 Seismic Model Based on Horizon Velocity Interpolation

The basic modeling process is the same as mentioned in the previous section, except horizon interpolated velocity model is used as input. The modelled seismic section generated by this technique is shown in Fig 5.24. It can be noticed that this seismic model reveals affordable sub-surface picture clearly illustrating some structures. However some closely packed layers are beyond the resolution of seismic velocities.

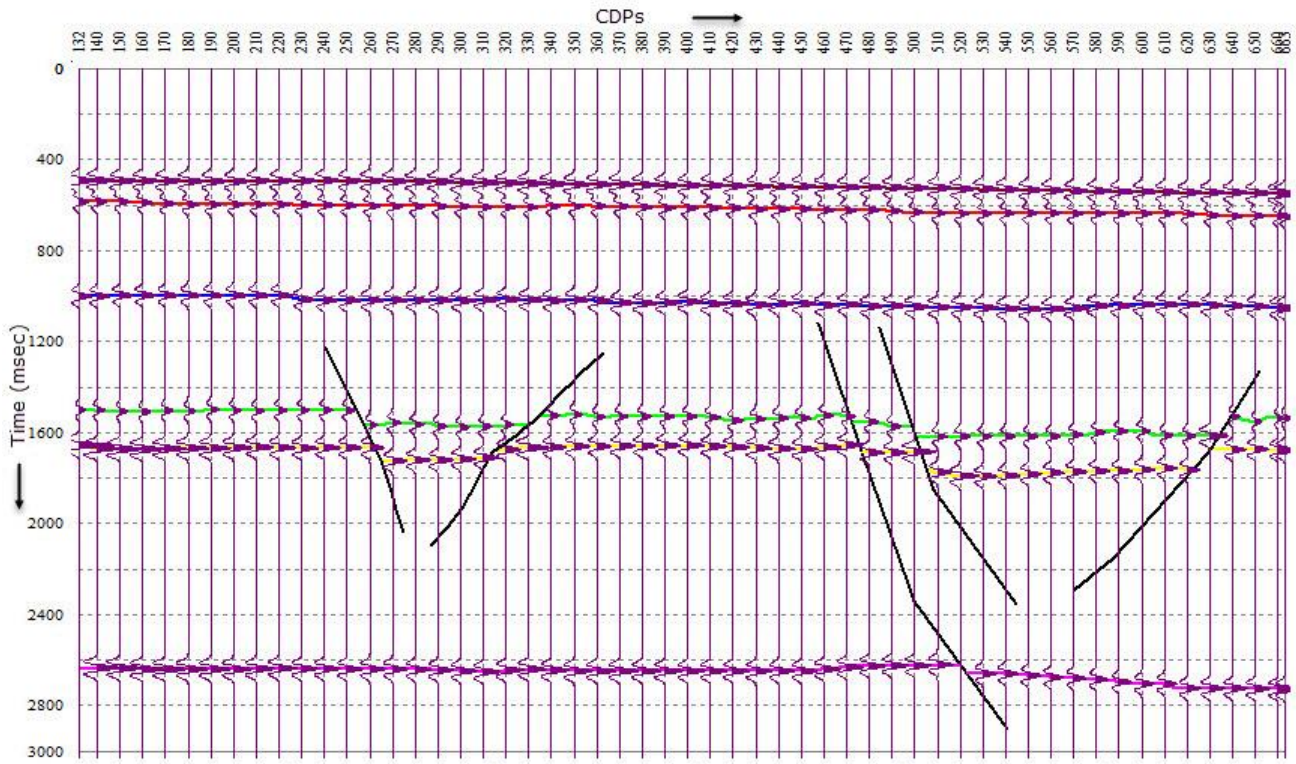

Figure 5.24 2D seismic model generated by using horizon velocity interpolation.

5.4 Conclusions

Rock physics studies has confirmed the presence of anomalous zone across the seismic line 20017-BTM-02. Most stratigraphic interpretation begins with the interpretation of structure. Color-encoded displays of attribute values aid in interpretation, correlation and the offset of the patterns helps establish throw across faults. The principle interest in the attribute interpretation was to get acknowledge by the variation along the bedding. Lateral variations in the section suggested stratigraphic or other changes. Getting familiar with the geology help in finding the significance especially in low frequency zones to define the limits of productive concession.

2D seismic model based on spatio-temporal velocity interpolation and horizon velocity interpolation have been generated as discussed in earlier sections. It can be observed that 2D seismic model based on spatio temporal velocity interpolation does not demonstrate subsurface structure so it can't be used in velocity modeling and rock physics analysis, though it can be used for time to depth conversion. Contrary to this, 2D seismic model based on horizon velocity interpolation displays the real subsurface structure which authenticate the interpretation.

Chapter 6

6. Amplitude versus Offset/Angle Modeling

6.1 Introduction

Fluid substitution is a vital component of the seismic rock physics analysis such as Amplitude versus Offset/Angle (AVO/AVA). It provides a tool for fluid identification and quantification in reservoir and is commonly performed using Gassmann's equation (Gassmann, 1951).

This equation is based on several assumptions; rock is homogeneous and isotropic, and that the pore space is completely connected. These assumptions are violated if the rock framework is composed of multiple minerals with large contrasts in elastic stiffness (Berge, 1998). However, Gassmann's equation is free of assumptions about pore geometry, although the pore system must be connected and fluids must be moveable.

The objective of fluid substitution is to model the seismic properties; seismic P & S wave velocities and density of a reservoir at a given reservoir condition such as pressure, temperature, porosity, mineral type, and water salinity as well as pores fluid saturation. Gassmann's equations can model various fluid scenarios such as 100% water saturation or hydrocarbon with only oil or only gas saturation and generates P and S wave velocities and density of the reservoir with changing fluid conditions.

6.2 Input Parameters for Petrophysical Logs

The petrophysical log of Fateh-01 has been used to calculate the V_P, Vs and RHO_B of Upper Goru and Lower Goru formations. The LAS file is loaded in the Wavelets software for the specific zone in which the required formations data exist. V_P is calculated using the DT log and then using the empirical relations Vs and RHO_B has been calculated. The detail of different parameters has been given in Table 14.

V_P is calculated for the depth range of 1700 to 2100 meters in which the reservoir sands and seal shale are present. Then using the Blocky average tool in the wavelets software the average values of the interval velocities of the shale and sand layers have been computed which is shown in Fig 6.1.

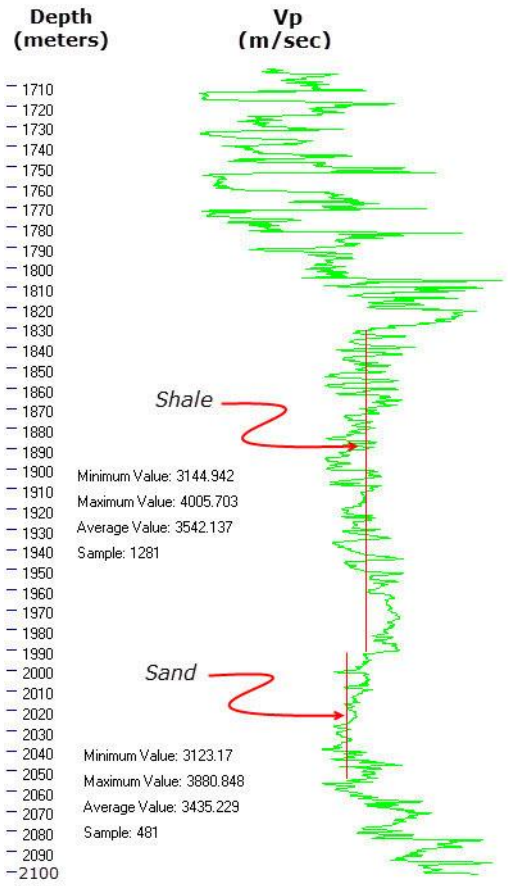

Figure 6.1Primary velocities calculate using DT log for 1700 m to 2100 m depth range of Fateh-01 using Wavelets software.

6.2 Zoeppritz Energy Partition Equations

The partition of energy when a plane wave hits an interface between two layers of varying velocities and densities is expressed by Zoeppritz equations. (Sheriff and Geldart, 1995). When the incident angle is not zero, four waves are generated: reflected P-wave and S-wave and transmitted P-wave and S-wave as shown in Fig. 6.2. The Zoeppritz equations were not the first to describe the amplitudes of reflected and refracted waves at a plane interface. Cargill Gilston Knott used an approach in terms of potentials almost 30 years earlier, in 1899, to derive Knott's Equations. Both approaches are valid but Zoeppritz approach is more easily understood.

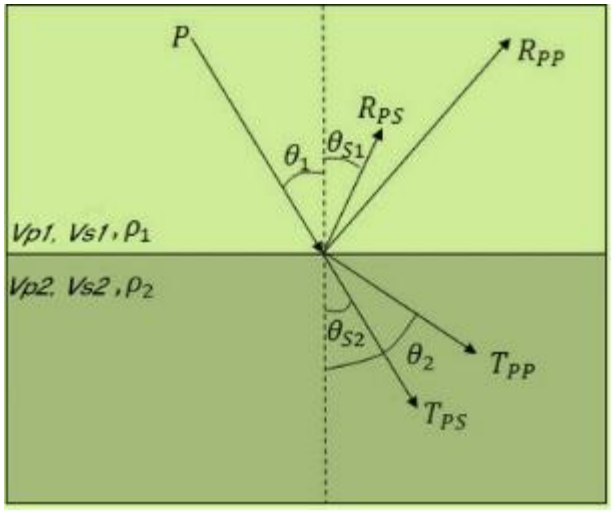

Figure 6.2 Partition of Energy when a P is incident at an interface with an angle.

The Zoeppritz equations give the amplitudes (reflection coefficients) R_P, R_S, T_P, and T_S of the reflected P- and S-waves and the transmitted P- and S-waves respectively and are given in matrix form as:

$$\begin{bmatrix} \cos\theta_{P1} & -\sin\theta_{S1} & \cos\theta_{P2} & \sin\theta_{S2} \\ \sin\theta_{P1} & \cos\theta_{S1} & -\sin\theta_{P2} & \cos\theta_{S2} \\ Z_1\cos 2\theta_{S1} & -W_1\sin 2\theta_{S1} & -Z_2\cos 2\theta_{S2} & -W_2\sin 2\theta_{S2} \\ \frac{V_{S1}}{V_{P1}}W_1\sin 2\theta_{P1} & W_1\cos 2\theta_{S1} & \frac{V_{S2}}{V_{P2}}W_2\sin 2\theta_{P2} & -W_2\cos 2\theta_{S2} \end{bmatrix} \begin{bmatrix} R_P \\ R_S \\ T_P \\ T_S \end{bmatrix} = \begin{bmatrix} \cos\theta_{P1} \\ -\sin\theta_{S1} \\ -Z_1\cos 2\theta_{S1} \\ \frac{V_{S1}}{V_{P1}}W_1\sin 2\theta_{P1} \end{bmatrix}$$

Where $Z_i = \rho_i V_{Pi}$, $W_i = \rho_i V_{Si}$.

6.3 Amplitude versus Offset/Angle (AVO/AVA)

AVO is the finger print of lithology and fluid. It has been found that Gas-sand reflection coefficients generally become more negative with increasing offset. High Gas Oil Ratio (GOR) light oil-saturated rocks may exhibit significant AVO anomalies. For large negative P-wave reflection coefficients, gas-sand and brine-sand reflection coefficients are distinct for all shale velocities. *Lower the shale velocity, greater the separation.* On the other hand for large positive P-wave reflection coefficients, gas-sand and brine-sand reflection coefficients are well separated only for the lowest shale velocities. These properties are used to model reflection coefficients for gas and brine saturated reservoirs.

Offset is a surface data acquisition geometry based parameter we record seismic data as a function of offset, while the angle defines the subsurface direction at which the seismic ray strikes the horizon of interest, with respect to its normal. Zoeppritz equations and all its

approximations are dependent on angle therefore the surface offsets (AVO) must be transformed into angle of incidents (AVA). There is a nonlinear relationship between offset and angle and the link between AVO and AVA is ray tracing in overburden as shown in Fig 6.3.

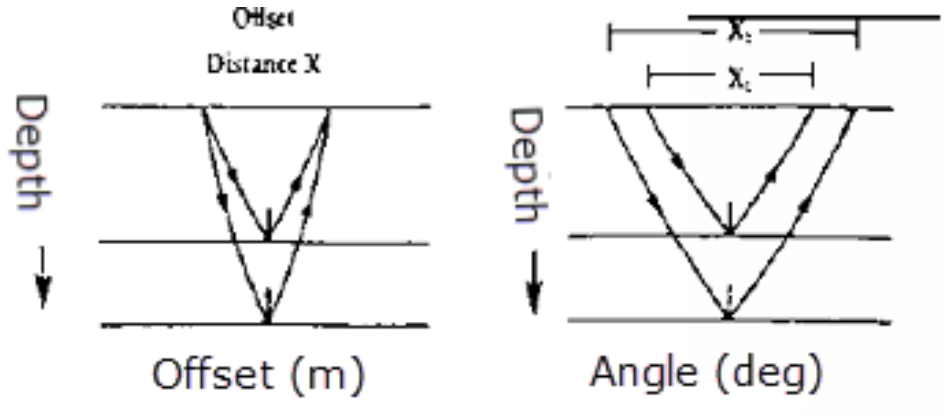

Figure 6.3 Relationship between Offset and Angle demonstrated through Ray-Tracing.

6.4 Gassmann Fluid Substitution and AVO Modeling of Bitrisim Reservoir

The complete processing workflow for Gassmann Fluid Substitution and AVO/AVA Modeling of Bitrisim reservoir is given in Fig 6.4. The petrophysical logs along with seismic velocities are used to get the P wave velocity and density for the Upper Goru formation (Shale) and the Lower Goru reservoir (Sandstone). S wave velocities for the two formations are then determined using rock physics empirical relations. The P wave velocity, S wave velocity and density of the reservoir are input to the Gassman Fluid Substitution program to model various fluid scenarios; water saturated, oil saturated or gas saturated. In the current study our interest is to derive models for water saturated and gas saturated reservoir. The derived P & S wave velocities and densities, for both water and gas saturated cases, are then input to the Zoeppritz equations for computing reflection coefficient curves as a function of angle of incidence.

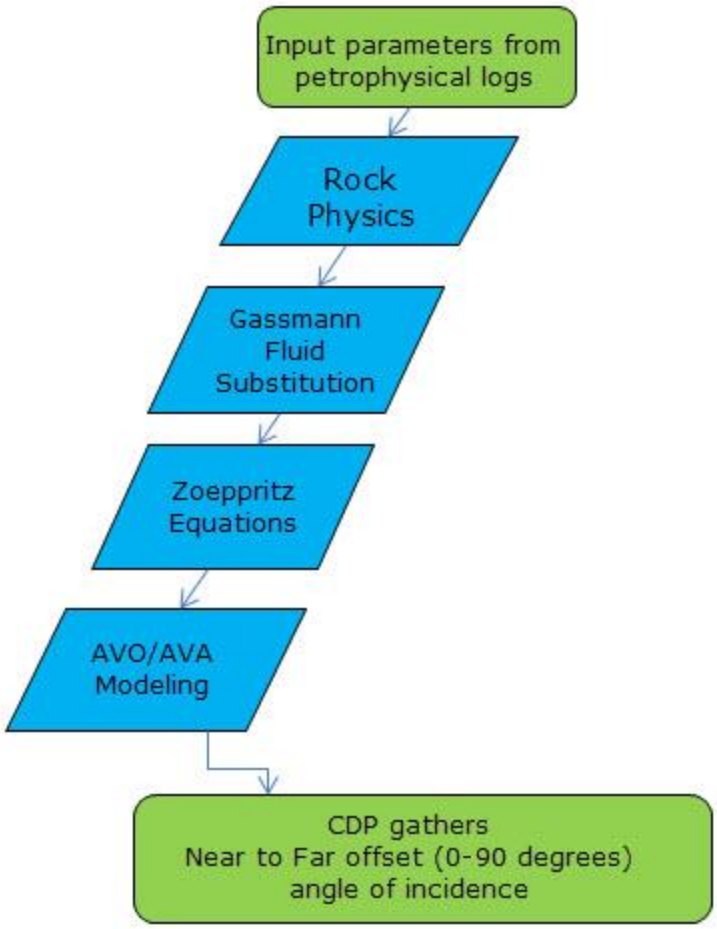

Figure 6.4 The Processing flowchart of Gassmann Fluid Substitution and AVO/AVA Modeling.

The input parameters for Gassmann fluid substitution are derived from well data and petrophysical logs. Fig 6.5 shows the Gassmann fluid substitution program along with input parameters and computed results for water, oil and gas saturated reservoirs.

These parameters include;

- Oil & Gas API Gravity
- Pressure
- Temperature
- Porosity
- Water saturation
- Salinity
- Volume of shale
- Gas Oil Ratio
- P & S wave velocities
- Density

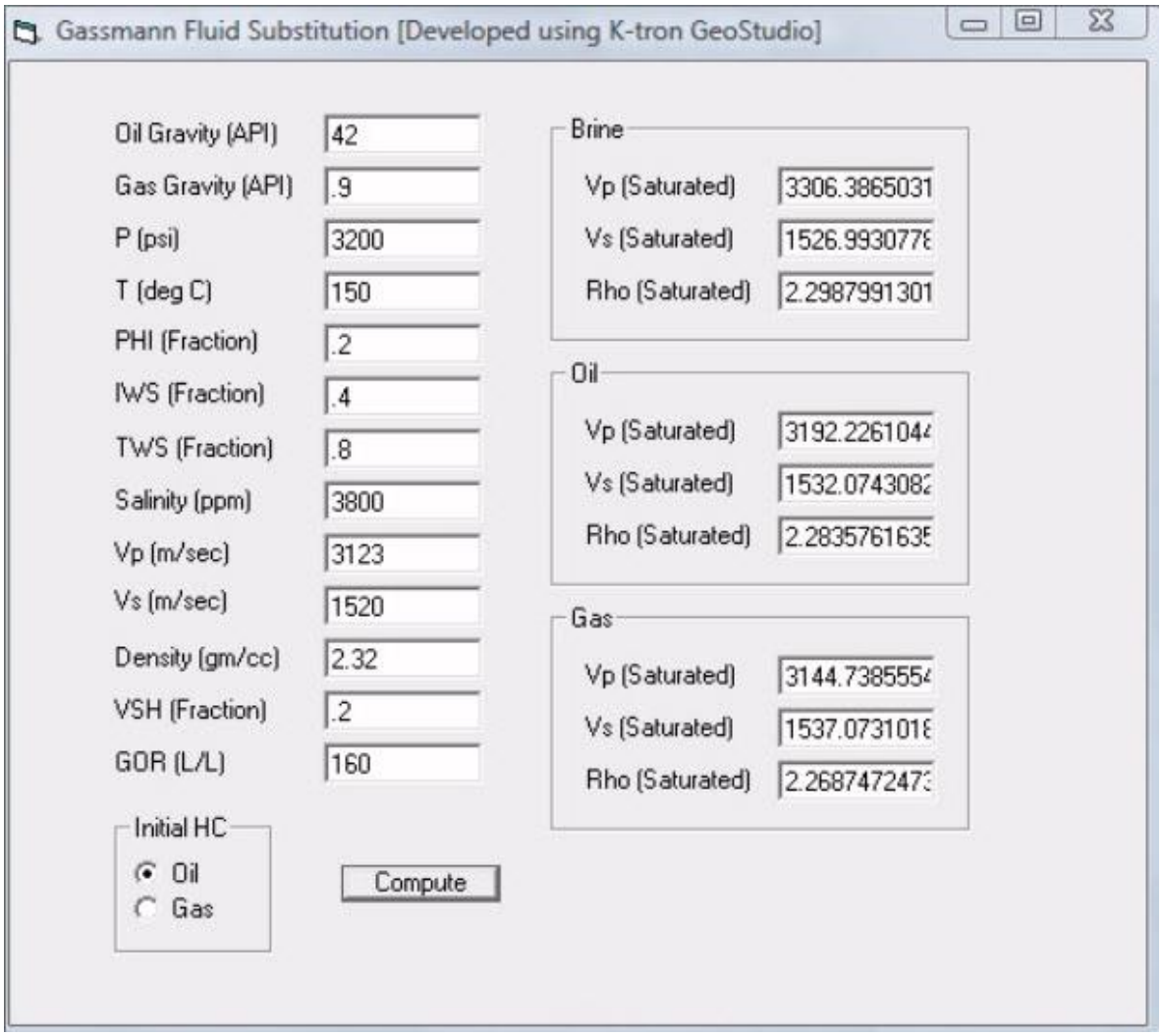

Figure 6.5 Interface of Gassmann Fluid Substitution program along with input parameters.

Table 14 Detail of the parameters used for AVO/AVA Analysis for the seal and reservoir of Bitrisim.

Parameters	Upper Goru	Lower Goru	
Lithology	Shale	Sandstone	
Thickness (meters)	160	60	
Condition	*Unsaturated*	*Water Saturated*	*Gas Saturated*
Vp (m/sec)	3539	3306	3144
Vs (m/sec)	1878	1527	1537
RHO_B (g/cc)	2.39	2.29	2.27

AVO/AVA has same response to both oil and gas. The above parameters for both water and gas saturated cases are input to the Zoeppritz equations to get amplitude response curves for a range of angles of incidence. Fig 6.6 shows the amplitude response graphs of reflected P- and S-waves and the transmitted P- and S-waves due to energy partitioning for the gas saturated case.

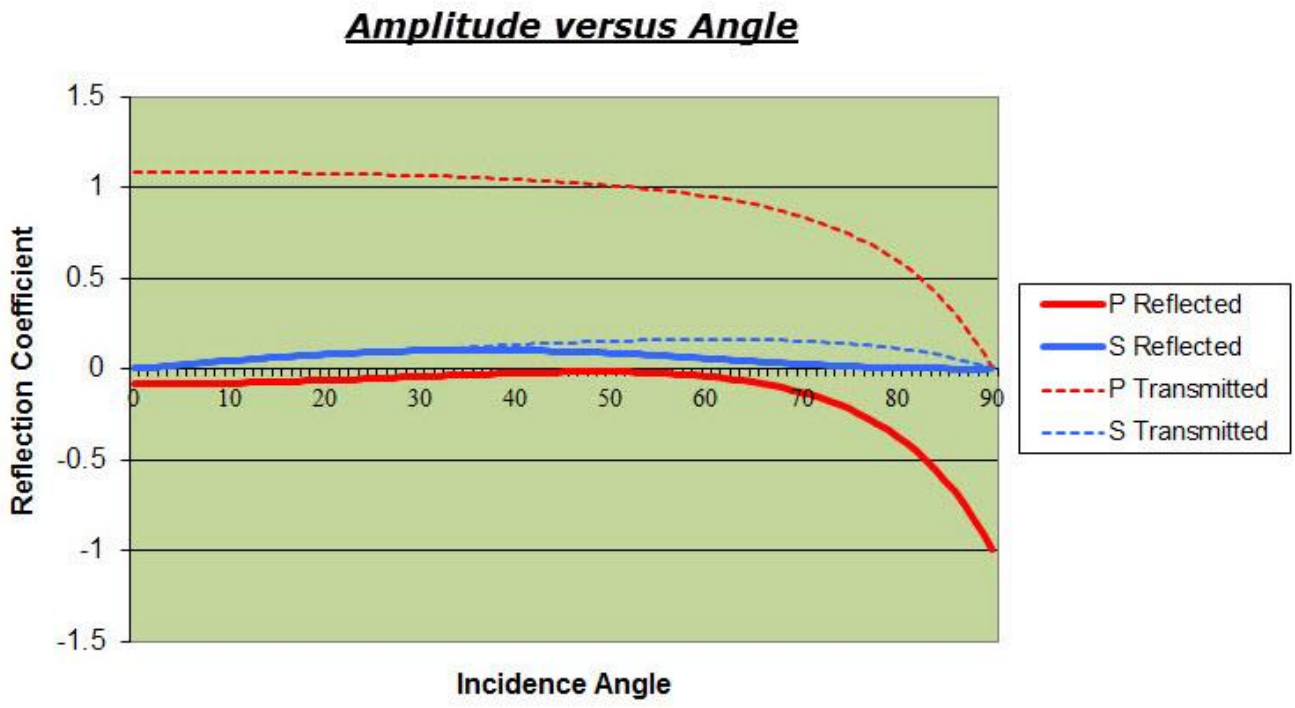

Figure 6.6 Zoeppritz based Reflection coefficient curves as a function of angle of incidence for reflected P- and S-waves and the transmitted P- and S-waves.

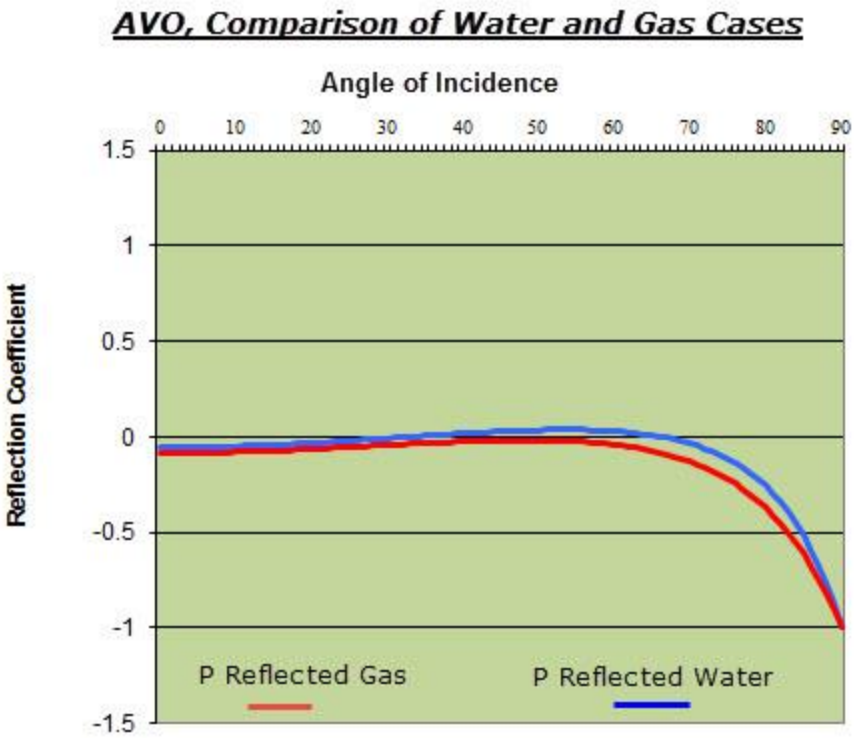

Figure 6.7 Reflection coefficient curves, for both water and gas saturated cases, as a function of angle of incidence ranging from 0 to 90 degrees.

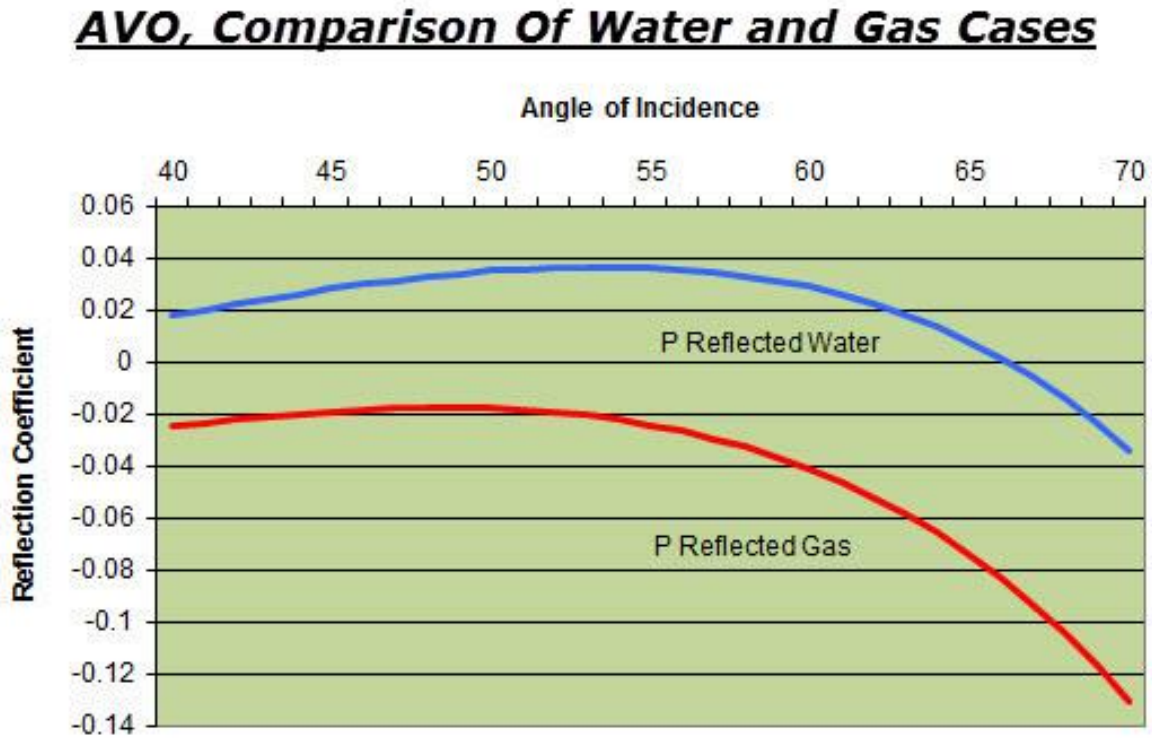

Figure 6.8 Reflection coefficient curves, for both water and gas saturated cases, as a function of angle of incidence ranging from 40 to 70 degrees.

The P wave reflection coefficient curve is used in AVO/AVA modeling to generate model CDP gathers at varying angle of incidence. A computer program AVOTrace composed by (Hameed ,2013) is written in K-tron Visual OIL which inputs the Zoeppritz computed reflection coefficients from a text file. It outputs a X-Works SEC file that can be used to generate model CDP traces with amplitudes varying with angle (offset) as shown in Fig 6.9.

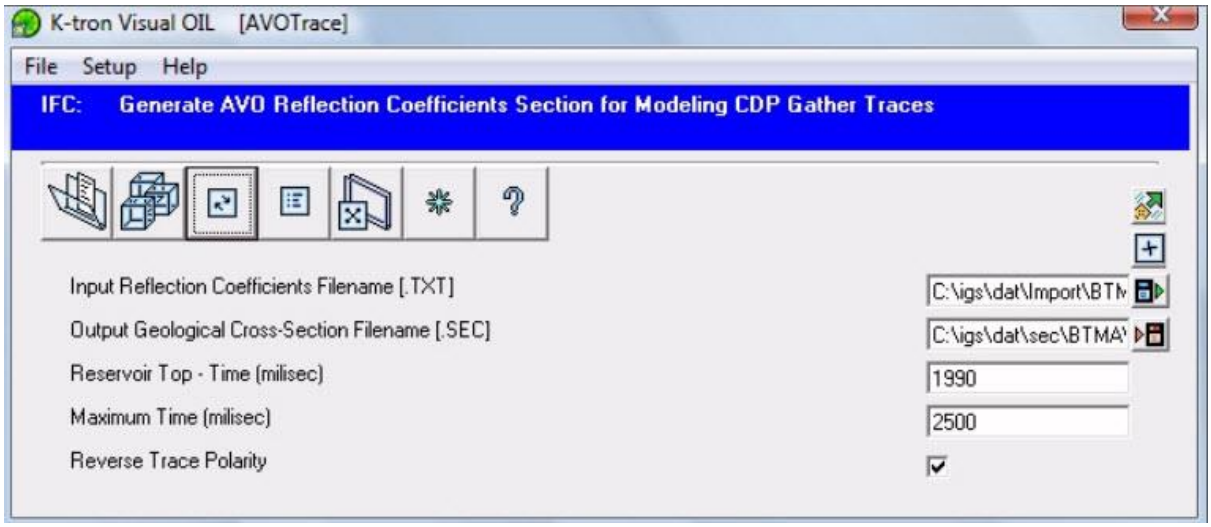

Figure 6.9 K-tron Visual OIL based interface of AVOTrace Program.

2D Modeling is applied to the SEC file created for the Lower Goru reservoir to generate the AVO model. Fig. 6.10 shows the results of AVO modeling with CDP traces generated over the SEC file with varying reflection coefficients.

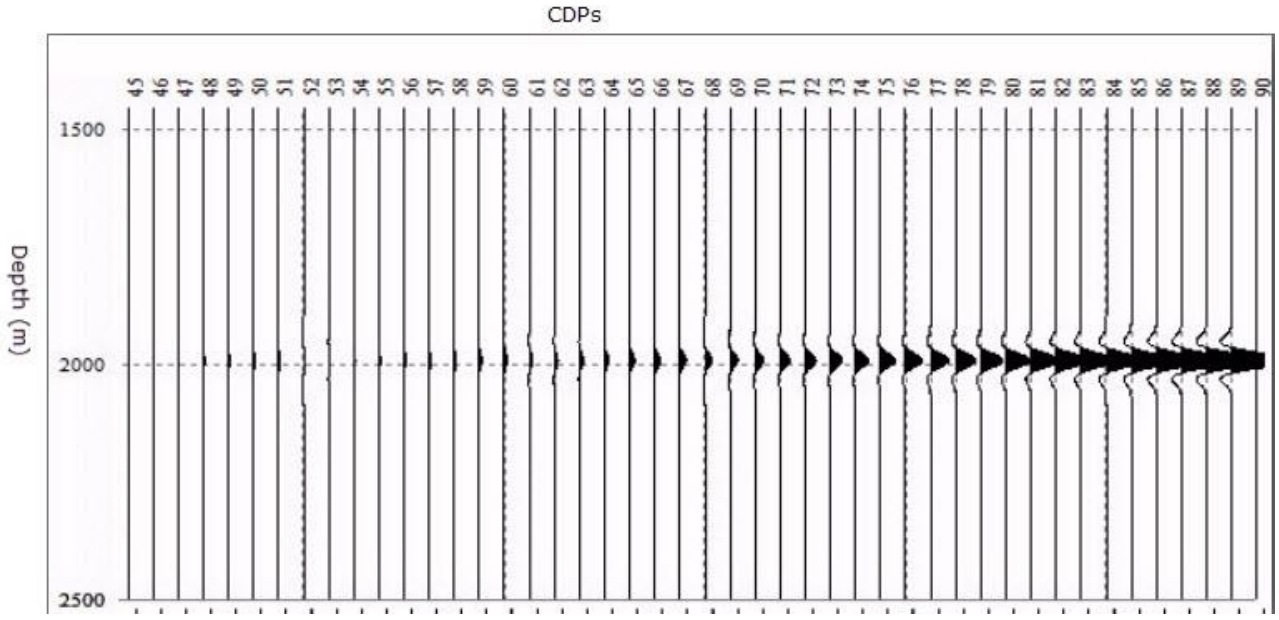

Figure 6.10 Polarity reversed AVO Modelled Traces with amplitudes increasing with offset (angle) for the saturated Lower Goru reservoir.

7. Conclusions and Recommendations

On the basis of detailed structural and stratigraphic interpretation of the study area using Fateh_01 and Icchri_01.

7.1 Conclusions

Following conclusions have been made:

- Six reflectors are marked on the interpreted seismic sections using formation tops; Kirthar (Reflector1), Laki (Reflector 2), Lower Ranikot (Reflector 3), Upper Goru(Reflector 4), Lower Goru(Reflector 5) and Chiltan (Reflector 6).
- Study area is in extensional regime having step faulting along with horst and graben structures which is confirmed by the seismic attribute analysis.
- Velocity is generally increasing with the depth due to compaction of rocks.
- The velocity analysis of the area allows the conversion of time section to depth sections which presented the real scenario of sub surface.
- Both the wells drilled in the study area are in horst block and both are abandoned due to non-commercial production.
- Synthetic seismogram matches with the marked horizons confirming the interpretation.
- An average of 847 meters crustal extension confirms the study area to be in extensional regime.
- The versatile description of 1D and 2D Rock physics studies confirmed the presence of soft and hard lithologies inter bedded with each other throughout the Goru formation.
- The reflection strength attribute computed across a seismic line though confirmed the reflector marking but remain unsuccessful in identifying oil-gas accumulation.
- Instantaneous phase attribute provided good results and the precise positions of faults.
- The increase of amplitudes with offset is an established indicator of hydrocarbons especially gas sands. The AVO/AVA analysis, for the current study, clearly indicate oil and gas sands with good deviation of hydrocarbons saturated reflection coefficients curve for saturation cases.

7.2 Recommendations

- Velocity analysis indicates vertical as well as lateral variations in seismic velocities which highly influence the time to depth conversion, seismic modeling and rock physics analysis.

- It has been found that seismic derived velocity data needs to be calibrated using borehole velocities and then smoothed and interpolated to build a velocity model.

- The spatio-temporal and horizon slice interpolation algorithms indicate that horizon interpolation generates a robust velocity model.

- Build a velocity model of the area using horizon slice based interpolation which can be used in further analysis including Pre-Stack Depth Migrations which is very sensitive to velocity data.

8. References

Ahmed, N., Mateen, J., Shehzad, K. Ch., Mehmood, N., Arif, F., 2011. Shale gas potential of lower Creta54ceous Sembar formation in Middle and Lower Indus Basin, Pakistan. SPE-PAPG Annual Technical Conference, 22-23 November, p. 235-254.

Berge, P. A., 1998. Pore compressibility in rocks, in Thimus, J.-F., Abousleiman, Y., Cheng, A.H.-D., Coussy, O., and Detournay, E., Eds., Biot Conference on Poromechanics: Universit´e Catholique de Louvain, pp.351–356.

Castagna. J.P., Batzle. M.L., and Eastwood. R.L., 1985. Relationships between compressional-wave and shear-wave velocities in clastic silicate rocks. Geophysics, V.50, pp. 571-581.

Coffeen, J.A., 1986. Seismic exploration fundamentals, Penn Well Publishing Company, Tulsa, Oklahoma.

Dewar, J., and Pickford, S. 2001. Rock Physics For The Rest Of Us –An Informal Discussion. Cseg Recorder.

Dix, C. H., 1955. Seismic Velocities for Surface Measurements. Geophysics, 20, 68-86.

Farr, T. G., et al., 2007. The Shuttle Radar Topography Mission, Review of Geophysics., Vol. 45, RG2004. doi:10.1029/2005RG000183.

Gadallah, J., and Fisher, I., 2009. Exploration Geophysics, Springer-Verlag Berlin Heidelberg. DOI: 10.1007/978-540-85160-8.

Gardner, G.H.F., Gardner, L.W., and Gregory, A.R., 1974. Formation velocity and density – the diagnostic basics for stratigraphic traps: Geophysics, 39, 770-780.

Gassmann, F., 1951. Uber die Elastizit ¨at Por ¨oser Medien: Vier. der Natur. Gesellschaft in Zurich, Vol.96, pp.1–23.

Hameed, N. 2013. Integrated Seismic Interpretation, Crustal Shortening and Rock Physics Studies of Missa Keswal Area With special emphasis on Gassmann Fluid Substitution and Amplitude Versus Offset Modeling, M.Sc. Dissertation, Department of Earth Sciences, Quaid-i-Azam University, Islamabad, Pakistan.

Kadri, I. B., 1995. Petroleum Geology of Pakistan. Karachi: Ferozsons (Pvt) Ltd.

Kemal, A., H.R. Balkwill, and F.A. Stokes, 1992, Indus basin hydrocarbon play: Proceedings of International Petroleum Seminar, Ministry of Petroleum and Natural Resources, Islamabad, Nov.1991, G. Ahmad, A. Kemal, A.S.H. Zaman and M. Humayon (eds.), p.78-105.

Khan, K.A., 1995. Seismic and its Super Computing Challenges, Pakistan Journal of Hydrocarbon Research, Vol.7 (2).

Khan, K.A., 2000. Integrated Geo Systems - A Computational Environment for Integrated Management, Analysis and Presentation of Petroleum Industry Data, In: T. C. Coburn and J. M Yarus (Eds.), Geographic Information Systems in Petroleum Exploration and Development, American Association of Petroleum Geologists, AAPG Book on Computers in Geology, pp.215-226.

Khan, K. A., Akhter, G., Ahmed, Z., Khan, M.A., and Naveed, A., 2006. Wavelets - A Computer Based Training Tool for Seismic Signal Processing, Pakistan Journal of Hydrocarbon Research, Vol.16(1), pp.37-43.

Khan, K.A., Akhter, G., Ahmad, Z., and Rashid, M., 2008. Development of a Projection Independent Multi-Resolution Imagery Tiles Architecture for Compiling an Image Database of Pakistan, Proceedings of 2nd International Conference on Advances in Space Technologies Islamabad, Pakistan, pp.164-170. doi:10.1109/ICAST.2008.4747706

Khan, K.A., 2009. Seismic Methods, Digital Courseware Series, 2nd Edition.

Khan, K.A., Akhter, G., and Ahmad, Z., 2009. The Real meaning of Geoscience Data and Process Integration, Proceedings of IAMG International Conference, Computational Methods for Earth, Energy and Environmental Sciences, Stanford Univ., CA.

Khan, K.A., Akhter, G. and Ahmad, Z., 2010. OIL - Output Input Language for Data Connectivity between Geoscientific Software Applications, Computers & Geosciences, Vol.36(5), pp. 687-697. doi:10.1016/j.cageo.2009.09.005.

Khan,K.A, 2010. Seismic The Next Step Series: Seismic Attributes, OIST, Islamabad.

Khan, K.A., and Akhter, G., 2011. Work flow shown to develop useful seismic velocity models, Oil & Gas Journal,Vol.109(16), pp.52-61.

Khan, K.A., Akhter, G., and Ahmad, Z., 2012. Integrated geoscience databanks for interactive analysis and visualization, International Journal of Digital Earth, Online: 09 Dec 2011. doi:10.1080/17538947.2011.638990.

Khan, K.A., 2013. Seismic - The Next Step Series: Rock Physics Analysis, OIST, Islamabad.

McQuillin, R., Bacon, M., and Barclay, W., 1984. An introduction to seismic interpretation, Graham & Trotman Limited Sterling House, 66 Wilton Road LondonSW1V1DE.

Peterson, R.A., Fillipone, W.R., and Coker, F.B., 1955. The synthesis of seismograms from well log data, Geophysics. Vol.20, pp. 516-538.

Robinson. E. S., and Coruh. C., 1988. Basic Exploration Geophysics, John Wiley and Sons, Inc. Newyork.

Shah, S.M.I., Ahmed, R., Cheema, M.R., Fatmi, A.N., Iqbal, M.W.A., Raza, H.A., and Raza, S.M., 1977. Stratigraphy of Pakistan. Geological Survey of Pakistan, Memoirs, v. 12, p.137.

Shah, S.M.I., 2009. Stratigraphy of Pakistan. Geological Survey of Pakistan, Memoirs, v.22.

Sheriff, R. E. and Geldart, L. P., 1995. Exploration Seismology, 2nd Ed., Cambridge Univ. Press.

Taner, M.T., and Koehler, F., 1969. Velocity spectra – digital computer derivation and applications of velocity functions, Geophysics, Vol.34, pp.859-881.

Taner, M.T., 2001. Seismic attributes, rock solid images, CSEG Recorder, Hoston, USA, pp.48-56.

Telford, W. M., Sheriff, R. E., and Geldart, L. P. 1990. Applied geophysics. Cambridge University Press.

Zaigham, N. A., Mallick, K.A., 2000. Prospect of hydrocarbon associated with fossil-rift structures of the southern Indus basin, Pakistan. AAPG Bulletin, V.84, No. 11, November, pp. 1833-1848.

www.gsp.gov.pk